The role of different PEPC isoforms in the growth and physiology of the model CAM plant, *Kalanchoë fedtschenkoi*.

Osita Williams Nwokeocha

Doctor of Philosophy

School of Natural and Environmental Sciences

Newcastle University

February 2023

Declaration

This thesis is submitted to Newcastle University for the degree of Doctor of Philosophy. The research detailed within was performed from 2018 to 2021. The work was supervised by Professor Anne Borland and Dr Maxim Kapralov. I certify that I have previously submitted no part of the materials offered in the thesis for a degree or any other qualification at this or any other university.

Osita Williams Nwokeocha

Abstract

Crassulacean acid metabolism (CAM) is one of plants' three types of photosynthesis. CAM evolved from C_3 via changes in protein sequence and temporal gene expression. Compared to C_3 and C_4 photosynthesis types, CAM shows resilient photosynthetic ability under limited water availability. A key step in CAM photosynthesis involves phosphoenolpyruvate carboxylase (PEPC), which catalyzes nocturnal carboxylation of phosphoenolpyruvate (PEP) to form oxaloacetate which is reduced to malate. PEPC is controlled transcriptionally and post-translationally. The two most abundant isoforms of PEPC in *Kalanchoë fedtschenkoi* are *KfePEPC1* (kaladp0095s0055.1) and *KfePEPC2* (Kaladp0048s0578.1), with the former being abundantly expressed in both light and dark periods while the latter is expressed abundantly in the dark period. In this study, we investigated the roles of different PEPC isoforms in the growth and physiology of the model CAM plant *Kalanchoë fedtschenkoi*. Our partners at Oak Ridge Laboratories USA created mutants of *KfePEPC1* and *KfePEPC2* genes using the novel gene-editing technique CRISPR. The aim of this thesis was to conduct physiological and biochemical analyses for independent lines of each of these mutated genes and thereby establish the physiological roles of PEPC1 and PEPC2.

The effect of knocking down the *KfePEPC1* gene includes a significant loss in PEPC enzyme activity and protein abundance along with a switch from nocturnal CO_2 fixation and stomatal opening to daytime CO_2 uptake and stomatal opening, as shown in the mutant *kfepepc1* line1. In addition, the *kfepepc1* line1 mutant had a significant drop in the amount of malic acid stored at dawn and increased starch accumulation at night compared to the wildtype. The same mutants also showed increased transpiration rate, reduced water use efficiency, reduced stomatal density with larger pore lengths and increased pigment content in drought conditions. In contrast, the *kfepepc1* Line 2 mutant retained all the attributes of CAM observed in wildtype. Still, the mutation significantly perturbed PEPC protein abundance, altered stomatal regulation, reduced stomatal density, and increased saturated water content under drought conditions in the *kfepepc1* Line 2 mutant. These different effects observed in the *kfepepc1* mutant lines could be attributed to how completely the *KfePEPC1* gene was knocked down in the lines. Overall, results indicated that the *KfePEPC1* gene is essential for CAM in *K. fedtschenkoi*.

The effect of knocking down the *KfePEPC2* gene was also examined. Both lines of the *kfepepc2* mutants retained all the attributes of CAM observed in wildtype, although down-regulation of diel transcript abundance of the *rbc*L gene during the middle of the daytime was observed. Furthermore, the ability of the *kfepepc2* mutants to regulate stomatal opening, especially towards the end of the light period, was significantly compromised, and growth was significantly suppressed. In addition, the *KfePEPC2* mutation caused a reduction in stomatal density and increased pore length. These observations indicated that the *KfePEPC2* gene isoform is implicated in other important non-photosynthetic functions, which are key to physiological performance in *K. fedtschenkoi*. At the same time, the effect of knocking down both *KfePEPC1* and *KfePEPC2* together was even more severe. In addition to losing the ability to do CAM, the mutation led to the loss of PEPC enzyme activity, protein abundance, inability to accumulate malic acid overnight, and highly suppressed growth in all the *kfepepc1/2* mutant lines.

Observations from this work indicate that the different isoforms of the PEPC gene investigated play pivotal but contrasting roles in optimizing CAM and photosynthetic activity of *K. fedtschenkoi*. To successfully bioengineer CAM into C_3 plants, both PEPC genes must be functional in the bioengineered system.

Acknowledgements

I want to first and foremost acknowledge God Almighty for his goodness to me, for seeing me through all these years, and for blessing me with a beautiful family, a blossoming career, and a bright future.

I express my sincere gratitude to my supervisor, Professor Anne Borland, for accepting to be my supervisor and mentor my budding academic career, helping me settle into Newcastle quickly, and being a constant presence in my research from inception to the end of it. I want to thank my second supervisor Dr Maxim Kapralov for their high-level professionalism in supervising this work and the significant contributions he made throughout this research. Finally, to my progression panel members, Dr Tahar Taybi and Dr Vasilios Andriotis, I want to say thank you for diligently accessing my yearly progress during the research, making valuable contributions and feedback to the research work, and giving me a listening ear whenever I come to you.

I want to appreciate my dear wife, Mrs Udodirim Precious Osita-Nwokeocha, and my lovely daughter Chimamanda Victoria Osita-Nwokeocha. You guys are my backbone, my source of strength, and for standing by me through thick and thin, I want to thank you from the depth of my heart; I love you guys deeply, and I will always be there for you all.

I also wish to acknowledge my parents, Mr and Mrs Clement Nwokeocha, and my siblings Mrs Chinemerem Nwosu (Nee Nwokeocha), Mr Kelechi Nwokeocha and Mr Obinna Nwokeocha. Thank you all for your prayers and support all these years.

Finally, I want to thank the Nigerian government through the academic staff training and development (AST&D) programme of the tertiary education trust fund (TETFUND) for sponsoring this thesis.

Table of Contents

List of Figures

List of Tables

List of equations

Abbreviations

ALMT	Aluminium-activated malate transporter
ANOVA	Analysis of variance
APS	Ammonium persulphate
ATP	Adenosine triphosphate
BSA	Bovine serum albumin
BTPC	Bacteria type PEPC
β - Carboxylation	C_4 carbon fixation pathway as the sole mechanism to fix CO_2 by PEP and RuBisCO
C_3	C_3 carbon fixation pathway as the sole mechanism to fix CO_2 by RuBisCO
CAM	Crassulacean acid metabolism
CO_2	Carbon dioxide
CRISPR-Cas9	Clustered regularly interspaced short palindromic repeats and CRISPR associated protein 9
DSB	Double stranded breaks
ECL	Enhanced chemiluminescence
FAO	Food and agricultural organisation
Fd-GOGAT	Ferredoxin-dependent Glutamate synthase
G6P	Glucose-6-phosphate
GAANTRY	Gene Assembly in *Agrobacterium* by Nucleic acid Transfer using Recombinase technologY
GDP	Gross domestic product
Gsi	Integrated CO2 uptake
H_2O_2	Hydrogen peroxide
HCO_3^-	Bicarbonate
LSD	Least significant difference
NAD-ME	NAD-malic enzyme
NADPH	Nicotinamide adenine dinucleotide phosphate (reduced)
NHEJ	Non homologous end joining
PAM	Protospacer adjacent motif
PCI	Potential conductance index
PEP	Phosphoenolpyruvate
PEPC	Phosphoenolpyruvate carboxylase
PEPCK	Phosphoenolpyruvate carboxylase kinase
PP2A	Protein phosphatase 2A
PPDK	Pyruvate orthophosphate dikinase
PPFD	Photosynthetic photon flux density
PTPC	Plant type PEPC

qRT-PCR	Quantitative real-time polymerase chain reaction
RNAi	RNA interference
ROS	Reactive oxygen species
RuBisCO	Ribulose-1,5-bisphosphate carboxylase/oxygenase
SDS	Sodium dodecyl sulphate
sgRNAs	single-guide RNAs
SPI	Stomatal pore area index
SWC	Saturated water content
T-DNA	Transfer DNA
tDT	Tonoplast dicarboxylate transporter
TEMED	Tetramethylethylenediamine
Tm	Melting temperature
TRi	Integrated rate of transpiration
WGD	Whole-genome duplication
WUE	Water use efficiency
WUEi	Instantaneous water use efficiency
ZFNs	Zinc finger nucleases

Chapter 1 General Introduction

1.1 Crassulacean acid metabolism (CAM) for sustainable agriculture in a warmer, drier world.

Photosynthesis manufactures complex organic molecules such as adenosine triphosphate (ATP) and reduced nicotinamide adenine dinucleotide phosphate (NADPH) in plants, algae and certain bacteria species using CO_2 and solar energy (Blankenship 1992; DePaoli et al. 2014). Moreover, it is fundamental to other plant processes, including respiration, growth, and reproduction. In addition, photosynthesis supplies substrates, such as oxygen and carbohydrate, as by-products needed to support vital processes in plants, crops and biomass used for livestock production (Singh and Thakur 2018). Of the various types of photosynthesis in plants today, the C_3 is the ancestral type of photosynthesis in most terrestrial plants and ultimately the most abundant photosynthetic pathway in crop plants (Raines 2011; Yang et al. 2015b). Unfortunately, the efficiency of C_3 photosynthesis has come under threat due to challenges posed by climate change, compromising global food security (Muhammad et al. 2021). A significant challenge facing C_3-type photosynthesis is the massive amounts of water needed to maintain optimal productivity of C_3 plants due to the increased tendency of transpiration transpirational water loss attributed to rising temperature, an effect of climate change (Borland et al. 2009; Hanjra and Qureshi 2010; Edwards 2019).

Water use efficiency (WUE) is the ability of a plant to assimilate a unit of carbon for every unit of water consumed (Yuan et al. 2020). The higher the water use efficiency of a plant, the better the plant's ability to maintain optimal growth, especially in limited water availability. C_3 plants lose a lot of water via transpiration as their stomata open during the day to absorb CO_2 from the atmosphere (Borland et al. 2009). This translates to poor water-use efficiency and has made it extremely challenging for C_3 plants to thrive in arid, semi-arid and marginal lands where the soil water availability and rainfall are meagre (Borland et al. 2009; Borland et al. 2014; Yang et al. 2015a). Poor water use efficiency and the rising earth's temperature from global warming have rendered lands hitherto conducive for agriculture almost inhabitable for plants, have affected crop productivity, and are posing a serious challenge to global food security and slowing down the fight against climate change (Hanjra and Qureshi 2010; Yang et al. 2015a). This is indeed an issue of concern because with the world's

population projected to increase by 50% by 2050 and 71% by the year 2100, increasing global food production is essential. Hence, increasing crop productivity to feed a rapidly growing world population via optimising the efficiency of photosynthesis is central to achieving this goal (Murchie et al. 2009; Yang et al. 2015a). The problem of water shortage in plant production poses a real threat to global food security because, at the moment, an extensive and expensive irrigation process is required to provide much-needed water to agricultural farms (Hanjra and Qureshi 2010). Not only is this practice non-sustainable, it will not provide the needed permanent solution to the problem but only a reprieve with the rate of global use of available freshwater for irrigation purposes standing at 31-38% as of 2020 (Walczak 2021).

There is believe also that the oxygenation activity of the RuBisCO enzyme can impact the efficiency of C_3 photosynthesis. With RuBisCO oxygenation reaction, one molecule of 2-phosphoglycolate (2-PG), a known enzyme inhibitor, and one molecule of 3-phosphoglycerate (3-PGA) are produced and as against two molecules of 3-phosphoglycerate (3-PGA) produced when carboxylation reaction occurs (Bowes et al. 1971). The inhibitory potential of 2-GP can perturb the functioning of enzymes like triose phosphate isomerase and sedoheptulose 1,7-bisphophatase critical to the Calvin cycle, thereby threatening the efficiency of photosynthesis in plants by initiating an energetically costly process known as photorespiration (Edwards 2019). However, recent studies have shown that photorespiration is indeed beneficial to plants. As a metabolic process, photorespiration recycles up to 75% of 2-phosphoglycolate (2-PG) generated via RuBisCO oxygenation to 3-PGA, involved in nitrogen assimilation and phospholipid biosynthesis (Busch 2020).

Several attempts have been made to solve these problems of crop limitations, including increasing CO_2 availability and reducing photorespiration by engineering C_4 photosynthesis into C_3 plants (Murchie et al. 2009). However, discovering that some plants evolved a specialised type of photosynthesis called Crassulacean acid metabolism (CAM) holds promise for crop improvement. CAM plants have demonstrated the ability to overcome the limitations facing the C_3 pathway by using temporal separation of key photosynthetic events, which has further created viable means of dealing with these problems whilst allowing the plants to benefit from the physiological advantages that come with the pathway (Winter et al. 2015a). CAM solves the problem of water-use efficiency by; switching stomatal behaviour to drastically reduce water loss via transpiration, thereby optimising photosynthesis and

increasing plants' productivity in marginal lands (Borland et al. 2014; Bräutigam et al. 2017; Yin et al. 2018). Furthermore, CAM plants adopt a diel shift in CO_2 uptake pattern, in which stomata open at night when the temperature is less hot, and the transpiration rate is lower (Borland et al. 2014). This diel shift in mechanism has solved particular challenges plants face in arid and semi-arid climates (Abraham et al. 2016).

CAM pathway can provide feasible solutions to problems plaguing sustainable agriculture by allowing crops to thrive and massively increase their productivity in the face of dwindling water supply. This is possible because water-use efficiency (WUE), an integral feature of CAM, is key to drastically reducing the water required to grow and increasing the productivity of staple crops (Yang et al. 2015a). However, introducing this CAM feature to C_3 crops is challenging and requires bioengineering CAM into C_3 plants by manipulating the genes and proteins of the C_3 pathway to allow for the expression of these novel traits from CAM (DePaoli et al. 2014).

Significant progress has been made in understanding the minimal set of genes and proteins required for the establishment and efficient operation of CAM, fulfilling the primary steps in bioengineering CAM (Liu et al. 2021; Winter and Smith 2022). This has also been helped by creating a computational model for CAM that includes gene regulatory networks, signalling pathways, and metabolic network fluxes. Thus, bioengineering CAM into C_3 plants is feasible (Borland and Yang 2013). Liu et al. (2021) reached a recent milestone in CAM bioengineering when they successfully engineered a tobacco plant to overexpress a CAM-specific *AaPEPC* gene from *Agave americana* and reported an increase in biomass production and tolerance to drought stress compared to the wild type. Even though more studies are underway, the initial success has laid a solid foundation for a complete switch from C_3 to CAM by engineering more CAM-related genes for carboxylation, decarboxylation, stomatal movement, and carbohydrate turnover (Liu et al. 2021; Yang et al. 2015a).

CAM enzymes are pivotal to the overall performance of the pathway, and phosphoenolpyruvate carboxylase (PEPC) is probably the most important enzyme involved in the nocturnal phase of the CAM pathway. The primary function of the PEPC enzyme is to catalyse the fixing of atmospheric carbon dioxide (CO_2) in the form of bicarbonate (HCO_3^-) to phosphoenolpyruvate (PEP) to form oxaloacetate and inorganic phosphate (Osmond 1978; Borland et al. 2009; Winter and Smith 2022; Shu et al. 2022). PEPC is encoded by a

multigene family (Deng et al. 2016) that gives rise to different isoforms that play a range of crucial roles in plants, from photosynthetic roles in the case of the CAM and C4 pathways to non-photosynthetic roles in the case of the housekeeping isoforms involved in like carbon and nitrogen metabolism, stomatal regulation, seed development and response to abiotic stresses (Shu et al. 2022; O'Leary et al. 2011). PEPC's involvement in the regulation of the stomatal movement has attracted the interest of researchers who are trying to fully understand the stomatal biology of CAM plants. So far, there is a general agreement that CAM stomata open in response to low internal CO_2 concentration (Winter and Smith 2022; Santos et al. 2022). Guard cells that surround stomatal pores and regulate their aperture, also play key roles in transporting ions like potassium and solutes like malate (Lefoulon et al. 2020). There are indications that the diel rescheduling of several stomata-related genes which include *CBL-interacting protein kinase 23 (CIPK23),* and *Regulatory component of ABA receptor1 (RCAR1)* and *Catalase 2 (CAT2)* genes in CAM plants as against their C_3 orthologues may impact stomatal movement in CAM plants (Moseley et al. 2019). Therefore, to successfully engineer CAM into C_3 photosynthesis, understanding how the different isoforms of PEPC genes are implicated in nocturnal CO_2 fixation, inversing stomatal opening to the night period, circadian clock regulation, and carbohydrate metabolism is essential (Yang et al. 2017). This thesis aims to use recently created CRISPR-Cas9 mutants of *K. fedtschenkoi,* where the expression of *KfePEPC1* and *KfePEPC2* genes has been knocked down to understand the roles of different isoforms of *PEPC* genes in the CAM pathway. Knocking down PEPC also provides an opportunity to examine how CAM biochemistry interacts with other physiological and anatomical attributes associated with drought tolerance in CAM plants. This general introduction will describe the phases of the CAM process, consider the ecology of CAM and how it sits alongside other drought resistance strategies before considering in detail the molecular genetics, biochemistry, and regulation of PEPC.

1.2 Process of CAM.

The diel cycle of CAM photosynthesis falls into four phases. The phases represent both the acidification and deacidification process that characterises CAM plants. These plants nocturnally source CO_2 to sustain the process of photosynthesis over 24 hours (Osmond 1978; Ceusters et al. 2011). The phases are described as follows;

1.2.1 Phase 1: The nocturnal CO_2 uptake (Primary carboxylation) phase.

In phase 1 of CAM, nocturnal uptake of atmospheric CO_2 or refixation of respiratory CO_2 occurs (Figure 0.1 andFigure 0.2). Towards the end of the photoperiod and the start of the night, CAM plants start to open their stomata to capture carbon dioxide (CO_2) from the air in the form of bicarbonate (HCO_3^-), a reaction that is catalysed by the enzyme carbonic anhydrase (Lüttge 2004; Boxall et al. 2020; Winter and Smith 2022). The 3-C substrate needed for nocturnal carboxylation comes from the breakdown of starch and/or soluble sugars synthesised and stored via the gluconeogenic processes during the photoperiod. These carbohydrates are broken down at night via glycolysis to phosphoenolpyruvate (PEP), a three-carbon substrate for primary carboxylation (Borland et al. 2016a; Winter and Smith 2022). Carboxylation of PEP is catalysed by a cytosolic enzyme called phosphoenolpyruvate carboxylase (PEPC), which is activated at night via phosphorylation by a dedicated PEPC kinase enzyme called phosphoenolpyruvate carboxylase kinase (PEPCK) (Cushman 2001; Dodd et al. 2002; Borland et al. 2014). As a result of primary carboxylation, oxaloacetate is the first by-product formed.

Oxaloacetate is quickly reduced to malate in a reaction catalysed by the enzyme malate dehydrogenase and transported via an aluminium-activated malate transporter (ALMT) or a tonoplast dicarboxylate transporter (tDT) to the large vacuoles located in the mesophyll cells of the leaf as malic acid (Hatch et al. 1982; Kim Hong et al. 2008; Yuan et al. 2020). The process of storing malate as malic acid is energised by one or both of the two tonoplast-localised H^+ pumps, the V-ATPase and the V-PPiase (Winter and Smith 2022). This phase of the CAM cycle is characterised by increased CO_2 uptake, a high concentration of malic acid building up in the vacuole, and a relatively low rate of water loss via transpiration because during the dark period, the air is cooler, therefore ensuring enhanced water-use efficiency, a vital attribute in CAM plants (Borland et al. 2009).

1.2.2 Phase 2: The transition phase

The second phase of CAM is the phase that occurs from the end of the dark period until the beginning of the photoperiod (Figure 0.2) and marks the beginning of the switch from β-carboxylation to C_3 carboxylation (Nimmo et al. 1984; Dodd et al. 2002). During this phase, there is a sharp increase and then a decrease in the rate of CO_2 uptake due to PEPC and RuBisCO enzymes being active at once (Osmond 1978; Dodd et al. 2002). This phase is typically short because overnight malate accumulation has been achieved. PEPC becomes

less active due to a gradual dephosphorylation process catalysed by protein phosphatase 2A (PP2A), evident in the drop of PEPC kinase activity (Carter et al. 1990; Nimmo 2000). This results in increased sensitivity of PEPC to malate inhibition, and RuBisCO activity gradually increases along with RuBisCO activase, ensuring RuBisCO is available in the active form (Nimmo et al. 1984; Martín et al. 2011). The key feature of this CAM phase 2 is that PEPC and RuBisCO, the two main enzymes involved in CO_2 accumulation in CAM, are active simultaneously, thereby having an overlapping effect (Lüttge 2010a; Winter and Smith 2022). As the photoperiod progresses, a process known as carbamylation involves the reversible binding of activator CO_2 and a light-dependent non–enzymatic modification activates RuBisCO. RuBisCO activate protein is needed to facilitate the dissociation of inhibitory sugar phosphates from the active site of Rubisco in an ATP-dependent manner making RuBisCO active (Perdomo et al. 2017). RCA protein is synthesized in the cytosolic ribosomes and transported to the chloroplast. This activation enables RuBisCO enzyme to become the dominant carboxylation enzyme as PEPC activity drops off entirely due to dephosphorylation and inactivation (Maxwell et al. 1999; Griffiths et al. 2002).

1.2.3 Phase 3: The secondary carboxylation phase.

Phase 3 of CAM is the phase where secondary carboxylation takes place (Figure 0.1 and Figure 0.2). This phase sees the translocation of the malic acid stored overnight from the large vacuole into the cytosol via an aluminium-activated malate transporter (ALMT) or a tonoplast dicarboxylate transporter (tDT) and, in the case of *Kalanchoe* species, to the mitochondria, where malate is broken down to release CO_2 (Borland et al. 2014; DePaoli et al. 2014; Dever et al. 2015; Hartwell et al. 2016; Yuan et al. 2020; Boxall et al. 2020). This process is catalysed by NAD-malic enzyme, and the CO_2 released goes into the Calvin-Benson cycle for fixation by ribulose-1,5-bisphosphate carboxylase/oxygenase (RuBisCO). RuBisCO activity in this phase of CAM is activated via a reversible binding of activator CO_2 and modulation by carbamylation of active sites and, in many cases, by removal of specific inhibitors to carbamylated sites (Maxwell et al. 1999; Griffiths et al. 2002; Ceusters et al. 2021a). The ability of activated RuBisCO to bind with multiple sugar complexes in a non-productive manner leads to the dead-end formation of inhibited complexes that need to be remodelled by a dedicated molecular chaperone known as RuBisCO activase (Parry et al. 2008; Shivhare and Mueller-Cajar 2017). This phase occurs during the photoperiod when the air is warmest, but the stomatal closure resulting from the CAM process ensures that water loss from transpiration is curtailed. The inactivity of PEPC at this time, together with

stomatal closure, effectively rules out direct atmospheric CO_2 uptake (Borland et al. 2009; Borland et al. 2014; Yang and Liu 2015; Dever et al. 2015; Hartwell et al. 2016; Boxall et al. 2017; Boxall et al. 2020). The CO_2 captured during primary carboxylation, which occurred during phase 1 of CAM and stored as malic acid, is broken down by NAD-malic enzyme (NAD-ME) or phosphoenolpyruvate carboxykinase for CAM species in the Bromeliaceae, Liliaceae, Clusiaceae and Asclepiadaceae families (Osmond 1978). This process increases the affinity of RuBisCO by 60-fold to its CO_2 substrate during light period fixation and significantly reduces photorespiration (Lüttge 2010a, b; Winter and Smith 2022). There is an estimated 2.5% (v/v) increase in the internal CO_2 concentration behind closed stomata during this phase of CAM (Lüttge 2010a). Meanwhile, the oxygen concentration during this phase is much higher at about 25% (Spalding et al. 1979; Miszalski et al. 1998; Pedersen et al. 2018). The pyruvate released at this stage is converted to phosphoenolpyruvate by pyruvate orthophosphate dikinase (PPDK), recycled via gluconeogenesis to the carbohydrate source (predominantly starch in *Kalanchoe* species) and subsequently used during primary carboxylation in phase 1 (Dever et al. 2015; Boxall et al. 2020).

1.2.4 Phase 4: Direct fixation of atmospheric CO_2

This phase of CAM involves directly fixing CO_2 from the atmosphere and commences when malate stores have been depleted from the vacuole. Phase 4 occurs at the end of the photoperiod and is characterised by decreasing intercellular CO_2 concentration. When favourable environmental conditions permit the stomata to open just before dark, the plants fix CO_2 using the C_3 pathway mediated by RuBisCO (Winter and Smith 2022). There is also evidence that in CAM plants, the activity of PEP kinase starts to increase, resulting in the availability of phosphorylated PEPC, which also gets involved in CO_2 uptake during this phase. This possibility also creates a situation where both PEPC and RuBisCO are active, as seen in some *Clusia* species (Roberts et al. 1997).

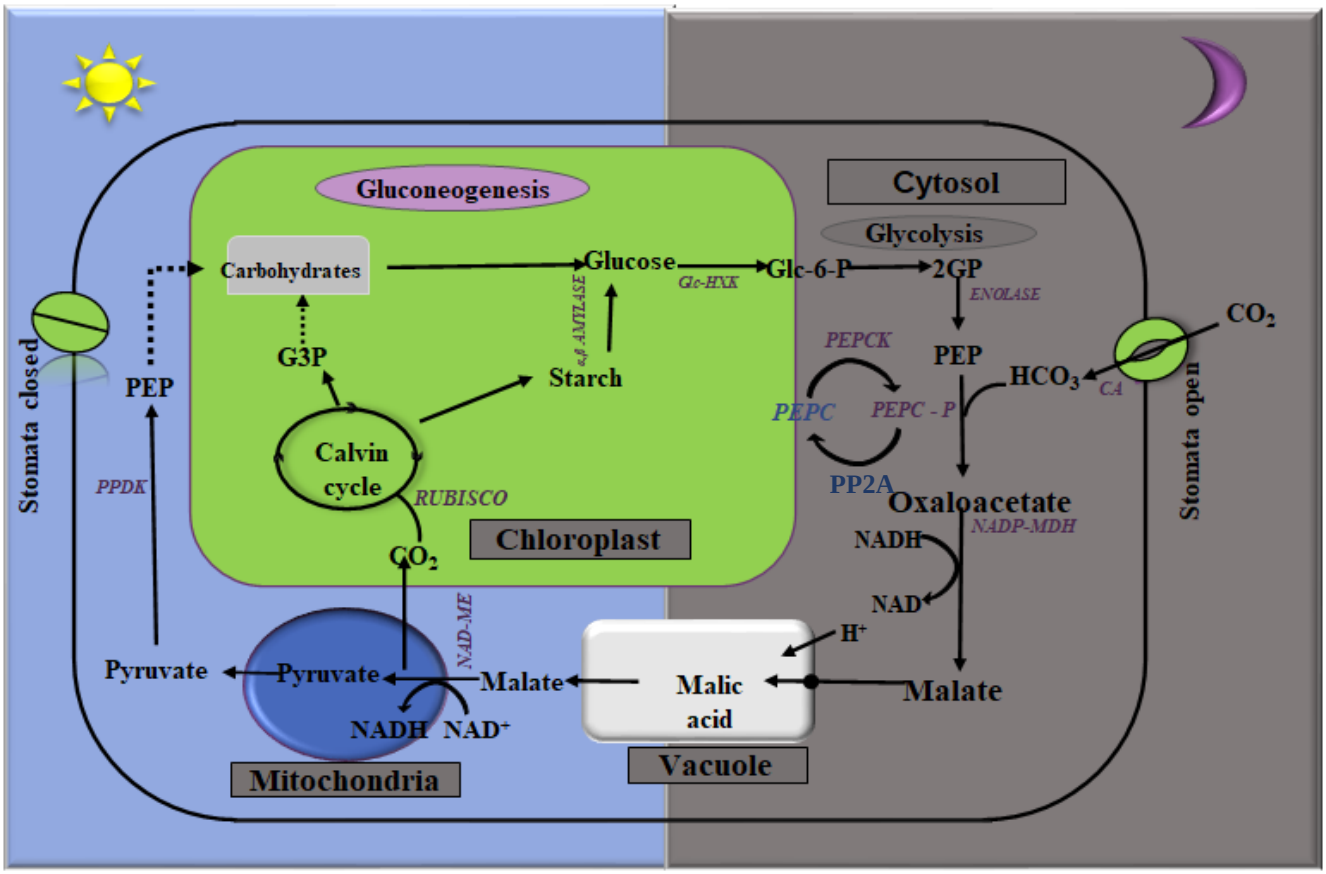

Figure 0.1. Diagram showing the CAM pathway. At night, the stomata open and CO_2 is absorbed; phosphoenolpyruvate carboxylase (PEPC) catalyses the carboxylation of phosphoenolpyruvate (a C3 acid) to form oxaloacetate, which is later reduced to malate and is stored in the vacuole of the leaves. During the day (Light period), the stomata are closed, malate is decarboxylated to release CO_2, PEPC is deactivated, and Ribulose-1, 5-biphosphate carboxylase/oxygenase (RuBisCO) catalyses the reassimilation of CO_2 into the Calvin Benson cycle while pyruvate goes into the production of starch that is stored in the plant.

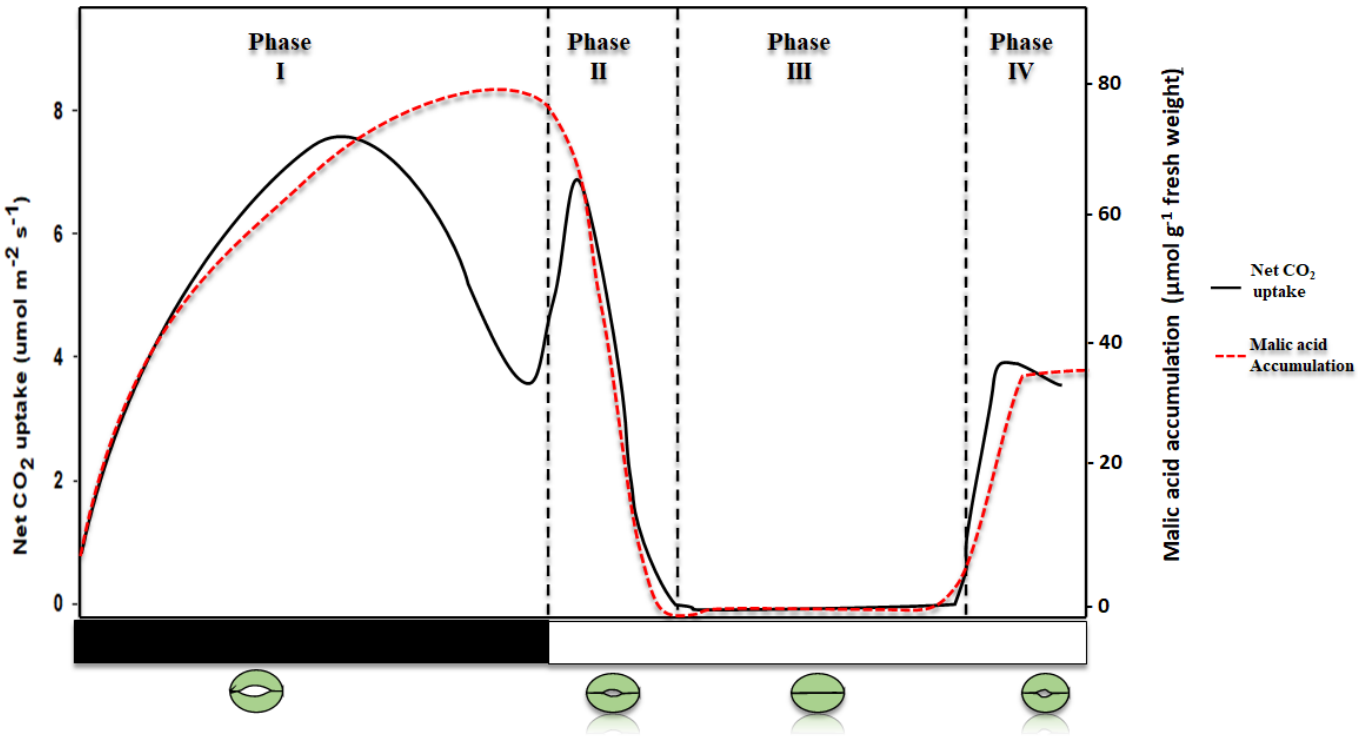

Figure 0.2. Diagram showing the amount of CO_2 uptake (black strip) and diel malate accumulation (red strip) in the four (4) phases of CAM. Most of the dark period (phase 1) is characterised by massive uptake of CO_2 as the phosphorylated PEPC enzyme is active, and stomata remain open; hence there is an increased amount of malate stored. At the end of the dark period (phase 2), there is a brief spike in CO_2 uptake due to two carboxylating enzymes PEPC and RuBisCO being active. As the PEPC enzyme becomes inactive due to dephosphorylation, malate accumulation starts to drop off, and stomata close. With the light period (Phase 3) in full force, net CO_2 uptake completely drops along with malate accumulation and stomata are closed. At the end of the light period (phase 4), as stomata start to open, CO_2 uptake starts to pick up because the RuBisCO enzyme is active and fixing atmospheric CO_2. This leads to an increase in malate accumulation.

1.3 Ecology of CAM and its relationship with other drought resistance strategies.

Globally, CAM plants are distributed in various zones ranging from temperate to mountains in the old world and the tropics (Lüttge 2004). For example, CAM plants of the Cactaceae and Crassulaceae families can be found in the northern deserts and prairies of the American continent; those of the Agavaceae family are prominently found in Mexico and also in semi-arid/arid regions of the New World, while Madagascar is home to a good number of CAM plants from the Crassulaceae family, especially of the *Kalanchoë* (Teeri et al. 1978; Descoings 2006; Lüttge 2010a; Garcia-Moya et al. 2011). Different environmental stressors exist in these climate zones, and one or a combination defines the type of adaptation these plants require to thrive (Lüttge 2010a). CAM ecology greatly depends on the environment the CAM plants are in and what type of environmental stress adopting CAM photosynthesis

would help them adjust to (Lüttge 2004). For instance, in CAM plants growing in hot tropical or temperate arid or semi-arid deserts, the primary environmental stress they face is a severe water shortage in the soil due to low precipitation, leading to drought (Borland et al. 2009; Borland et al. 2014; Yang et al. 2015a). Even so many epiphytes prefer to use CAM photosynthesis as a tool to cope with low water availability (Gilman and Edwards 2020).

Drought is of great concern because of its destructive effect on agricultural production and the knock-on effect on global food security efforts (Martignago et al. 2020). Drought results in a reduction in growth and increased oxidative stress, which destroys vital cells of the cell, eventually leading to the death of the plant (Lüttge 2004; Yang and Liu 2015; Rustioni and Bianchi 2021). Plants have adopted different strategies to avoid or cope with the drought problem, from making morphological and anatomical changes such as succulent leaves, roots and sunken stomata to adopting specialised photosynthetic pathways such as C4 and CAM (Chandler and Bartels 2008). Oxidative stress is a significant problem plants deal with when facing drought stress. It originates as a natural phenomenon in the standard metabolism of oxygen and its by-products and can induce cellular injuries by protein oxidation, lipid peroxidation, and DNA damage, finally leading to plant cellular death (García-Caparrós et al. 2021).

Extensive studies on the CAM pathway have confirmed that one of the key benefits to CAM plants is higher water-use efficiency, which is tightly linked to their ability to tolerate drought stress (Borland et al. 1998; Borland et al. 2009; Yang et al. 2015a). Hence, adopting CAM to avoid or cope with the side effects of drought is a well-known strategy of most C_3/CAM switching plant species (Dodd et al. 2002; Broetto et al. 2002; Ślesak et al. 2008; Chia-Yun et al. 2018). In addition, CAM plants can increase the activity of enzymes that specialise in scavenging reactive oxygen species (ROS) to deal with oxidative stress (Miszalski et al. 2003; Nosek et al. 2019). For example, Broetto et al. (2002) and Ślesak et al. (2008) both reported that inducing CAM in *M. crystallium* by subjecting it to salt stress led to increased activity of the superoxide dismutase enzyme, which has antioxidant properties and catalyses the dismutation of superoxide radicals (H_2O_2).

In the remaining parts of this section, I shall examine how CAM and succulence help plants handle drought stress and how CAM influences stomatal patterning to reduce water loss.

1.3.1 How does drought tolerance benefit from CAM's relationship with succulence?

Succulence is an attribute that confers on a plant the ability to store significant amounts of water in tissues to use under drought conditions (Grace 2019). Succulence is a morphological adaptation used to limit drought stress and is an excellent example of convergent evolution in plants. Depending on the variation of some parameters, succulence can either exist as a cell form or as storage in plants (Griffiths and Males 2017; Grace 2019). Succulence can occur in plants' leaves, stems, roots, bulbs, and tubers, but the leaves and stems are the most common succulent part of plants (Ogburn and Edwards 2010; Males 2017). Some of the main features of succulence in plants include the ability to store large amounts of water in tissues for later use, a low surface area to volume ratio which provides maximum water storage volume and minimal surface area for transpirational water loss, thick cuticles, highly sensitive to environmental stimuli, and low hydraulic conductance (Ogburn and Edwards 2012; Griffiths and Males 2017; Grace 2019). The evolution of succulence in plants occurred continuously with varying diversity within the plant kingdom (perhaps up to 12,500 species) and existed in water-limited environments (Ogburn and Edwards 2010; Griffiths and Males 2017; Grace 2019). However, the role of succulence in promoting drought resistance in plants is not fully understood. This is because succulence is a complex syndrome rather than a simple trait and consists of several anatomical changes in plants (Males 2017).

Griffiths and Males (2017) and (Males 2017) identified CAM as the photosynthetic pathway integral to the ecophysiology of plants with succulent features but not the only pathway as some succulents make use of other photosynthetic pathways like the spatially-separated C4 pathway. However, CAM is the dominant photosynthetic mode in succulents due to the large vacuole required by CAM plants for storing organic acid produced during the nocturnal carboxylation process (Lüttge 2004). The relationship between CAM and succulence cannot be established because CAM is a very complex mechanism. Also, less information is available to fully explain the evolutionary connections between CAM, succulence, and biochemical activities (Males 2017). However, the process underpins nocturnal carboxylation and offers a way to relate the two processes (Males 2017). Furthermore, the nocturnal opening of stomata enhances water-use efficiency due to reduced leaf-air vapour pressure deficit; and provides the physiological conditions necessary for drought avoidance in storage succulence (Lüttge 2004; Males 2017).

1.3.2 Influence of Stomatal patterning on CAM's drought tolerance strategy.

The ability to resist drought stress and enhanced water-use efficiency has enabled the continued existence of CAM plants in arid, semi-arid, and marginal land where drought is an enormous challenge (Borland et al. 2009; Winter et al. 2015b; Yang et al. 2015b). Hence CAM is considered an ecophysiological adaptation to drought, which is achieved by reversing stomatal opening and opting for nocturnal carbon assimilation to gain a significant advantage over water stress (Lüttge 2008; Ceusters et al. 2016). To effectively achieve this feat, plants that use CAM photosynthesis have reprogrammed genes controlling stomatal behaviour to ensure that stomata remain closed during the daytime and thus reduce the rate of water loss via evapotranspiration (Yang et al. 2020). With evidence to show that C_3 stomatal genes show a rescheduled diel transcript expression to their CAM orthologues, this shows that reprogramming of stomatal genes is necessary for CAM plants (Niechayev et al. 2019).

Stomatal closure is one way plants respond to environmental stress like drought (Li et al. 2014; Ceusters et al. 2016). Because stomata play a strategic role in balancing carbon gain and transpirational water in plants, shutting stomata down is a logical strategy to mitigate the side effects of drought in plants, including shoot water loss (Visentin et al. 2020). This stomatal closure response is induced by the production of abscisic acid associated with the formation of reactive oxygen species like hydrogen peroxide (H_2O_2) and the promotion of the expression of genes linked to the drought response(Li et al. 2014).

The developmental stage when plants decide their stomatal density is not clear but there are suggestions that environmental stimuli like light can influence this (Feitosa-Araujo et al. 2020). Notwithstanding, another way plants respond to drought is to reduce their stomatal density (Caine et al. 2019). Reduced stomatal density is an attribute of most succulent plants and a critical patterning strategy for CAM plants which ensures high water storage capacity, low external surface area to volume ratio, and high water-use efficiency for CAM leaves (Borland et al. 2018). However, a lower stomatal density can lead to stomata with a large pore length (guard cell size) due to fewer spatial limitations (Barrera Zambrano et al. 2014). In C_3-CAM intermediates, however, no evidence of a salt-stress-induced transition from C_3 to CAM photosynthesis led to a significant reduction in stomatal density (Pereira et al. 2021; Heyduk et al. 2016). Therefore, the benefit of this patterning strategy is not only felt in CAM plants' ability to deal with the problem of drought; it also contributes to optimal performance in photosynthesis which can be measured using a parameter known as the stomatal pore index

(Sack et al. 2003; Bucher et al. 2016). The stomatal pore index (SPI) measures the influence of the number of stomata (stomatal density) present in the leaf of a plant and the size of its guard cell opening (pore length) on the efficiency of gas exchange (Bucher et al. 2016). This parameter is related to leaf hydraulic conductance correlated to photosynthetic rate across plant species (Brodribb et al. 2005). Since it is well known that drought can lead to plants altering the stomatal anatomy to cope with the stress, there is a possibility that SPI responds to changing abiotic conditions on both inter and intraspecific levels though the mechanism behind this is not well understood.

1.4 PEPC: regulation and phylogeny.

Phosphoenolpyruvate carboxylase catalyses the carboxylation of phosphoenolpyruvate to form oxaloacetate in CAM and C_4 plants (Nimmo 2000; Cushman 2001). PEPC is also involved in anaplerotic processes in plants performing CAM as well as C_4 and C_3 photosynthesis. An enzyme has an anaplerotic effect if it catalyses the replenishment of the tricarboxylic acid (TCA) cycle with C_4-dicarboxylic acids used for anabolic purposes, for example, amino acid biosynthesis in most plants and some bacteria (Peters-Wendisch et al. 1997). PEPC anaplerotic reactions are key to replenishing intermediates for the tricarboxylic acid cycle, malate formation in guard cells during the stomatal opening, nitrogen-fixing in legumes, and are also implicated in the growth of plants (Nimmo 2000; Sánchez et al. 2006; Edwards 2019).

1.4.1 PEPC activity in CAM photosynthesis.

Studies have shown that the circadian oscillator rather than light-dark transitions control carbon flux through PEP carboxylase in CAM plants (Nimmo 2000). PEPC is activated at night when the serine residue near the N-terminus of the protein becomes phosphorylated by phosphoenolpyruvate carboxylase kinase (PEPC-kinase) (Nimmo 2000; Taybi et al. 2004; Borland and Taybi 2004; Theng et al. 2007; Boxall et al. 2017). This process makes the enzyme sensitive (lowers the Km) to phosphoenolpyruvate (PEP) and positive effectors like glucose-6-phosphate and triose phosphate and less sensitive to malate inhibition (Borland and Taybi 2004). As the dark period ends, the role PEPC plays in CAM photosynthesis gradually reduces. The CO_2 captured overnight and stored as malate is actively involved in this process, and high malate content which builds up overnight is believed to feedback and curtail transcription of the PEPC kinase gene, which in turn leads to inactive PEPC (Borland et al, 1999) The main reason behind the involvement of malate in PEPC regulation is to avoid a

futile cycle between PEP and malate (Nimmo 2000; Borland and Taybi 2004). The deactivation of PEPC involves undergoing dephosphorylation, a process catalysed by the enzyme phosphatase 2A (PP2A), which renders PEPC sensitive to allosteric inhibition from malate (Nimmo et al. 1984; Nimmo 2000; Martín et al. 2011).

1.4.2 Regulation of PEPC enzyme.

PEPC activity is subject to regulations, just like most proteins found in living organisms. The essence of this regulation is to ensure temporal separation of PEPC's involvement in CAM photosynthetic activity as regards other key CAM enzymes (Dodd et al. 2002; Chomthong and Griffiths 2020). In CAM plants, the diel activity of the PEPC enzyme is achieved via two primary levels of regulation; a transcriptional level of regulation and a posttranslational level of regulation (Taybi et al. 2004; Chia-Yun et al. 2018; Taybi et al. 2017; Nimmo 2000; Theng et al. 2007). The transcriptional level of PEPC regulation involves regulating the amount of PEPC protein via the change in the abundance of the mRNA which encodes PEPC (Theng et al. 2007). The second level of regulation over the PEPC enzyme is a posttranslational level of regulation. This level of regulation occurs in the dark and involves the phosphorylation of the PEPC enzyme by phosphoenolpyruvate carboxylase kinase (PPCK) (Nimmo 2000). This level of regulation ensures the phosphorylated form of the enzyme is less sensitive to allosteric malate inhibition and drives nocturnal carboxylation, the key feature of the CAM process (Boxall et al. 2020; Chomthong and Griffiths 2020). In the CAM model plant *Kalanchoë fedtschenkoi*, three (3) isoforms of *KfePPCK* genes exist. Boxall et al. (2017) investigated genetically perturbing PPCK activity in CAM plants by silencing the *KfePPCK1* gene in *Kalanchoë fedtschenkoi* and reported that PPCK is essential for maximal and sustained dark CO_2 assimilation. The genetic perturbations in PPPCK also led to a loss of oscillations in the circadian clock feedbacks perturbing the central clock itself and further proved that the enzyme activity is a key component of the entire CAM process (Boxall et al, 2017).

1.4.3 Phylogeny of phosphoenolpyruvate carboxylase (PEPC) genes.

The independent emergence of CAM from the C_3 pathway incorporated the appearance of a similar phenotype in their distinct evolutionary lineages, a process described as convergent evolution (Yang et al. 2017). In *Kalanchoë* species for instance, the process that gave rise to CAM photosynthesis involved CAM genes achieving convergent evolution by either the convergence of protein sequence or the rewiring of diel gene expression from their C_3

orthologues (Yang et al. 2017; Shu et al. 2022). The functionally diverse and ubiquitous isoforms that encode PEPC in all plants serve as an important evolutionary starting point for the emergence of CAM photosynthesis (Cushman and Bohnert 1999; Silvera et al. 2014). PEPC belongs to a small gene family, and each isogene within the family encodes for a specialised function (Silvera et al. 2014). Phylogenetic analysis of plant PEPC genes revealed a single origin and later split into two forms; hence PEPC genes have two types based on their origin and diverse roles. The PTPC (plant-type) and the BTPC (bacterial-type) (Deng et al. 2016; Silvera et al. 2014; Shu et al. 2022). To investigate the convergent evolution of CAM PEPC genes from their C_3 orthologues, Shu et al. (2022) studied the 3D protein structure PTPC. This was done using the SWIS- MODEL server and showed that PTPC has three (3) templates of 3D protein structure which are: (a) 5vyj.1.A., (b) 3zgb.1.A, and (c) 5fdn.1.A structures respectively. C_4 PEPC proteins have the 3zgb.1.A 3D structure, CAM PEPC proteins has the 5vyj.1.A and 3zgb.1.A 3D protein structures, and C_3 PTPC has the 3zgb.1.A and 5fdn.1.A 3D protein structures respectively. These 3D structures were modelled using a SWIS-MODEL which integrated up-to-date protein sequence and structure database as the structural templates and showed the configuration of the PEPC protein (Shu et al. 2022). Aside from convergent evolution, the evolutionary history of PEPC genes also shows gene duplication and gene loss events (Shu et al. 2022). The diversity in function of *PEPC* genes in CAM plants suggests the presence of CAM-specific and house-keeping isoforms of the gene, and the CAM-specific isoform encodes the β-carboxylation of PEP to form oxalacetate by the PEPC enzyme (Dodd et al. 2002; Taybi et al. 2004; Silvera et al. 2014; Yang et al. 2017). Furthermore, house-keeping isoforms of PEPC genes in CAM plants are responsible for carbon-nitrogen interactions, seed formation and germination and stomatal regulation (Silvera et al. 2014; Christin et al. 2014; O'Leary et al. 2011; Deng et al. 2016).

Data collected from sequencing the entire genome of *K. fedtschenkoi*, a model CAM plant, showed the presence of five (5) PEPC genes (Shu et al. 2022; Yang et al. 2017). The key feature in the phylogeny of plant-type PEPC genes in *K. fedtschenkoi* is the presence of 5vyj.1.A and 3zgb.1.A 3D protein structure, with six (6) gene duplications and one (1) gene loss occurring as a result of whole-genome duplication events in their evolution (Shu et al. 2022). Of all the plant-type PEPC genes identified in *K. fedtschenkoi*, *KfePEPC1* and *KfePEPC2* have the highest diel transcript abundance, with *KfePEPC1* showing abundant transcripts throughout the light and dark periods while *KfePEPC2* showed abundant transcripts only in the dark period (Yang et al. 2017).

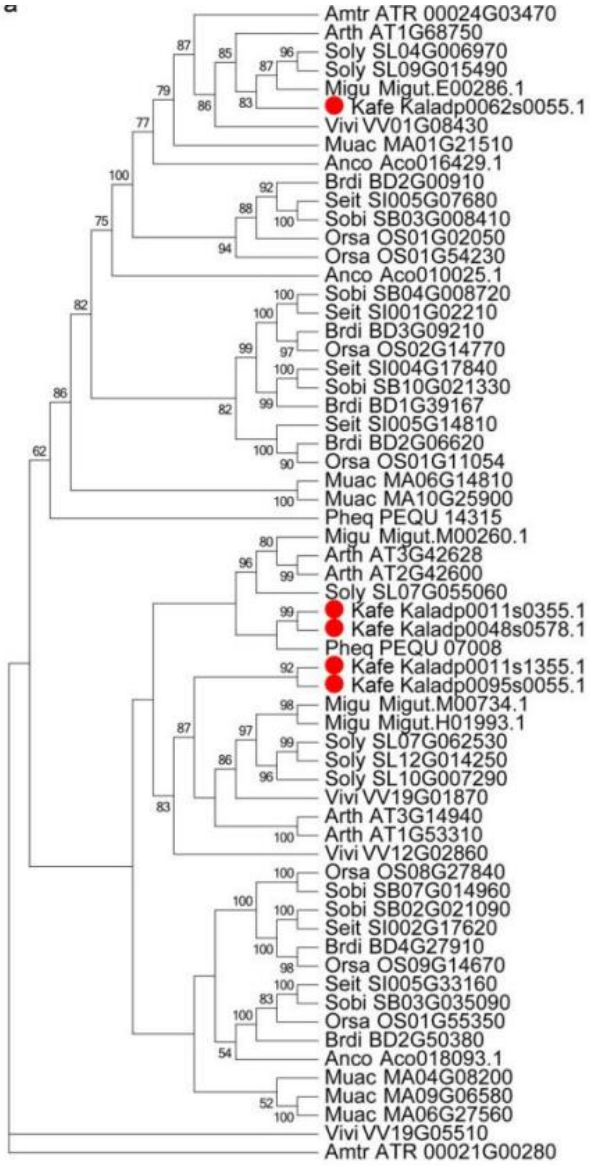

Figure 0.3. A maximum likelihood phylogenetic tree of the phosphoenolpyruvate carboxylase (PEPC) constructed from protein sequences. The *Kalanchoë fedtschenkoi KfePEPC* genes are identified with the red dots (Yang et al. 2017).

1.5 CAM Metabolites

The CAM pathway relies heavily on carbon supplied by metabolites like starch and soluble sugars. This reliance is evident in the carbon flux established from storing carbohydrates to malic acid at night and from malic acid to storing carbohydrates during the daytime (Christopher and Holtum 1996). The primary role of metabolites is to provide substrates like phosphoenolpyruvate (PEP) used in the CAM process and serve as sinks for carbohydrates needed for plant growth (Borland et al. 2016a; Ceusters et al. 2009). Studies have shown that

an optimised system of carbon supply and demand in CAM is crucial to the effective running of the CAM pathway and maintaining the plastic nature of the whole process (Taybi et al. 2017). Carbon supply is a major limiting factor to dark CO_2 uptake, the storage carbohydrate source notwithstanding (Ceusters et al. 2009). This is also important in explaining the comparable and even higher productivity level observed in CAM plants to their C_3 counterparts due to the sufficient supply of exportable carbon needed for growth (Ceusters et al. 2009; Shameer et al. 2018; Lüttge 2004). CAM plants can be divided into two groups based on the carbohydrate storage type they adopt (a) starch and glucans storing group and (b) soluble sugars storing group (Christopher and Holtum 1996).

For CAM plants in the starch and glucan storing group, starch is their primary carbon source and, by extension, the carbohydrate store of higher plants (Borland et al. 2016a; Christopher and Holtum 1996). This carbon source exists as transitory starch formed as a product of the Calvin cycle and broken down at night to provide the three (3) carbon CO_2 acceptor PEP for nocturnal carboxylation (Dodd et al. 2002; Taybi et al. 2017; Weise et al. 2011). This diel change in the starch level is a critical feature of CAM photosynthesis (Weise et al. 2011). Starch degradation is essential to the entire CAM pathway (Borland et al. 2016a). There are two known starch degradation pathways, (i) the hydrolytic pathway, which involves the use of a β-amylase enzyme, mainly plastidic BAM3 and disproportionating enzymes (DPE1) to catalyse the breakdown of starch to maltose and glucose, and (ii) the phosphorolytic pathway, which involves α-glucan phosphorylase 1 (PHS1) catalysing the nocturnal breakdown of starch to produce glucose 1-phosphate (Ceusters et al. 2021b). Most CAM plants adopt the phosphorolytic pathway of starch degradation (Ceusters et al. 2021b). The final product of this process, glucose-6-phosphate (G6P), undergoes glycolysis to produce PEP providing ATP via substrate-level phosphorylation to offset the energetic cost of the CAM cycle (Shameer et al. 2018). C_3 plants, on the other hand, adopt the hydrolytic pathway with studies on the starch breakdown in *Arabidopsis thaliana* showing that maltose and glucose as the major products exported from the chloroplast at the end of the process (Stitt and Zeeman 2012; Fulton et al. 2008).

CAM plants that fall within the soluble sugar storing group, soluble sugars such as glucose, fructose, and sucrose and be a source of carbon input and a carbohydrate store (Ceusters et al. 2009; Christopher and Holtum 1996). These plants accumulate soluble sugars in their vacuoles and extrachloropastic compartments (Christopher and Holtum 1996).

1.6 CAM molecular genetics and bioengineering.

The evolution of the CAM pathway is strongly believed to have occurred from the C_3 pathway with evolution operating on an already existing low flux pathway for amino acid metabolism (Bräutigam et al. 2017). Not much has been known about how plants genetically and metabolically evolved from C_3 to CAM until recently, even though there is a good understanding of carbohydrate turnover, starch cycling, and other enzymatic mechanisms in CAM plants (Chen et al. 2002; Dodd et al. 2002). Recently, studies have started to emerge that are helping to understand further how this transition from C_3 to CAM happened. For example, current knowledge from studying *Yucca* species which show both C_3 and CAM now opine that ancestral patterns required for CAM may have pre-dated the actual emergence of CAM in this plant genus despite differences in transcript profiles, metabolite profiles and shared time-structured expression of CAM genes in both CAM and C_3 *Yucca* species (Heyduk et al. 2021). An ancestral pattern of low flux was observed in C_3 plants that enable the synthesis of amino acids using organic acids. This led to the suggestion that to establish CAM, this flux capacity was increased in the existing C_3 carboxylation pathway without the need to rewire or day/night change in the schedule of carboxylating enzymes (Bräutigam et al. 2017; Heyduk et al. 2019).

1.6.1 CAM molecular genetics

Model systems have been developed in recent times to further gain vital knowledge into the inner workings of the CAM pathway. These systems all have one in common: adopting functional genomics approaches to deliver significant advances in understanding CAM's genetic blueprint (Hartwell et al. 2016). In addition, some CAM plants have had their transcriptome and genome sequencing. For example, a high throughput transcriptome sequencing study of *Agave tequilana* and *Agave deserti* has been done to understand how both species evolved significant drought tolerance abilities (Gross et al. 2013). For the Clusiaceae family, a restriction site-associated sequencing of 64 species providing more insight into the evolution of CAM in *Clusia* suggested that ancestrally, CAM evolved about four times in *Clusia* (Luján et al. 2021). Also, the sequencing of genomes of two CAM monocot plants, pineapple (*Ananas comosus*) and moth orchid (*Phalaenopsis equestris*), using a high-throughput DNA sequencing technique, confirmed the transition from C_3 photosynthesis to CAM, diel expression of CAM-related genes and possible involvement of gene duplication in the evolution of CAM photosynthesis (Cai et al. 2015; Ming et al. 2015).

However, there is recent interest in molecular studies of CAM plants of the genus *Kalanchoë* which have seen potential to provide further insights into the building blocks of CAM (Hartwell et al. 2016; Yang et al. 2017). The model CAM plant, *Kalanchoë fedtschenkoi* which had its sequence published by Yang et al. (2017), marked a very significant milestone in the molecular studies of CAM photosynthesis. It was the first time an obligate eudicot CAM plant genome was fully sequenced, and this has contributed immensely to the understanding of the convergent evolution of CAM genes from C_3 orthologs, as well as key genes implicated in the processes such as nocturnal CO_2 uptake, stomatal movement, heat tolerance, circadian clock operation and carbohydrate metabolism.

Following the success of various sequencing projects, there have been various investigations into the functional involvement of some genes in the CAM pathway by genetically altering their abundance in plants. A range of biotechnological tools has been developed to enable genomic manipulation so that it is now possible to gain in-depth knowledge of a range of different genes in CAM (Liu et al. 2016). Tools such as RNA interference (RNAi) and, most recently, CRISPR-Cas9 gene-editing techniques have been used to create mutant genotypes of obligate and facultative CAM plants with suppressed expression of the genes of interest (Boxall et al. 2017; Liu et al. 2019a; Boxall et al. 2020; Dever et al. 2015).

Dever et al. (2015) reported that silencing the expression of *KfeNAD_ME_b1* and *KfePPDK* genes significantly affected malate decarboxylation in *K. fedtschenkoi*. This adverse effect is due to perturbing the activities of the NAD-malic enzyme and pyruvate orthophosphate dikinase (PPDK) enzyme. This genetic manipulation also affected the circadian regulation of PEPC phosphorylation during the dark period and led to the mutants fixing their CO_2 during the light period. This observation confirmed the essential roles of NAD-ME and PPDK in underpinning secondary CO_2 fixation in CAM plants. Boxall et al. (2017); Boxall et al. (2020) observed the importance of PPCK and PEPC enzymes in the CAM pathway by creating mutant genotypes with suppressed expression of *KfPPCK1* and *PPC1* genes in *K. fedtschenkoi* and *K. laxiflora* respectively using RNAi. Their results showed that suppressing the diel expression of the *KfePPCK1* gene led to a 66% reduction in the amount of nocturnal CO_2 fixed, reduced malate accumulation at dawn and decreased nocturnal starch turnover. Suppressing the diel expression of the *PPC1* gene led to total loss of nocturnal CO_2 fixation and a switch of daytime CO_2 fixing, reduction in malate accumulation, and the loss of daytime stomatal closing ability. This observation will be tested in this work with CRISPR-

Cas9 mediated *Kfepepc1* mutants of *K. fedtschenkoi*. Liu et al. (2019a) investigated the role of blue light receptor Phototropin 2 in the CAM activity of *K. fedtschenkoi* by knocking out the *KfePHOT2* gene using the CRISPR-Cas9 loss of function technique. This mutation reduced stomatal conductance and CO_2 fixation in the late afternoon (phase 4 of CAM photosynthesis) and increased stomatal conductance and CO_2 fixation during the dark period (phase 1 of CAM photosynthesis). Ceusters et al. (2021b) studied the process of re-routing chloroplastic starch degradation from the amylolytic route to the phosphorolytic route to provide PEP substrate for nocturnal carboxylation. To achieve this, RNAi was used to suppress the diel expression of the *KfePHS1* gene hence perturbing the activity of α-glucan phosphorylase (PHS1) enzyme in *K. fedtschenkoi*, generating *kfephs1* mutants. This mutation reduced nocturnal starch degradation and dark CO_2 uptake, reduced water-use efficiency, and stunted growth in the *kfephs1* mutants. This study confirmed that in *K. fedtschenkoi* phosphorolytic starch degradation is preferred in CAM plants to degrade chloroplastic starch and provide PEP for nocturnal carboxylation.

1.6.2 How to tackle CAM bioengineering

With what is known about the possible candidate genes for CAM and the quest to bioengineer CAM photosynthetic machinery into C3 plants, there is a need to develop an informed approach to tackle CAM bioengineering. Presently, limitations to CAM engineering include technical challenges arising from a lack of robust biosystem design capabilities for reconfiguring signalling and metabolic pathways in plants (Yuan et al. 2020). However, two approaches have emerged for the genetic improvement of complex organisms such as plants, microbes and animals which are (1) biosystems design and (2) synthetic biology, which is based on genome editing (Yang et al. 2019; Yuan et al. 2020; DePaoli et al. 2014).

The biosystem design approach to CAM bioengineering adopts a Design-Build-Test-Learn (cycle), which involves four phases. These phases are (I) bio-designed genetic circuits and assembly of multigene constructs, (II) delivery of designed devices, (III) plant engineering, and (IV) evaluation of engineered plants (Yuan et al. 2020). This approach ensures that with the identification of the genes required for the engineering; these genes are correctly assembled and provide a solution to the problem of deploying more complicated genetic circuits caused by experimental bottlenecks and sloe generation of plants by using protoplast based and *Agrobacterium*-mediated leaf infiltration transient expression to analyse transgene expression and subcellular protein localisation quickly (Zhang et al. 2011; Yuan et al. 2020).

In delivering the genes into the plant cells, the approach avoids conventional methods such as the physical and chemicals. Instead, it adopts a novel method which can stably stack multiple genes within *Agrobacterium* virulence plasmid Transfer -DNA (Yuan et al. 2020). This method is called Gene Assembly in *Agrobacterium* by Nucleic acid Transfer using Recombinase technologY (GAANTRY) and has been used to generate transgenic potato plants (McCue et al. 2019). For phase three (3) of this approach, tissue culture-based plant transformation is avoided because the process is not suitable for many plants, is time-consuming with low efficiency, and can cause genetic and epigenetic changes. Instead, generating gene-edited dicotyledonous plants via de novo meristem induction is used without in vitro cultures (Maher et al. 2020). Finally, to evaluate the performance of the process, the biodesign approach uses a combination of omics (genomics, transcriptomics, proteomics, metabolomics, and fluxomics) to ensure it is done quickly and efficiently (Yuan et al. 2020).

Just like the biosystem approach, the synthetic biology approach to CAM engineering favours a process where relevant CAM genes can be introduced to C_3 plants together rather than moving them individually. In addition, it uses an advanced computational approach that utilises experimental data from the analysis of genes or proteins to group them into dynamic network models, which can be tested and validated using synthetic biology tools (DePaoli et al. 2014). Synthetic biology provides a system for validating the computational modelling of photosynthesis and provides an experimental toolbox for realising computational designs through multigene engineering in plants (DePaoli et al. 2014). The synthetic biology approach would involve the construction of the synthetic network, targeted protein degradation, and transferring the network to the host organism.

.

1.7 CRISPR-Cas9: an efficient genome editing system

Accurately targeting and editing genes is essential to engineering crops genetically and investigating functional genomic analysis in plants (Xing et al. 2014). In the quest to achieve this goal, techniques like transfer DNA (T-DNA) insert, physical and chemical mutagens, and RNA – interference (RNAi) has been developed to successfully manipulate genes by introducing mutations that either suppress or promote the function of genes of interest. However, RNAi has a few drawbacks that include incomplete loss of function and extensive off-target activities (Liu et al. 2016; Liu et al. 2019a). Nevertheless, these techniques have been pivotal in investigating the molecular basis of CAM photosynthesis to provide a clear

understanding of how CAM plants underwent convergent evolution from their C_3 ancestors, in-depth operations of the circadian clock vis-á-vis regulation of genes involved in CAM, and enzyme kinetics of key enzymes like PEPC, and PPCK (Abraham et al. 2016; Borland and Taybi 2004; Yang et al. 2017; Cushman 2001). Zinc finger nucleases (ZFNs) and TAL effector nucleases were recently developed as solutions to the problems encountered in tRNAi, but protein design, synthesis, and validation problems hindered the effective adoption of these techniques (Doudna and Charpentier 2014; Xing et al. 2014). Eventually, a novel approach with massive potential to unlock several opportunities that seemed impossible in the past has emerged. This novel approach is the clustered regularly interspaced short palindromic repeats and the CRISPR-associated protein 9 (CRISPR-Cas9).

CRISPR-Cas9 is a defence mechanism adopted by many bacteria and archaea species against bacteriophage infections and plasmid transfer (Liu et al. 2016; Jiang and Doudna 2017). This defence mechanism is an adaptive RNA-guided immune system encoded by a CRISPR locus that enables Cas genes to provide acquired immunity against bacteriophage infection and plasmid transfer (Jiang and Doudna 2017). The CRISPR system is grouped into six (6) types (I-VI), and the type adopted for genome editing research is type II (Jiang and Doudna 2017). Type II CRISPR system derived from *Streptococcus pyogenes* consists of three (3) genes, one encoding for Cas9 nuclease and two non-coding RNA genes (Xing et al. 2014). It employs a single DNA endonuclease, Cas9, to identify dsDNA substrates and causes a double-strand break by cleaving each strand at a specific site with a distinct nuclease domain (HNH or RuvC). DSB introduces a mutation via a pathway known as non-homologous end-joining (NHEJ), which is error-prone (Xing et al. 2014; Liu et al. 2016; Liu et al. 2019a). This thesis will use CRISPR-Cas mutants of *K. fedtschenkoi,* which colleagues created at the Oak Ridge National Laboratory in the USA.

The *KfePEPC* mutants used for this study were created by colleagues at the Oak Ridge National Laboratory, TN, USA using a method described by (Zhang et al. unpublished). The single guide RNAs (sgRNAs) targeting the *KfePEPC1* and *KfePEPC2* genes, respectively, were designed using the sgRNAcas9 software. First, the Gibson Assembly method was used to assemble the CRISPR-Cas9 vectors. This process involved using an isothermal, single-reaction to assemble multiple overlapping DNA molecules by the concerted effort of a 5'exonuclease, a DNA polymerase and a DNA ligase (Gibson et al. 2009). Next, the assembly were transformed into the *Agrobacterium tumefaciens* strain GV3101. The transformants

were selected via their ability to resist kanamycin. Finally, the T1 plants were screened using the Sanger sequencing method to confirm the success of the knockdown.

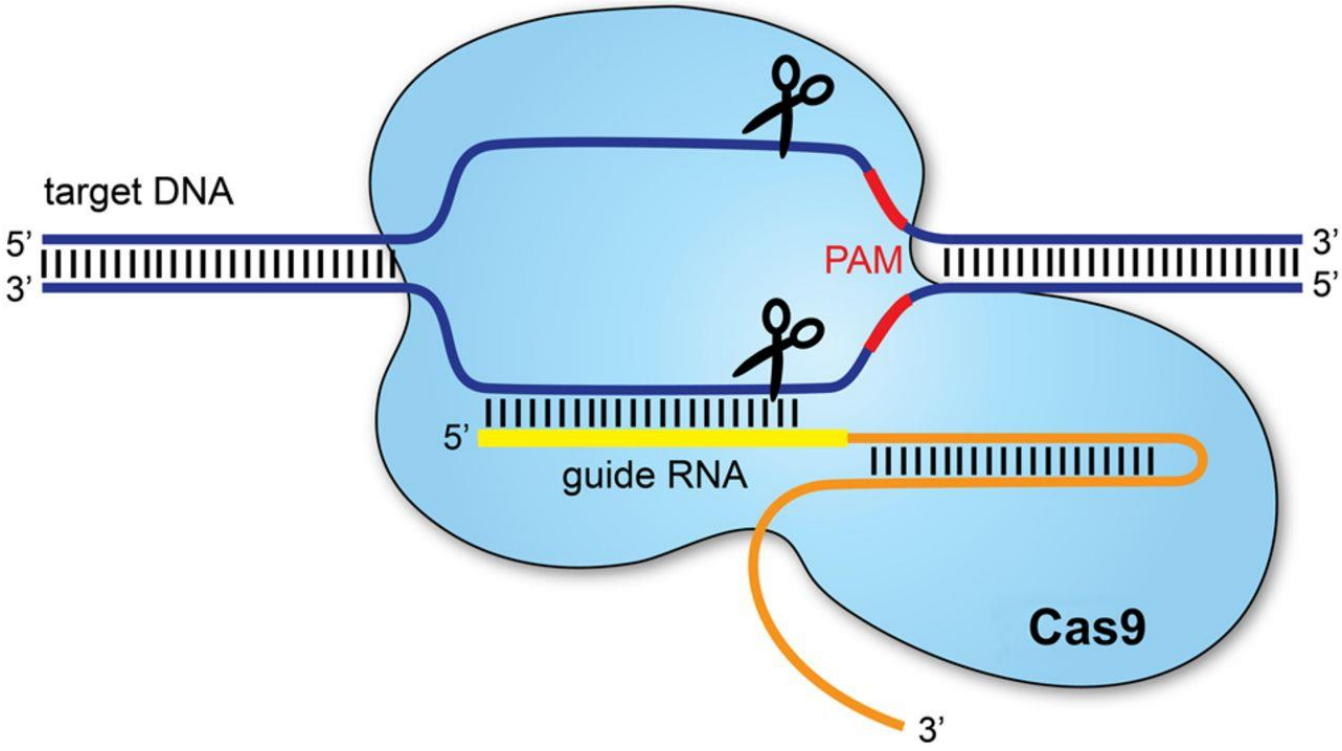

Figure 0.4. Schematic diagram of the CRISPR-Cas9 loss of function technique. Cas9 protein is directed to its target by a section of RNA called a synthetic single-guide RNA (sgRNA). The section of RNA which binds to the genomic DNA is 18–20 nucleotides with a specific sequence of DNA of between 2 and 5 nucleotides called a protospacer adjacent motif (PAM) lying at the 3' end of the guide RNA for the DNA cut to happen (Redman et al. 2016).

1.8 Biology of *Kalanchoë fedtschenkoi*

Kalanchoë fedtschenkoi Hamet et Perr 'Marginata', the model plant used for this study, is a eudicot and an obligate CAM plant that belongs to the family Crassulaceae. The species was named after Boris Alexjeewitsch Fedtschenko of the Imperial botanical garden in St Petersburg, Russia (Smith et al. 2019).

The plant is native to Madagascar, where it has the most extensive species diversity, Brazil and a few tropical areas in Asia and Africa (Hartwell et al. 2016; Abdel-Raouf 2012). The genus *Kalanchoë, to* which the plant belongs, comprises 125 species, with close to half (60) of them found in Madagascar alone. These species are divided into three (3) groups namely (a) Kitchingia, (b) Bryophyllum, and (c) Eukalanchoe (Hartwell et al. 2016; Gehrig et al. 2001). The plant is terrestrial with a perennial life cycle and has a growth habit classified as a

shrub (Descoings 2006; Oloyede et al. 2007). The leaves are simple, ovate, cuticular, succulent, amphistomatous, densely packed and numerous (Oloyede et al. 2007; Abdel-Raouf 2012). It grows up to 75cm tall, with thin green to greenish-purple stems from when young to brown when matured (Smith et al. 2019). Reproduction for the plant is vegetative and asexual. Detaching the leaf from the plant causes the leaf margins to form bulbils within the depressions between the crenations and the plant flowers between June and September, peaking around August (Smith et al. 2019).

Apart from being used for scientific studies, there are other potential uses of the plant, most commonly as ornamentals to beautify homes, gardens and parks (Oloyede et al. 2007).

1.9 Aims and objectives

1.9.1 Aims of the study.

The publication of the *Kalanchoë fedtschenkoi* genome (Yang et al 2017) and the ease of genetic transformation of this species (Hartwell et al, 2016) present the opportunity to investigate the roles of various genes implicated in the CAM pathway of this model CAM plant. Our colleagues at Oakridge national laboratories in the United States of America recently created mutants of *K. fedtschenkoi* where *KfePEPC1* (kaladp0095s0055.1) and *KfePEPC2* (Kaladp0048s0578.1) genes have been knocked down singly and in combination using a novel CRISPR-Cas9 loss of function technique. Our aim in this study is to conduct physiological and biochemical analyses for independent lines of each of these mutated genes and thereby establish the physiological roles of PEPC1 and PEPC2 in *K. fedtschenkoi*.

1.9.2 Objectives of the study.

Objective 1: Investigate the effect of knocking down *KfePEPC1* and *KfePEPC2* genes on the biochemistry of C_3 and β-carboxylation in *K. fedtschenkoi.*

Objective 2: Investigate the effect of knocking down *KfePEPC1* and *KfePEPC2* genes on the CAM physiology and leaf gas exchange properties of *K. fedtschenkoi.*

Objective 3: Investigate the effect of knocking down *KfePEPC1* and *KfePEPC2* genes on the growth and drought tolerance ability of *K. fedtschenkoi*.

Chapter 2 Material and methods

2.1 Plant material

Kalanchoë fedtschenkoi, a CAM model plant (Yang et al. 2017), was used for experiments carried out in this study. Our colleagues at Oakridge National Laboratories, United States of America, used the CRISPR-Cas9 loss of function technique to generate plants deficient in *KfePEPC1* and *KfePEPC2* with two independent transformations for each gene. In addition, two transformations were made for *KfePEPC1* and *KfePEPC2* together to generate double mutant lines, respectively.

The wildtype and mutant lines were propagated vegetatively by placing older leaves (leaf pair 10, numbered from the growing tip) in a propagating tray filled with vermiculite, covered with a transparent lid and placed in a growth room for up to 8 weeks with a 12-h photoperiod. Once the plantlets formed around the edge of the leaves and produced roots, they were transferred to the soil. For the transfer to soil, the soil mixture used contained John Innes No. 2 soil-based compost, perlite, sand and chopped barks at a ratio of (3:2:1:1).

Leaf pair 8 (counting from the top of the plant) was used because the leaves were matured and could do CAM to measure net CO_2 uptake and stomatal conductance (gas exchange). At the same time, for biochemical and molecular assays, leaf-pair seven (7) were collected, wrapped, labelled correctly in foil, snap-frozen in liquid nitrogen and stored in a -80 ^{o}C freezer till needed.

Figure 2.1. *Kalanchoë fedtschenkoi* CAM model plant for the study. (a) Wildtype, (b) *kfepepc1* Line 1 mutant, (c) *kfepepc1* Line 2 mutant, (d) *kfepepc2* Line 1 mutant, (e) *kfepepc2* Line 2 mutant, (f) *kfepepc1/2* Line 1 mutant, and (g) *kfepepc1/2* Line 2 mutant respectively. Three biological replicates of each phenotype were used for all the sampling.

2.2 Plant growth analysis

The protocol for plant growth analysis involved the measurement of several parameters, including plant height, fresh/dry weight of shoots and roots, leaf area, and the number of leaves.

The height of the wildtype and mutant *Kalanchoë fedtschenkoi* was determined using a procedure described by Martin et al. (2012). A meter rule was used to measure the height from the soil surface to the tip of the uppermost fully developed leaf extended vertically for each plant.

The fresh weight of the samples was determined by uprooting different plants from the wildtype and mutant strains of the plant, washing the roots with water to remove the soil particles, carefully cutting the root out from the shoot, and weighing them separately taking

note of the weight. In contrast, the dry weights will be determined after drying the samples in a 70°C oven for 48 hours, after which the dried stock (shoot and root) was weighed, and the weight was recorded.

The number of leaves was measured by physically counting and recording the number of leaves on the plants every week for six (6) weeks. All the growth analysis data were collected and presented as an average of three biological replicates.

The leaf area was measured by detaching all the leaves of the plants and taking a photograph of the leaves. ImageJ software 1.46r (Java 1.6.0_20, 64-bit http://imageJ.nih.gov/ij) was used to sketch each leaf's outline and calculate the total leaf areas of 3 biological replicates of each genotype.

2.3 Gas exchange analysis

Photosynthetic activity and gas exchange of the plants was assessed by measuring net CO_2 uptake (µmol m^{-2} s^{-1}), stomatal conductance (mmol H_2O $m^{-2}s^{-1}$) and transpiration rate (mmol m^{-2} s^{-1}). Three biological replicates of each genotype were measured over a 24-hr light/dark cycle using the LI-6400XT Portable Photosynthesis System (LI-COR® Biosciences). Fully expanded leaves of age eight were clamped into the leaf chamber fluorometer, supplied with a LED light source and a temperature sensor. The ambient CO_2 concentration was set at 400 µmol CO_2 mol^{-1} air, and the light and temperature were set to track the conditions established in the growth chamber where the assay was conducted (day/night temperature of 25°C/19°C) and a diurnal photosynthetic photon flux density (PPFD) of 250 µmol $m^{-2}s^{-1}$ at plant height). Relative humidity was maintained at 50 and 60% to avoid any condensation that could potentially damage the LiCOR machine or affect readings. The data were recorded every 15 minutes and were plotted against time. The data are presented as the average of three biological replicates for each genotype. The instantaneous water–use efficiency was calculated by calculating the ratio of integrated CO2 uptake and integrated water loss from the transpiration rate over 24 hours. The integrated CO_2 uptake and transpiration rates were calculated by measuring the area under the diel leaf gas exchange curve at three-time points at night and during the day. The data were presented as the average of three biological replicates for genotype (wildtype and mutant lines).

2.4 Titratable acidity measurement.

Leaf pairs 7 and 8 numbered from the tip of the plant were sampled over a 24-hr period. These samples were collected at six (6) time points every four (4) hours, wrapped in foil, labelled correctly, snap-frozen in liquid nitrogen and stored in a -80 ^{o}C freezer. Approximately 300mg of the frozen powdered leaf was weighed into a 2 ml Eppendorf tube. 0.9 ml of 80% methanol was added and heated at 60^{o}C for 40 minutes. The mixture was centrifuged at 13,000 rpm for 10 mins, the supernatant was retained for titratable acidity and soluble sugar analyses, and the pellets were retained for starch analysis.

For titratable acidity analysis, 200 µl of the extract, 2ml of distilled water and three (3) drop of phenolphthalein was added to a beaker and titrated against 0.005M NaOH until the solution forms a uniform pink colour.

$$\text{Titratable Acidity } (H^{+}\ g^{-1}\ \text{fwt}) = \left(\frac{(NaOH\ titre \times 0.005)/0.2) \times 2) \times 1000))}{fwt}\right)$$

Equation 2.1. Titratable acidity calculation. NaOH titre is the difference between the initial and final levels of NaOH used for the titration. Fwt is the fresh weight of the tissue.

2.5 Soluble sugar and starch analysis.

The phenol–sulphuric acid described by Dubois et al. (1956) was used to measure the soluble sugar contents of methanol extracts. A standard curve was required to calculate the soluble sugar concentration of the extract and was prepared using a glucose standard of known concentration. Exactly 50 µl of the methanol extract and 450 µl of distilled water were added together in a glass tube and taken to a fume hood. In the fume hood, 0.5 ml of 5% phenol and 2.5 ml of concentrated sulphuric acid were added to the mixture, stirred with a glass rod, and cooled for 15 minutes. The absorbance of samples was measured at 483nm compared with the glucose standard to determine the concentration of soluble sugars (as glucose equivalents).

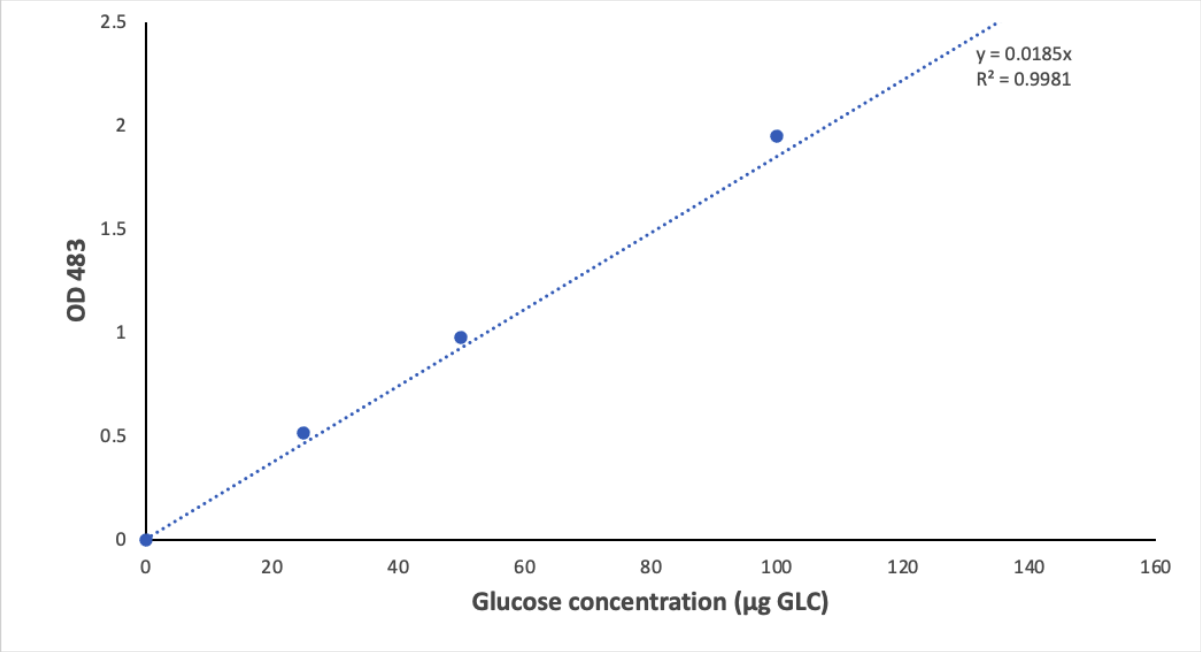

Figure 2.2. A glucose standard curve was used to measure the soluble sugar concentration of the plant extracts. The standard curve was prepared by measuring the absorbance of glucose standards with known concentrations.

The pellets retained after the methanol extraction were washed twice in distilled water, and 1.5 ml of 0.1M acetate buffer was added to the tube and placed in a water bath at 90ºC for 1 hr to allow the starch to gelatinize, and tubes were then allowed to cool. Exactly 0.3ml of 300-unit amyloglucosidase enzyme was added to the tube and incubated for 24 hours in a water bath at 45ºC to enable the enzyme to digest all the starch to glucose. The sample was removed from the 45 ºC water bath and microfuge at 13,000 rpm and 5ºC for 5 mins. Exactly 50µl of the digested sample and 450µl distilled water were added together in a test tube and placed in a fume hood. In the fume hood, 0.5ml of 5% phenol and 2.5ml of concentrated sulphuric acid were added to the mixture, stirred with a glass rod and allowed to cool for 15 minutes. The absorbance was measured at 483nm, and the values were recorded and read against the glucose calibration curve as described above. The starch content was calculated as the glucose equivalent of extracts with the formula below:

Starch content (µl Glc Equiv g^{-1} fwt) = $\left(\frac{\left(\frac{A}{G}/180\right)\times DF)}{fwt}\right)$

Equation 2.2. Calculation of glucose equivalents from starch degradation in leaf tissue. A is absorbance, G is the gradient of line calculated from the calibration curve, DF is the dilution factor (volume of the sample divided by the total volume of enzyme suspension in acetate buffer), and fwt is the fresh weight of tissue.

2.6 Phosphoenolpyruvate carboxylase (PEPC) extraction/activity assay, malate sensitivity, and protein assay.

PEPC enzyme activity was measured using the biochemical activity assay described by Borland and Griffiths (1997). Extraction of the enzyme was carried out in a cold room at 5 ^{o}C. Exactly 0.6 g of leaf tissue which was collected four hours into the photoperiod or four hours after dark, was blended in a grinding mortar with 1.5 ml of the extraction buffer [200mM Tris-base (pH 8.0), 2mM EDTA, 20% (w/v) PEG 20,000, 1mM dithiothreitol, 1mM benzamidine, 350mM $NaHCO_3$] and 0.05g of PVPP. The extract was strained through 2 layers of muslin and then centrifuged for 1 min at 13,000 g before desalting.

Extracts were desalted on a Sephadex G-25 M column using an elution buffer [100mM Tris-base (pH7.5), 1mM dithiothreitol, 1mM benzamidine, 5% (v/v) glycerol]. The extract was eluted through the column at 5^{o}C and collected for subsequent activity assay.

For measuring PEPC activity, the reaction was initiated by the addition of 100 µL desalted extract to 850 µL assay cocktail [65mM TRIS-base (pH7.8), 0.2 mM NADH, 10mM $NaHCO_3$, 5mM $MgCl_2$, and 2mM PEP]. PEPC activity was measured on a spectrophotometer at 340 nm as the rate of NADH consumption over 5 min with the reaction held at 30 ^{o}C. To assess the impact of malate inhibition on PEPC activity, exactly 50µL of 0.2M malate standard was added to 850 µL of the assay cocktail. The reaction was started by adding 100 µL of the extract to the cocktail. Malate sensitivity of PEPC was determined spectrophotometrically at 340 nm as the percentage inhibition of the reaction with and without malate over five minutes.

The Bradford (1976) method was used to measure the protein content of the extracts. A calibration curve of protein standards 0-140 µg was prepared from stock Bovine serum albumin (BSA). Stock BSA was prepared by dissolving 0.2g BSA in 100 ml water and then blended to give six (6) concentrations ranging between 0-140 µg protein in separate test

tubes. From each test tube, 0.1 ml of the solution was added to 4 ml of Bradford reagent made up of 100 mg of Coomassie Brilliant Blue G, 50 ml of 95% ethanol and 100 ml of 85 % orthophosphoric acid were mixed thoroughly. After 15 minutes, the absorbance was read to determine the protein concentration at 595nm. A protein calibration curve (Figure 2.3) was used to determine the concentration of protein standard. The protein content in the extracts used for the PEPC assays was measured by adding 100µL of the desalted extract to a cuvette, and then 4 ml of Bradford reagent was added and mixed thoroughly. After 15 minutes, the absorbance was read to determine the protein concentration at 595nm using the protein calibration curve.

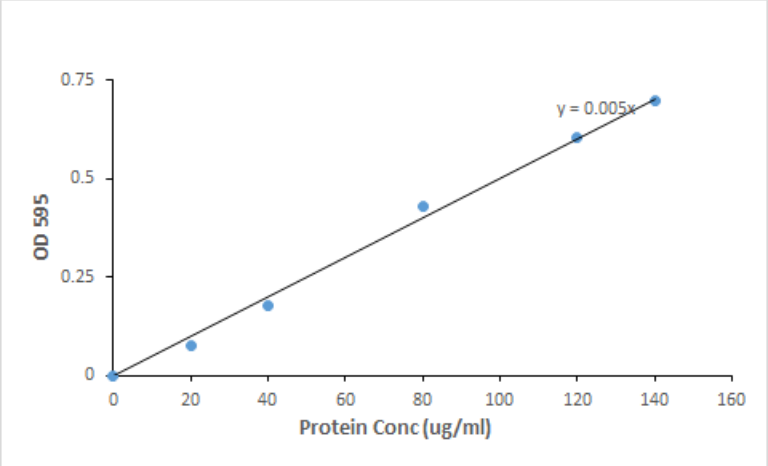

Figure 2.3. Calibration curve for protein standard. The calibration curve was designed by measuring the protein concentration of bovine serum albumin.

2.7 Western blotting.

Western blot is an essential and useful technique employed to examine the relative abundance of specific proteins in biological samples (Eaton et al. 2013). This study used the western blotting technique to determine the relative abundance of the PEPC, RuBisCO and RuBisCO activase proteins in the wildtype and the PEPC mutant lines of *Kalanchoë fedtschenkoi*. The results gave an insight into how knocking down the *KfePEPC1* and *KfePEPC2* genes impacted the abundance of the proteins screened. The Western blotting technique involves four steps, namely:

- Total protein extraction
- SDS electrophoresis

- Semi-dry blotting
- Antibody incubation and dictation

2.7.1 Total protein extraction

Exactly 500 µl of chilled extraction buffer (450 mM bicine pH 10.3, 50 mM CAPS, 1 % PEG 20,000), 25 µl of 1M DTT and 50 µl of 10% SDS was added to precisely 0.2g of snap-frozen and pre-ground leaf tissue in a labelled, frozen, and pierced Eppendorf tube. The extract in this tube was quickly snap-frozen in liquid nitrogen and then allowed to thaw on ice. The thawed sample was spun at 10,400 g for 10 min 30 sec at 4ºC. Exactly 350 µl of supernatant was added to a clean Eppendorf tube, and then 650 µl of ice-cold 80% acetone was added to the same Eppendorf tube on ice. The tube was quickly snap-frozen in liquid nitrogen and allowed to thaw on ice. The thawed samples were centrifuged at 10,400 g 7 min30 sec at 4ºC. The supernatant was discarded, and the pellets formed were resuspended in 100 µl of 4x SDS Lamelli Buffer (0.189g of Tris base, 2.5 ml of glycerol, 12.5 ml of 10% SDS, 1.25 ml of mercaptoethanol, and 3 ml of 0.02 % bromophenol blue)., the samples were incubated in a shaker at 60ºC for 20 minutes to aid resuspension of pellets and then stored at -80ºC. Before loading samples onto SDS page gel, the samples were re-incubated in a shaker at 60C for 20 minutes.

2.7.2 SDS electrophoresis

The SDS page gel used for the electrophoresis consisted of two gels, a stacking gel and a separating gel. Two clean glass plates were stacked together and held firmly with a casting frame to make the gel. A 15% separating gel was made by mixing 9.4ml of distilled water, 6.5ml separating gel buffer (3M Tris/HCL pH 8.8), 0.3ml 10% (w/v) SDS, 16.2ml 30% Acrylamide/bisacrylamide, Rotiporese 30. In comparison, 300 µl of 10% ammonium persulphate (APS) and 16µl of tetramethylethylenediamine (TEMED) were added last as hardeners. The mixture was poured into the plate cast, leaving enough space for the stacking gel mixture, and allowing for approximately 30 minutes to set before pouring the stacking gel. A 4% stacking gel was made by mixing 5.6ml of distilled water, 2.5ml of stacking gel buffer (0.5M Tris/HCL pH 6.8), 0.1ml of 10% (w/v) sodium dodecyl sulphate (SDS), 1.7ml 30% of Acrylamide Rotiporese 30, and 10µl of 2.5% Bromophenol blue, while 300µl of 10% APS, and 6µl of TEMED was added last to harden the mixture. The mixture was poured into a glass plate to fill it up, and the comb was immediately added to create the wells on the gel.

The gel was made to stand for approximately 1 hour to allow complete polymerization at room temperature.

The total protein extracts from the wildtype and PEPC mutant lines were loaded into an SDS page gel mounted in a cassette and placed in a Bio-rad mini-PROTEAN vertical electrophoresis system. The gel was run initially for 30 minutes at 70 volts, then for 1 hour at 150 volts for the constituent protein to vertically separate on the SDS gel according to the size, with the very heavy proteins travelling slowly and settling at the top end of the gel while the less heavy proteins were travelling faster on the gel and settling at the bottom of the gel. At the end of the run, the electrophoresis system was switched off disconnected from the mains, the cassette was dismantled to release the gel, the stacking gel and bottom of the separating gel were cut off, and the remaining gel was placed in a transfer buffer (5.82g tris, 2.93g glycine, and 200ml 100% methanol) ready for semi-dry blotting. The gel meant for protein staining was placed in fixative (80ml of methanol, 14ml of acetic acid and 6ml of distilled water for 100ml volume) for 3 minutes, after which the gel was stained overnight in a solution containing 10ml Coomassie blue (Bio-rad Cat. #1610786) and 2.5ml methanol. After the overnight staining, the gel was placed on a shaker and de-stained in 20% methanol for 1 hour, placed in a plastic bag and scanned to get an image of the protein separation.

2.7.3 Semi-dry blotting

The BIO-RAD Trans-Blot' Turbo transfer system was used to transfer the proteins separated on the SDS page gel onto a nitrocellulose membrane (Amersham ™ Protran ™ Premium 0.45 µm Nitrocellulose paper, GE Healthcare Cat No. 10600003). Three (3) layers of Whatman filter paper (100 x 150 mm) were soaked in transfer buffer and then carefully placed one after the other on the transfer plate and used a glass test tube to roll over the layers a few times to remove any air bubbles trapped. The nitrocellulose membrane was also soaked in the transfer buffer before carefully placing it on the filter papers. Then the gel was placed on the membrane with care taken to remove any air bubbles which may have become trapped in the process. Three (3) more Whatman filter papers soaked with the transfer were placed on the gel one after the other before sealing the transfer plate with the cover and slotting it into the machine. The blotting was done at 13 volts for 30 minutes, and after the run, the filter papers and gel were carefully removed and discarded safely. The nitrocellulose membrane was placed into a ponceau solution (SIGMA Ponceau solution; 0.1% Ponceau S (w/v) in 5%

acetic acid (v/v)), where it was allowed to incubate for 15 minutes at room temperature on a shaker. After incubation, the ponceau solution was recovered in a bottle wrapped in foil for re-use. The membrane was gently washed with distilled water, placed in a plastic wallet, cut to size to remove the areas where the protein did not transfer to and scanned to show that the protein transfer had been successful.

2.7.4 Incubation with antibodies

After scanning, the membrane was blocked for one (1) hour with 10 ml 1x TBS containing 5% of low-fat milk powder (Tesco). The milk was discarded after the incubation. The membrane was washed twice for 5 minutes each in buffer TBS-T (0.5 ml Tween 20, 2 ml Triton-X, 100 ml 10 xTBS buffer). All the primary and secondary antibodies used for the incubation were procured from Agrisera Antibody Limited. These include anti- PEPC purified from *Zea mays* (1:3000), anti-RbcL (1:1000) purified from Keyhole limpet hemocyanin conjugated synthetic peptide conserved across all plants, anti-RuBisCO activase (1:3000) purified from *Gossypium hirstum* and goat anti-rabbit (1:1000) was purified from goat IgG. All antibodies were made up in a 5 % milk solution and then used to treat the membrane one at a time overnight at 4°C. The milk solutions containing the primary antibodies were retained after the incubation period, and the membrane was washed twice for 5 minutes each in buffer TBS-T. The secondary antibody incubation was done using 10 ml of 1xTBS buffer containing 5% low–fat milk and goat anti-rabbit serum (1:1000) (Cat no. AS10 665) for 1 hour on a shaker at room temperature. The milk used was retained, and the membrane was washed twice in buffer TBS-T for 5 minutes each.

The solution used for the antibody detection was an enhanced chemiluminescence (ECL) substrate kit (high sensitivity) (Thermo Fisher Scientific Cat no. 32109), and the kit came with two solutions to be mixed at a ratio of 1:1. Exactly 1 ml of the mixed ECL solution was poured on a pat–dried nitrocellulose membrane, which was placed in a plastic wallet and kept in the dark for 5 minutes. The bands on the membrane were subsequently captured using the VisionWorks software of the Analytik Jena GELDOC-ITE 315 Gel documentation system.

2.8 RNA extraction and cDNA synthesis.

RNA extraction was conducted using 100 mg of frozen powdered leaf tissue collected from all the samples (wildtype and mutants) using the Qiagen RNAeasy Plant mini kit following

the manufacturer's instructions but with the addition of PEG 20,000 (100mg/ ml) to the RLC Buffer to avoid interference of the leaf's acidity with the isolation. The RNA obtained was eluted in 30 µl of RNAse-free water, and its concentration (ng μl^{-1}) was quantified by the Nanodrop™ spectrophotometer system. The synthesis of cDNA from the total RNA obtained was performed following the instructions of the Qiagen Quantitec Reverse transcription kit and diluted in Elution Buffer 1:4 for RT-qPCR analysis.

2.9 Transcript abundance of the genes using Real-time qPCR.

Real-time quantitative reverse-transcription PCR (qRT-PCR) has become arguably the preferred method of measuring the abundance of mRNA gene expression (Pfaffl 2006). In this study, the technique was employed to measure the relative change of the mRNA expression levels against an endogenous control and a non-treated control which is a cDNA calibrator prepared by combining RNAs extracted from wildtype *Kalanchoë fedtschenkoi* samples collected every four (4) hours over a day/night cycle of twenty-four (24) hours.

The primers used for this assay were designed using software Geneious® 11.0.3, Build 2017-10-31 12:45, Java Version 1.8.0_112-b15 and checked for efficiency. A standard curve was designed for the efficiency assay using a ten-fold dilution of the cDNA calibrator (125, 12.5, 1.25, 0.125, and 0.0125 ng μl^{-1}). Three technical replicates of each dilution were assayed using SensiFAST sybr No-ROX kit (supplied by SLS) on a Rotor-Gene Q instrument manufactured by Qiagen with the program: 95°C for 2mins, 40 cycles of 95°C for 5 secs, melting temperature for the primers (60 - 65°C) for 10 secs and 72°C for 10 secs. To confirm that the primers tested were working optimally, a coefficient of determination (R^2) of $\geq 98\%$ and efficiency between 0.9 and 1.10 was observed in line with reports by Pfaffl (2006).

The reference gene and gene of interest were evaluated using the same amplification conditions as the primer efficiency assay (95°C for 2mins, 40 cycles of 95°C for 5 secs, melting temperature (Tm) for 10 secs and 72°C for 10 secs). The experiments were conducted using three (3) biological replicates and two (2) technical replicates for both the wildtype and the mutants. The relative quantity was determined using the $2^{-\Delta\Delta Ct}$ method described by Livak and Schmittgen (2001) to normalize the data against the cDNA calibrator and reference gene thioesterase/thiol ester dehydrase-isomerase (TEDI) superfamily protein from *K. fedtschenkoi* (Phytozome Kaladp0068s0118.1) was used because it has a stable diel transcript abundance and in addition, a no template control (NTC) was used to confirm the absence of any contamination.

Table 2.1 The genes evaluated in the wild type and PPC mutant lines of *Kalanchoë fedtschenkoi* using Real-time qPCR. Both forward and reverse sequences are presented.

Gene name	**Annotation**	***K. fedtschenkoi* gene code**	***A. thaliana* gene code**	**Forward Primer (5' - 3')**	**Reverse Primer (5' - 3')**
KfePEPC 1	Phosphoenolpyruvate carboxylase 1	Kaladp0095s0055.1	AT1G53310.1	CGTGACTTCAGCAAACCAGC	AGGAGCATACTCGCTGGTTG
KfePEPC 2	Phosphoenolpyruvate carboxylase 2	Kaladp0048s0578.1	AT2G42600	TGGAGGTCCTACCCATCTGG	TGAATGGTGTCTGGTGGCTG
KfeTEDI	Thioesterase/thiol ester dehydrase isomerase	kalad0068s0118.1	AT5G48370	AGAAGAAGAGGCACGACGTG	GCAGGGAGTTTTCAGCATCG
***rbc*L**	RuBisCO large subunit	Kaladp0059s0137.1	ATCG00490	TGGGAATTTCAGGGTCTCGC	AAGCTTCCCCTTCGTCTTGG
KfePEPCK	Phosphoenolpyruvate carboxylase kinase	Kaladp0040s0194.1	AT4G37870	AGAGTGTGTGGAGAAGGAGC	GATGGGATGAGAGGCAGAGC

2.10 Drought treatment

Drought treatment was given to the plants to investigate how they would perform whilst stressed. The plants (wild type and mutants) were separated into two groups. One group was well–watered every two days for two weeks, while the other group was droughted for two weeks by withholding water. At the end of the two weeks, one leaf (age 8, counting from the tip of the plant) was cut from the stem of plants from both groups (well-watered and droughted) using a razor blade underwater to prevent emboli (air bubbles) from forming in the xylem.

2.11 Succulence measurement assay

The detached leaves were placed back of a beaker, held together with an elastic band so that the cut petiole remained submerged in water, covered with a clear plastic bag and left in a growth room set 25/19ºC and a 12-h photoperiod at a temperature and left to incubate for 24 hours.

After the incubation period, the leaves were patted dry of any excess water and weighed to 4 decimal places. Next, the leaves were placed on a flatbed scanner with a ruler in the scanner alongside the leaf so that a scale could be set on ImageJ, and the ImageJ was used to measure the leaf area.

The leaves were dried to constant weight in the oven for seventy-two (72) hours at 75 °C. The dry weight of the leaves was measured after drying, and the data collected was used to calculate the following parameters:

- Leaf dry mass per area (LMA)
- Leaf water mass per area (WMA)
- Saturated water content (SWC)

$$\text{LMA} = \frac{Dry\ weight}{Leaf\ area} \quad \text{(equation 1)}$$

$$\text{WMA} = \frac{Fresh\ weight - dry\ weight}{Leaf\ area} \quad \text{(equation 2)}$$

$$\text{SWC} = \frac{(Fresh\ weight - dry\ weight)}{Dry\ weight} = \frac{WMA}{LMA} \quad \text{(equation 3)}$$

Equation 2.3. The formula for calculating leaf dry mass per area (equation 1), leaf water mass per area (equation 2) and saturated water content (equation 3) from well-watered and droughted leaves of *K. fedtschenkoi*.

2.12 Chlorophyll and carotenoid measurement assay

Chlorophyll and carotenoid contents were measured using mature leaf pair 9 (counting from the tip of the plant) collected from wildtype and PEPC-mutants. Three biological replicates were sampled from both the well-watered and droughted plants. 1 ml of 80% acetone buffered with 2.5mM sodium phosphate pH 7.8 was added to 100 mg of ground powdered leaf tissue, and the extracts were subsequently placed in the dark in the – 80℃ freezer for a week. After the incubation period, the mixture was centrifuged at 16,000 gs for 10 mins at 4℃. The supernatants were collected in a fresh tube and protected from light by wrapping them in foil. The absorbance was read at 470 nm, 647 nm and 665nm. The following equations gotten from Porra et al. (1989) were used to calculate the chlorophyll contents of the plant leaves in (μg / mg):

Chlorophyll a = $12.25 \times A663 - 2.55 \times A647$…… (Equation 1)

Chlorophyll b = $20.31 \times A647 - 4.91 \times A663$……. (Equation 2)

Chlorophyll a + b = $17.76 \times A647 + 7.34 \times A663$…… (Equation 3)

Chlorophyll a to Chlorophyll b ratio = chla/chlb……(Equation 4)

Equation 2.4. The formula for calculating the chlorophyll a (equation 1), chlorophyll b (equation 2), the total chlorophyll (equation 3), and chlorophyll ratio (equation 4) content in well-watered and droughted leaves of *K. fedtschenkoi*. The results were expressed on a dry weight basis (μg/g DWT).

The formula used to calculate the total carotenoid content of the leaves in (μg / mg) was:

$$\text{Carotenoid} = \frac{(1000 \times (A475)) - (2.27 \times (chloA)) - (81.4 \times (chlo\ B))}{227}$$

Equation 2.5. The formula used in calculating the total carotenoid content of well-watered and droughted K. fedtschenkoi. Results are expressed on a dry weight basis (μg/g DWT).

2.13 Measuring stomatal density, pore length and stomatal pore index

Stomatal density was measured by obtaining the stomatal impressions using clear nail varnish to cut an area of approximately 2 cm^2 adjacent to the midvein and near the middle of a matured intact leaf of both the wild type and the *KfePEPC* mutants. Once the nail polish dried, a piece of clear Sellotape was used to peel off the stomatal imprint quickly, stick it onto a microscope slide and labelled. The slide collected was viewed using the x 20 stage lens on a microscope, the number of stomata was counted for every square of known distance and the 20 views were recorded per peel. The stomata were kidney-shaped and were found on both the upper (adaxial) and lower (abaxial) surface of the leaf (amphistomatic). Three (3) biological replicates of adaxial and abaxial stomata were measured per genotype, and the data were presented as the mean of sixty (60) measurements per genotype ± standard error of the mean. Three (3) photographs per peel viewed on the x 20 stage lens were taken, and ImageJ software 1.46r (Java 1.6.0_20, 64-bit http://imageJ.nih.gov/ij) was used as the measuring tool to measure the pore length. The results of the measured pore presented as the mean of 40 measurements per peel for both the upper and lower stomata ± standard error of the mean.

The stomatal pore area index (SPI) of the plants used in the study was determined. SPI measured the stomatal conductance was impacted by the stomatal density and pore length. SPI was calculated using the formula proposed by Bucher et al. (2016).

$$\text{SPI} = (\text{Guard cell length})2 \times \text{stomatal density}$$

Equation 2.6. The formula for calculating the stomatal pore area index (SPI) of *K. fedtschenkoi* wildtype and *KfePEPC* mutant stomata.

2.14 Statistical analysis

Data collected were analysed to determine whether there were significant differences in the data collected from wild–type and PEPC mutant lines. The analytical tools used included Analysis of variance (ANOVA), least significant difference (LSD) and student t-test, respectively. The statistical analyses used SPSS software (IBM Corp. Released in 2017. IBM SPSS Statistics for Windows, Version 25.0.0.1 Armonk, NY: IBM Corp).

Chapter 3 Effect of CRISPR-CAS knockdown of PEPC genes on transcript abundance and biochemical activity of C4 and C3 carboxylation processes in *Kalanchoë fedtschenkoi.*

3.1 Introduction.

Phosphoenolpyruvate carboxylase (PEPC) is one of the cytosolic enzymes involved in CAM photosynthesis. PEPC catalyses the nocturnal carboxylation of phosphoenolpyruvate to form oxaloacetate, a critical step in the CAM process (Cushman 2001). PEPC enzyme also catalyses the metabolic pathway that replenishes intermediates involved in the tricarboxylic acid pathway through a process known as anaplerosis (Arias-Baldrich et al. 2017; Peters-Wendisch et al. 1997; Cousins et al. 2007). The β-carboxylation role of PEPC in CAM plants has been implicated in the improved rate of photosynthesis and enhanced water-use efficiency, a beneficial attribute of CAM (Borland et al. 2009; Deng et al. 2016). In higher plants, PEPC has two gene subfamilies which are PEPC-1 (plant-type PEPC), and PEPC-2 (bacterial-type), with all these gene families, have chlorophyte algae as a common ancestor (Deng et al. 2016). PEPC found in CAM originates from PEPC-1m1, a clade derived from whole-genome duplication (WGD) of the eudicot PEPC-1 genome (Silvera et al. 2014). In *Kalanchoë fedtschenkoi,* a model CAM plant used for various research in CAM photosynthesis, five (5) isoforms of the *KfePEPC* gene exist. The *KfePEPC1* and *KfePEPC2* genes have been shown to have the highest diel transcript abundance (Yang et al. 2017). Boxall et al. (2020) reported that knocking down the *PEPC1* gene in *Kalanchoë laxiflora* resulted in the loss of nocturnal stomatal opening and CO_2 uptake. However, the extent to which the *PEPC2* gene isoform is involved in the primary carboxylation phase of CAM is yet to be studied. Apart from *KfePEPC* genes encoding for nocturnal carboxylation, isoforms of *KfePEPC* genes have also been implicated in encoding non – photosynthetic functions like stomatal regulation, growth and nitrogen assimilation in plants (O'Leary et al. 2011). Christin et al. (2014) reported that PEPC is ubiquitous in plants with all modes of photosynthesis (i.e., C_3, C_4 and CAM), indicating that different PEPC isoforms are responsible for non-photosynthetic functions.

In CAM plants, studies have shown that the circadian oscillator rather than light-dark transitions control flux through PEPC (Boxall et al. 2020). PEPC is controlled post-translationally by the activity of phosphoenolpyruvate carboxylase kinase (PPCK) via

phosphorylation of a serine residue near the N- terminus of the protein (Borland and Taybi 2004; Nimmo 2000; Theng et al. 2007; Boxall et al. 2017). The amount of PEPC protein is also regulated through the changes in abundance of PEPC mRNA at the transcriptional level, while the diel activation/deactivation of PEPC provides efficient means of optimising the nocturnal CO_2 uptake in CAM plants and is regulated at the post-translational level (Theng et al. 2007).

Phosphoenolpyruvate carboxylase kinase (PEPC Kinase or PPCK) is a cytosolic regulatory enzyme that phosphorylates PEPC at the end of the photoperiod in CAM plants (Taybi et al. 2004). This process renders PEPC less sensitive to malate inhibition as the enzymes drive CO_2 uptake during the dark phase. In the CAM model plant *Kalanchoë fedtschenkoi*, three (3) isoforms of *PPCK* genes exist. Boxall et al. (2017) investigated genetically perturbing PPCK activity in CAM plants by silencing the *KfePPCK1* gene in *Kalanchoë fedtschenkoi* and reported that PPCK is essential for maximal and sustained dark CO_2 assimilation and further proved that the enzyme activity is a key component of the entire CAM process. Currently, efforts are being made to understand further how PPCK is regulated. However, the extreme sensitivity of the PPCK enzyme to proteolysis during extraction from plant tissues, which leaves a shorter, yet active form of the enzyme seems to be a setback in achieving this objective (Martín et al. 2011).

RuBisCO in CAM plants plays a pivotal role as the enzyme is responsible for catalysing the refixing of CO_2 released from the decarboxylation of malate during the daytime (Ceusters et al. 2011; Wyka et al. 2004). Given RuBisCO's ability to bind with both oxygen and carbon dioxide, the problem of photorespiration can arise mostly in C_3 plants, affecting the efficiency of photosynthesis (Sage et al. 2012). However, CAM plants are believed to overcome this drawback, not by structural changes as seen in C_4 plants, but by a temporal shift in CO_2 uptake from daytime to nighttime (via PEPC) and making more CO_2 available during the daytime for RuBisCO to bind to during Phase three (3) of the CAM cycle (Griffiths et al. 2002; Maxwell et al. 1999). RuBisCO is usually active in CAM plants at the start of the photoperiod (Phase 2), just when PEPC starts to become inactive due to dephosphorylation (Dodd et al. 2002). RuBisCO is active throughout the light period (Phase 3) as decarboxylation of malate is taking place and CO_2 liberated needs to be refixed into the Calvin cycle, and RuBisCO remains active towards the end of the light period (Phase 4) as PEPC gradually becomes active, and stomata start opening in anticipation of nocturnal CO_2

uptake (Chia-Yun et al. 2018; Borland et al. 2014; Borland et al. 2009). The switch in the use of carboxylating enzymes (PEPC and RubisCO) over a diel period leads to unique and flexible carboxylation capabilities in CAM plants (Ceusters et al. 2021a). Hence PEPC being active throughout the day/night period will affect this flexibility. The ability of activated RuBisCO to bind with multiple sugar complexes in a non-productive manner leads to the formation of dead-end inhibited complexes that need to be remodelled by a dedicated molecular chaperone known as RuBisCO activase (Parry et al. 2008; Shivhare and Mueller-Cajar 2017). There are three (3) classes of RuBisCO activase, which belong to the superfamily of AAA+ proteins, but their primary sequences and mechanisms are distinct (Ng et al. 2020). In CAM plants, high carboxylation, electron transport capabilities, and high constant photon flux situations have been used to study and understand how RuBisCO activity is modulated. In C_3 and C_4 plants, RuBisCO is activated by reversible binding of activator CO_2 and modulation by carbamylation of active sites and, in many cases, by binding specific inhibitors to carbamylated sites (Griffiths et al. 2002; Maxwell et al. 1999; Ceusters et al. 2021a). Ceusters et al. (2021a) reported that in the case of CAM plants, the daytime activation of RuBisCO is slow, and there are indications that the process is regulated by the transcriptional regulation of the enzyme RuBisCO activase.

Molecular manipulation of the abundance and properties of enzymes/proteins is an approach that has yielded detailed insight into functional genomics and has opened more avenues to explore in terms of protein and gene function as more techniques are developed to facilitate the process. In CAM photosynthesis, molecular genetic manipulation has aided a clear understanding of how CAM plants underwent convergent evolution from their C_3 ancestors, how the circadian clock plays a pivotal role in the regulation of genes involved in CAM, as well as the enzyme kinetics of key enzymes like PEPC, and PPCK (Abraham et al. 2016; Borland and Taybi 2004; Yang et al. 2017; Cushman 2001). In the quest to study molecular aspects of plants and other organisms, techniques have been developed to successfully manipulate genes by introducing mutations that either suppress or promote the function of genes of interest. Some of these techniques include physical and chemical mutagens, RNA – interference (RNAi), and most recently, a technique already existing in some bacteria organisms that enable them to destroy the genome of viruses that attack them called Clusters of randomly interspaced short palindromic repeats and CRISPR – associated protein 9 (CRISPR-Cas9) (Liu et al. 2016). In this chapter, the CRISPR-Cas9 loss-of-function analysis technique has been used to knock down *KfePEPC1* and *KfePEPC2* genes individually in the

single mutants and together in the double mutants. The recent discovery of CRISPR-Cas9 technology adopted from *Streptococcus pyogenes* has become a game-changer in genome editing as the process guarantees precise gene targeting when compared to other genome editing techniques (Liu et al. 2019a). However, answers to several questions still elude scientists in CAM research. Some of these questions include: to what extent are the different isoforms of *KfePEPC* genes involved in the nocturnal carboxylation activity of PEPC enzyme? what effect will the knockdown of different *KfePEPC* genes have on the diel regulatory function of PPCK? and what happens to RuBisCO secondary carboxylation activity in CAM should PEPC activity be perturbed? This chapter has approached these questions, and the following hypotheses have been proposed.

Hypothesis 1: Crispr-CAS9 loss of function activity completely disrupts the expression of *KfePEPC1* and *KfePEPC2* genes.

Hypothesis 2: PEPC enzyme protein abundance and activity are diminished when the *KfePEPC1* gene is knocked down but not when the *KfePEPC2* gene is knocked down.

Hypothesis 3: Knocking down either of the *KfePEPC* genes (i.e., *KfePEPC1* and *KfePEPC2*) will perturb the diel expression and abundance of phosphoenolpyruvate carboxylase kinase *PPCK* and RuBisCO *rbc*L gene transcripts.

3.2 Material and methods

3.2.1 PEPC activity, malate sensitivity and protein assays

PEPC enzyme activity and malate sensitivity were measured using the assays described in section 2.6 (Chapter 2). Bradford (1976) method described in section 2.6 (Chapter 2) was used to measure the protein content of the extracts.

3.2.2 Immunoblotting

Total protein extracts from *Kalanchoë fedtschenkoi* used for the assay was prepared using the extraction method described in section 2.7 (Chapter 2).

3.2.3 RNA isolation, cDNA synthesis and gene expression analysis

RNA was extracted and cDNA synthesised from all the samples (wildtype and mutants) using methods described in section 2.8 (Chapter 2).

The real-time qPCR process used to measure the transcript abundance of the *KfePEPC1*, *KfePEPC2*, *rbc*L and *PPCK* genes in the wildtype and PEPC – mutant lines is described in section 2.9 (Chapter 2). The results were used to determine the difference in expression of the genes over a 24-hr period in the wild type and the mutant lines.

3.2.4 Statistical analysis

Data collected were analysed to determine whether there were significant differences in the data collected from wildtype and PEPC mutant lines using methods described in section 2.14 (Chapter 2).

3.3 Results

3.3.1 Transcript abundance of KfePEPC1 and KfePEPC2 genes.

Loss of function analysis brought about by double-stranded breaks (DSB) of type 2 CRISPR-Cas9 technology from *Streptococcus pyogenes* has provided a viable and precise means of editing genes for molecular studies (Liu et al. 2016; Liu et al. 2019a). Biallelic single *kfepepc1*, *kfepepc2* and double *kfepepc1/2* mutants, in which the indel mutations lead to disruption of protein-coding sequences, were used by our colleagues at Oakridge National Laboratory, TN, USA to create two independent lines for each gene or gene combination. T1 plants were selected at Oakridge using Kanamicin and then screened by the Sanger sequencing service of Eurofins Genomics LLC (Louisville, KY, USA). Our colleagues at Oakridge selected two independent lines each for *kfepepc1*, *kfepepc2* and double *kfepepc1/2* from the sequencing. These plants were sent to Newcastle for further analyses using qRT-PCR to examine if the CRISPR-Cas transformation perturbed the transcript abundance of *KfePEPC1* or *KfePEPC2*.

Figure 3.1 shows the transcript abundance of *KfePEPC1* in all genotypes. Reduced transcript abundance of *KfePEPC1* relative to that in the wild type was noted in the *kfepepc1* mutants, particularly in line 1 (Figure 3.1A). In the *kfepepc2* mutants, the transcript abundance of *KfePEPC1* was comparable to that observed in the wild type for the duration of the photoperiod and the first hours of the night (Figure 3.1B). However, from the mid to late dark period, transcript abundance of *KfePEPC1* was reduced in both lines (particularly line 1) of the *kfepepc2* mutants compared to that noted in the wild type.

Figure 3.2 shows the transcript abundance of *KfePEPC2* in all genotypes. In the *kfepepc1* mutants, the transcript abundance of *KfePEPC2* was like that of the wild type throughout the photoperiod. However, in the middle of the night, reduced transcript abundance of the gene was noted in both *kfepepc1* lines relative to that in the wild type (Figure 3.2A&B). In the *kfepepc2* mutants, transcript abundance of the *KfePEPC2* gene was significantly reduced relative to that of wild type for the duration of the dark period. However, the daytime expression was similar in both lines and wild type (Figure 3.2B).

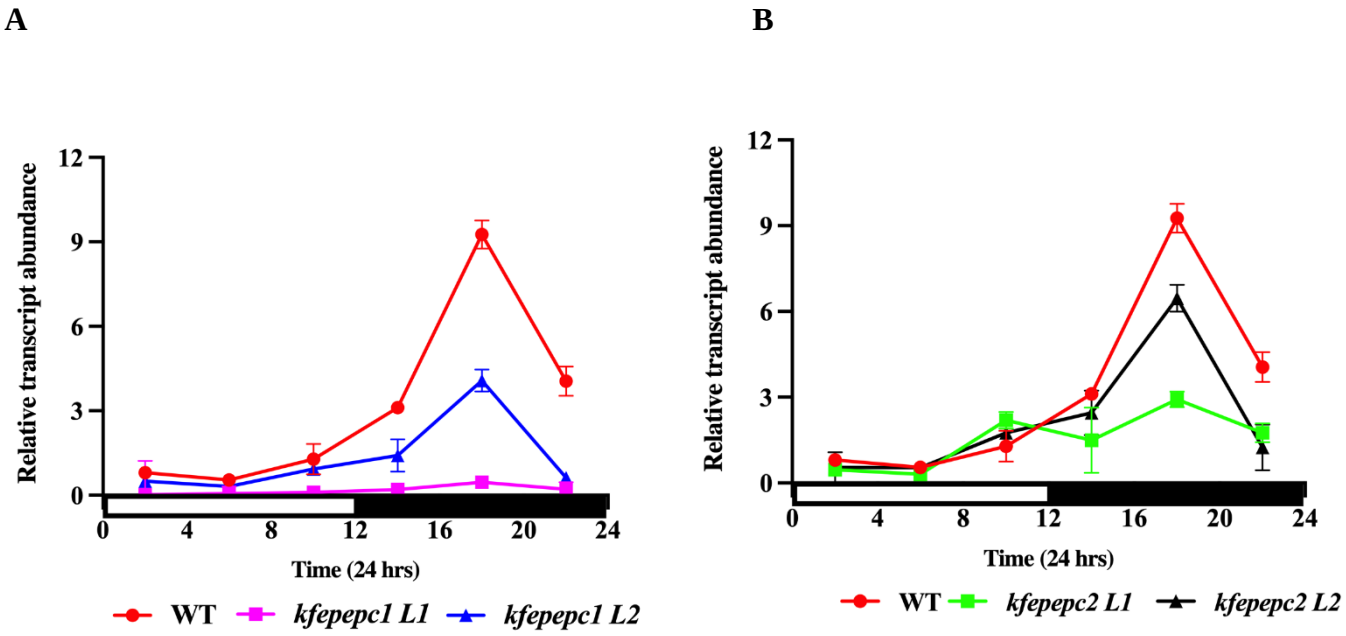

Figure 3.1. The diel relative transcript abundance of *KfePEPC1* gene in wild type (red), *kfepepc1* Line 1 (blue), *kfepepc1* Line 2 (purple), *kfepepc2* Line 1 (green) and *kfepepc2* Line 2 (black) of *Kalanchoë fedtschenkoi*. Leaf pairs 7 and 8 counting from the tip was used for this analysis. The error bars represent the standard error of six replicates (3 biological replicates, each with two technical replicates).

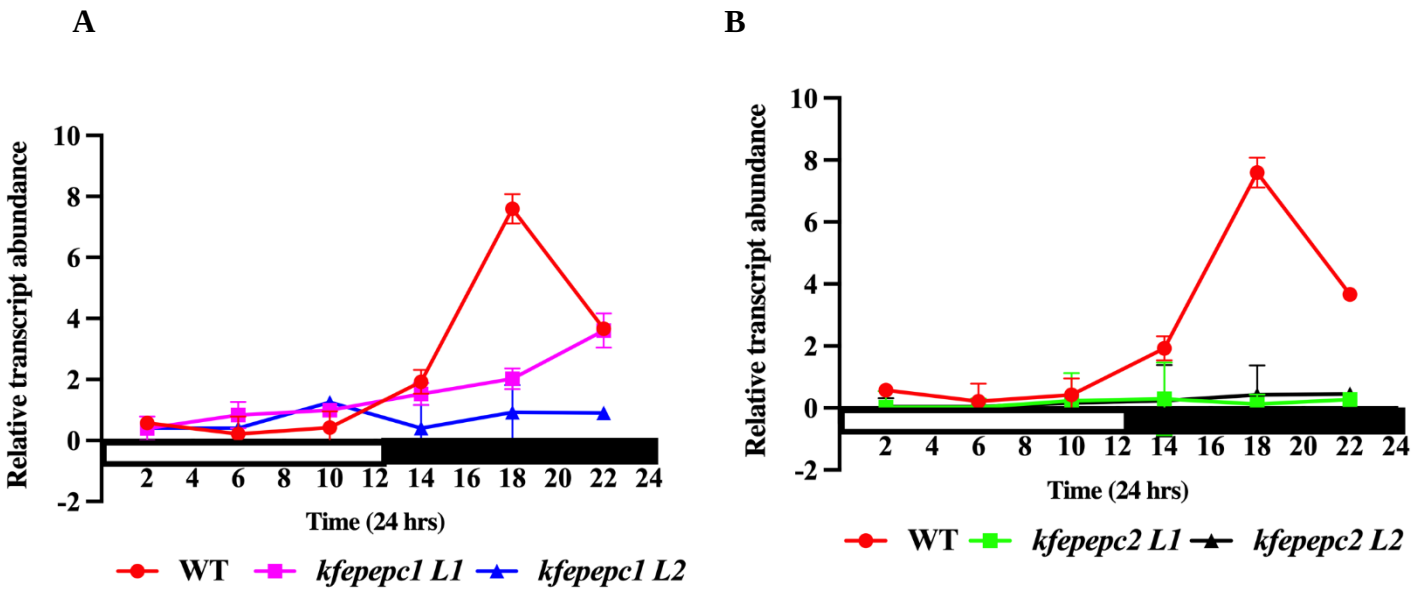

Figure 3.2. Diel relative transcript abundance of *KfePEPC2* gene in wild type (red), *kfepepc1* Line 1 (blue), *kfepepc1* Line 2 (purple), *kfepepc2* Line 1 (green) and *kfepepc2* Line 2 (black) *Kalanchoë fedtschenkoi*. Leaf pairs 7 and 8 counting from the tip was used for this analysis. The error bars represent the standard error of six replicates (3 biological replicates, each with two technical replicates).

3.3.2 PEPC activity and malate sensitivity.

Comparing the extractable *in vitro* PEPC activity of the mutants with wildtype shows how the mutation affected the biochemical activity of the enzyme. Knocking down the *KfePEPC1* gene led to a significant reduction ($p < 0.05$) in diel PEPC activity in *kfepepc1* Line1, but no significant reduction in enzyme activity was observed in *kfepepc1* Line 2 when compared to wildtype (Figure 3.3). There were no significant differences in the diel PEPC activity between wildtype and *kfepepc2* Lines 1 or 2 (Figure 3.3). When diel PEPC activity was measured in both lines of the double mutants *kfepepc1/2*, there was a significant reduction in the diel PEPC activity ($p < 0.05$) compared to the wildtype (Figure 3.3).

PEPC activity was measured in the presence and absence of malate to show percentage inhibition of PEPC activity and thereby assess any possible changes in the phosphorylation status of PEPC in the different mutants. Percentage inhibition results show that in wild type, the enzyme PEPC extracted during the day was inhibited more by malate than the enzyme extracted at night. Still, the difference was not significant at $P<0.05$ (Figure 3.4). In the single *KfePEPC1* and *KfePEPC2* mutants, the percentage inhibition of PEPC activity by malate had a similar pattern to what was observed in wildtype, although there was no significant

difference at (P<0.05) between the inhibition of the enzyme extracted during the daytime and the night-time. There was no observable day/night pattern of inhibition by malate in the double mutants, comparable to that observed in wild type and the single mutant lines. So double mutants appeared to have lost the day/night difference in malate sensitivity that was observed in other genotypes.

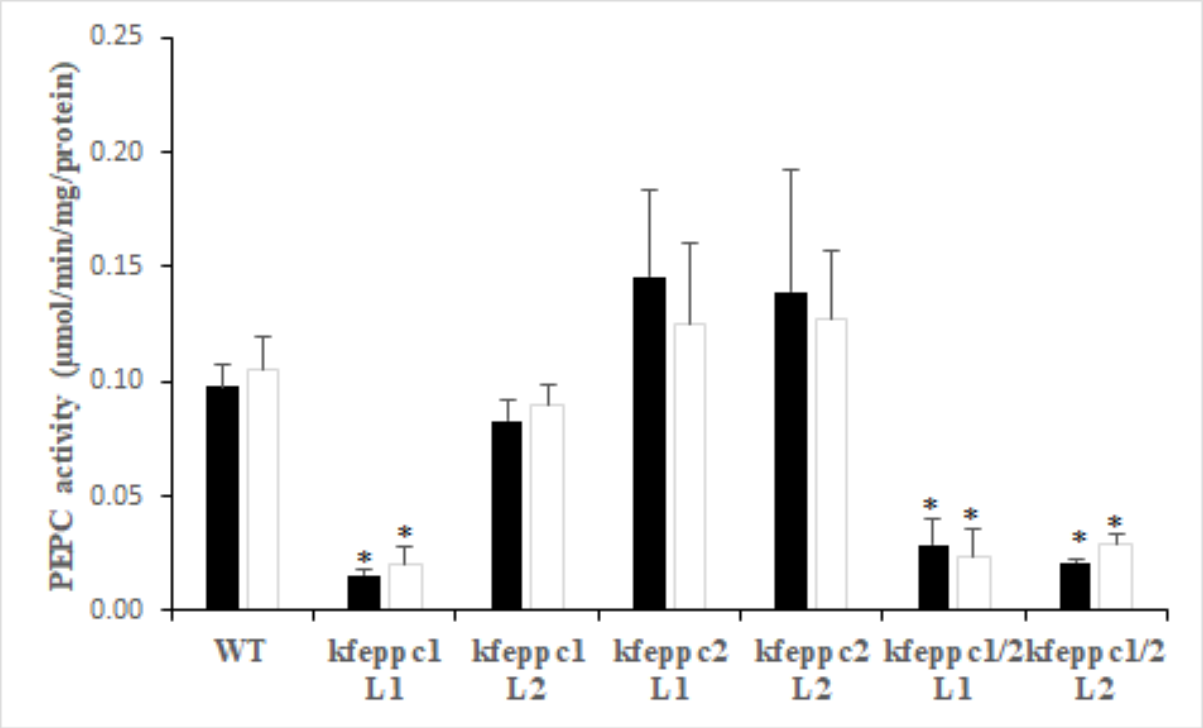

Figure 3.3. PEPC activity in *Kalanchoë fedtschenkoi* wildtype and mutants over a 24-hr night (black bars) and day (white bars) period. There was a significant reduction in diel (day/night) PEPC activity in *kfepepc1* Line 1, *kfepepc1/2* Line 1 and *kfepepc1/2* Line 2 mutants. In contrast, there was no significant reduction in diel PEPC activity in *kfepepc1* Line 2, *kfepepc2* Line 1, and *kfepepc2* Line 2 mutants, respectively. Three (3) biological replicates of each phenotype were used to analyse. * represents a significant difference at (P < 0.05).

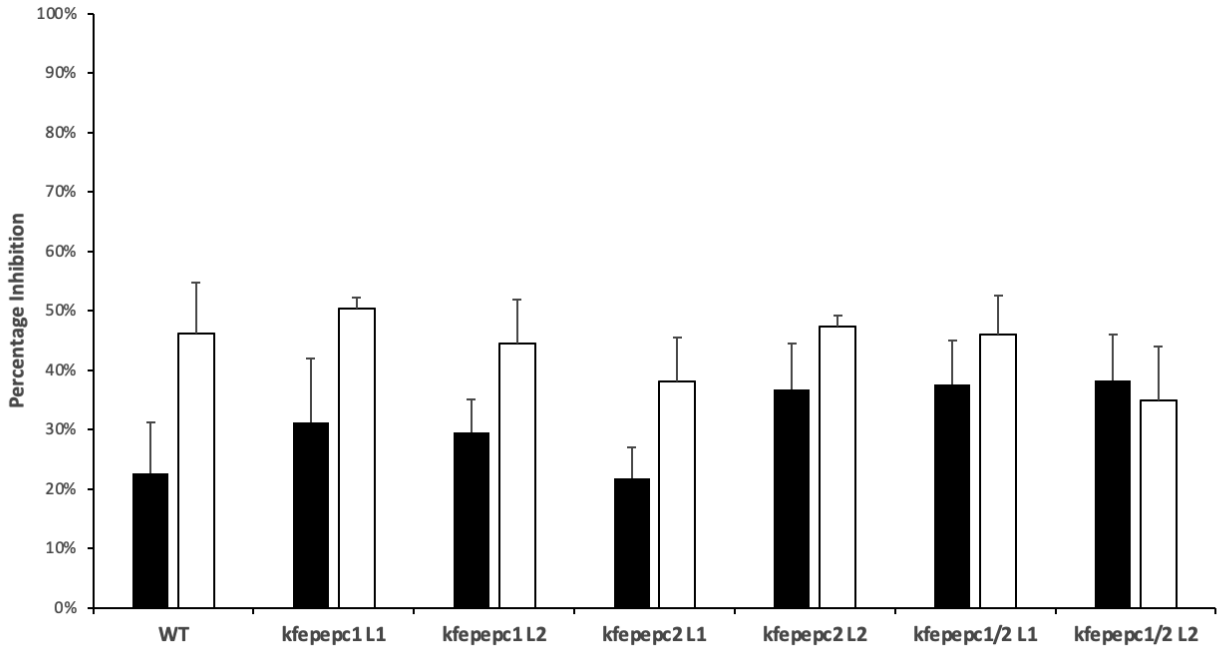

Figure 3.4. Percentage inhibition of malate on PEPC enzyme extracted from *Kalanchoë fedtschenkoi* wildtype and mutants over a 24 hrs night (black bars) and day (white bars) period. Results are the average of three biological replicates.

3.3.3 Abundance of PEPC, RuBisCO and RuBisCO activase proteins

Western blot analysis was conducted on all genotypes to identify the effect of knocking down *KfePEPC1* and *KfePEPC2* genes on the abundance of PEPC and RuBisCO proteins. Results show that the amount of PEPC protein was significantly reduced in both lines of the *kfepepc1* single mutants and both *kfepepc1/2* double mutants (Figure 3.5A). In the *kfepepc2* mutants, the amount of PEPC protein was like that in the wild type. The immunoblot results also showed that knocking down *KfePEPC1 or KfePEPC2* genes did not significantly affect the amount of RuBisCO or RuBisCO activase proteins in any mutants relative to the wild type (Figure 3.5B and Figure 3.6A). However, the double mutant *kfepepc1/2* Line 1 showed a somewhat reduced abundance of RuBisCO protein. Results in Figure 3.5C&D and Figure 3.6B&C confirmed that the proteins were successfully transferred from the SDS-page gel to the nitrocellulose membrane. The proteins successfully separated according to their sizes in the SDS-PAGE gel during the electrophoresis process.

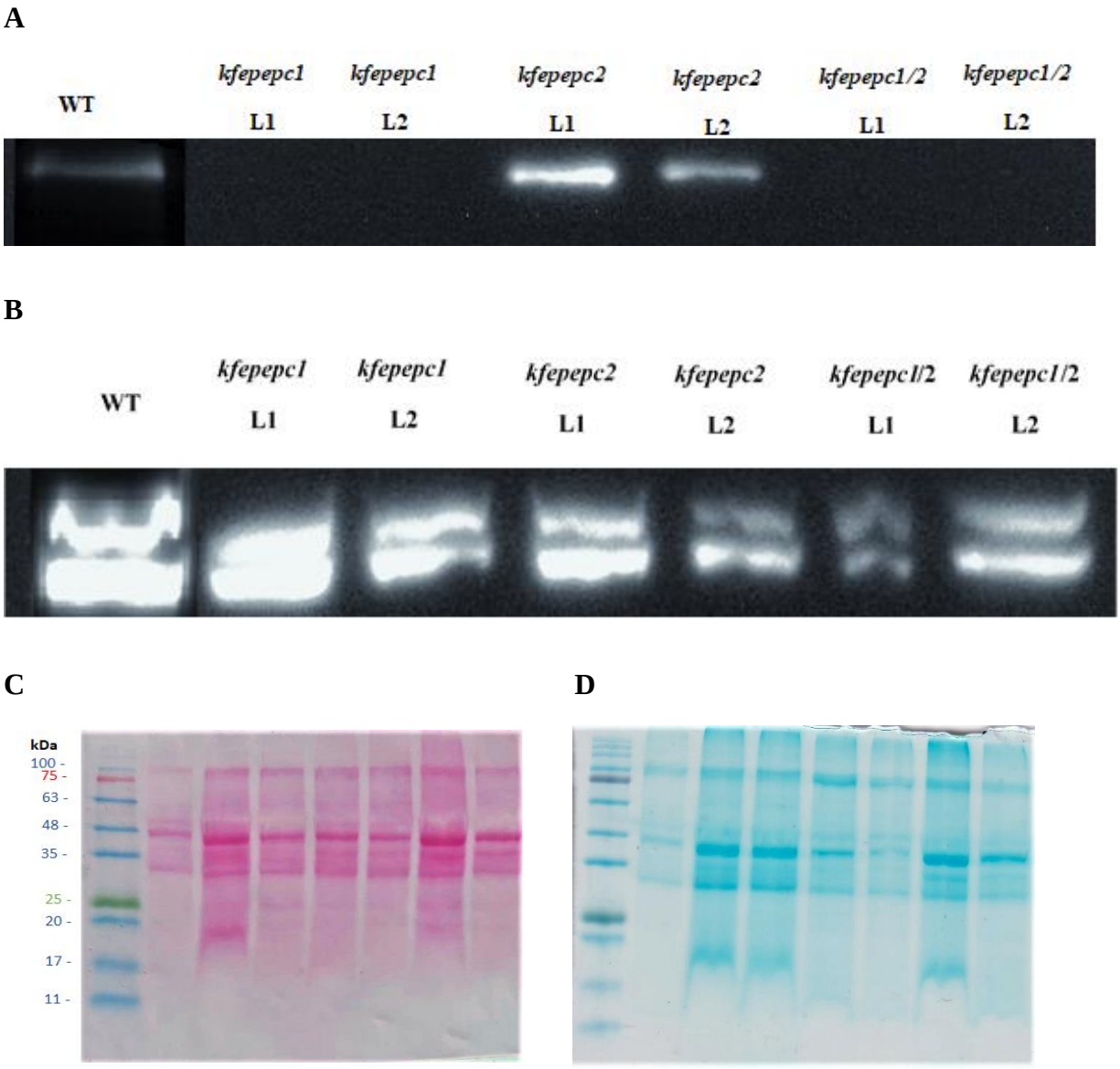

Figure 3.5. PEPC (A) and RuBisCO (B) protein abundance of wildtype and *KfePEPC* mutants of *Kalanchoë fedtschenkoi* collected at the end of the photoperiod. (C) The ponceau image of the SDS page transfer to nitrocellulose membrane and protein gel image (D) stained overnight in Coomassie blue solution to confirm that equal amounts of protein were loaded in each well.

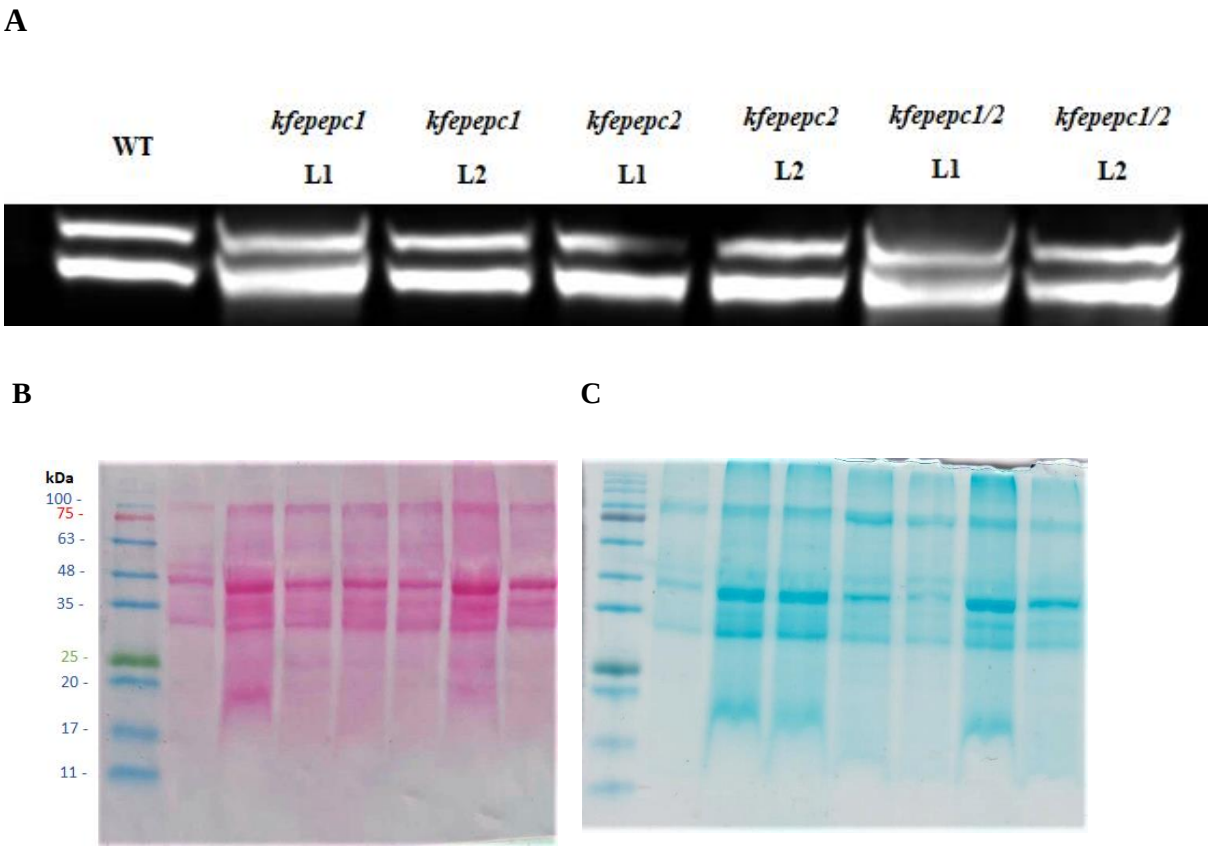

Figure 3.6. RuBisCO activase (a) protein abundance of wildtype and *KfePEPC* mutants of *Kalanchoë fedtschenkoi* collected at the end of the photoperiod. The ponceau image of the SDS page transfer to nitrocellulose membrane (b) and protein gel image (c) stained overnight in Coomassie blue solution to confirm that equal amounts of protein were loaded in each well.

*3.3.4 Transcript abundance of RuBisCO (*rbc*L) and KfePPCK genes in the KfePEPC mutants.*

To further understand the effect of knocking down *KfePEPC1* and *KfePEPC2* genes on carboxylation processes, the transcript abundances of RuBisCO large subunit (*rbc*L) and Phosphoenolpyruvate carboxylase kinase (*KfePPCK*) were measured over 24 hours in wildtype and the *kfepepc1* and *kfepepc2* mutants.

The results show that transcript abundance levels of the *rbc*L gene in *KfePEPC1* and K*fePEPC2* mutants were like that of the wild type during the night. In the middle of the photoperiod, there was a marked increase in *rbc*L transcripts in the wild type, but this increase was less marked in *kfepepc1* mutants and particularly in the *kfepepc2* mutants, which showed significant downregulation ($P \leq 0.05$) (Figure 3.7A&B).

Transcript abundance measurements for *PPCK* show significantly elevated transcript abundance of this gene at night in wild type, as previously reported by Boxall et al. (2020). However, in all the *kfepepc1* and *kfepepc2* lines, transcript abundance of *KfePPCK* at night was significantly (P< 0.05) reduced compared to that in the wild type (Figure 3.7A&B).

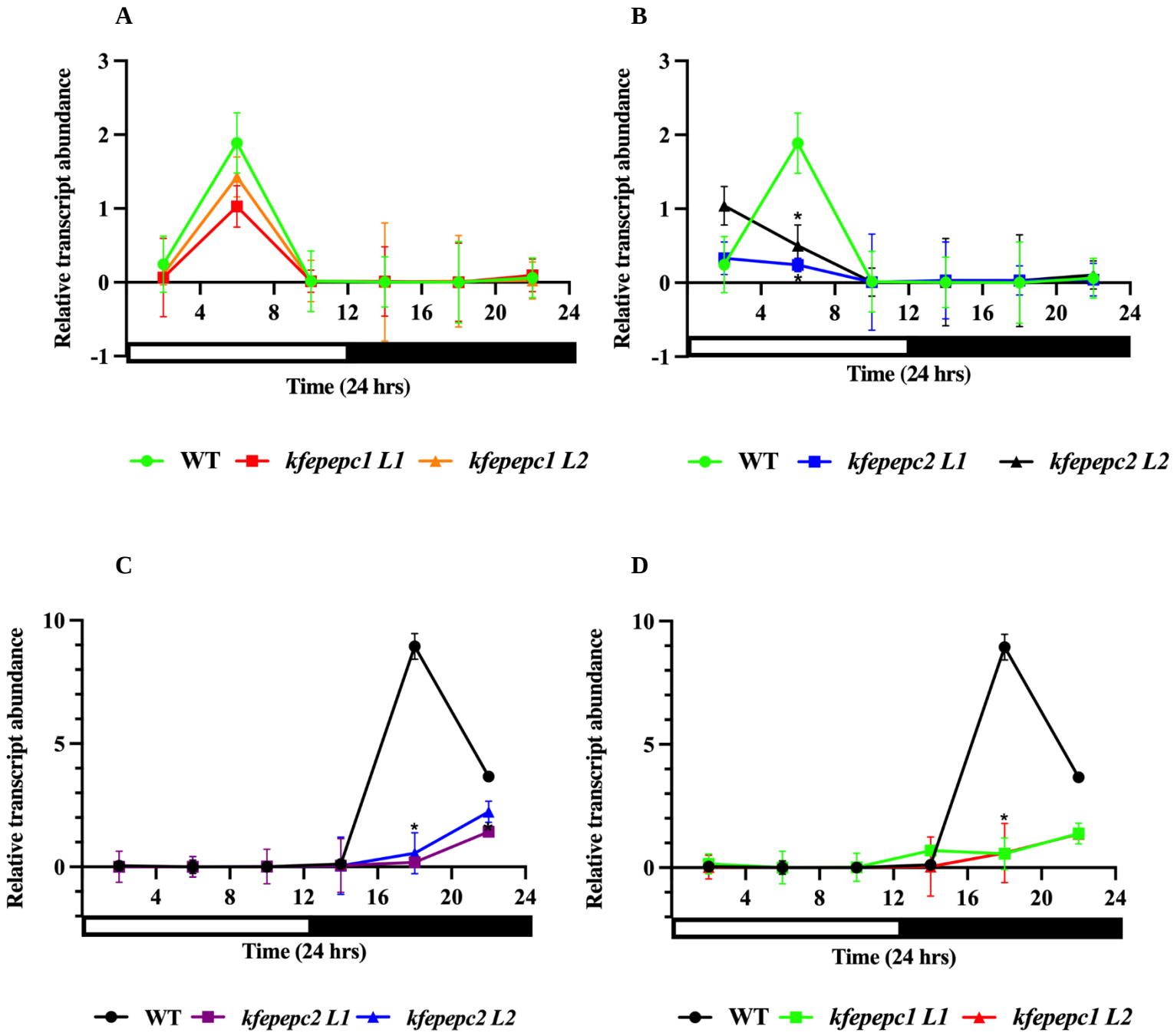

Figure 3.7. *rbc*L gene relative transcript abundance (a,b) in wild type (green), *kfepepc1* Line 1 (red), *kfepepc1* Line 2 (orange), *kfepepc2* Line 1 (blue), *kfepepc2* Line 2 (black) and *KfePPCK* gene relative transcript abundance (c,d) in wildtype (black), *kfepepc1* Line 1 (green), *kfepepc1* Line 2 (red), *kfepepc2* Line 1 (purple) and *kfepepc2* Line 2 (blue) over 24 hour period. Leaf pairs 7 and 8 counting from the tip were used for this analysis. * show significant difference at p<0.05.

3.4 Discussion.

3.4.1 CRISPR-Cas mutations in KfePEPC1 and KfePEPC2 genes disrupt diel transcript abundances of KfePEPC isogenes

This thesis examined CRISPR/Cas9 knockdowns of *KfePEPC1* and *KfePEPC2* genes to understand how these genes ultimately affect nocturnal CO_2 uptake (Chapter 4), an essential aspect of CAM photosynthesis. The results in the present chapter show that the gene-editing technology employed led to a significantly reduced diel transcript abundance of *KfePEPC1* and *KfePEPC2* genes in both lines of each of the single mutants when compared to the wildtype. Furthermore, CRISPR-Cas9 employed a 20 nucleotide guide RNA sequence (gRNA) to cleave the target *KfePEPC* genes, allowing the Cas9 protein to cut the genes, initiating a series of non-homologous end joining (NHEJ) events (Liu et al. 2019a). This observation confirms one of the hypotheses that Crispr-Cas9 loss of function activity disrupts the expression of the target genes.

The impact of knocking down the genes of interest (*KfePEPC1* and *KfePEPC2*) on the transcript abundance of each other was mixed and differed between the independent lines. For example, in *kfepepc2* Line 1, there was diel downregulation of *KfePEPC1*, while in *kfepepc2* Line 2, the gene expression of *KfePEPC1* was like that observed in the wildtype. In contrast, there was diel downregulation of *KfePEPC2* genes in both *kfepepc1* mutants (*kfepepc1* Line 1 and *kfepepc1* Line 2). These observations suggest a potential metabolic regulatory link between the diel transcript abundance of the *KfePEPC* genes, as knocking down one gene affects the expression of the other in various ways. Boxall et al. (2020) observed that silencing *PPC1* in *Kalanchoë laxiflora* led to an upregulation of *KfePEPC2* in one of the mutants where the gene was completely silenced, whilst no change in transcript abundance was observed in the mutant where *PPC1* was partially suppressed. This observation could be attributed to these genes having common origins due to gene duplication events which then led to the genes evolving. The results align with Silvera et al. (2014), who argued that gene duplication and neofunctionalization played roles in the *PPC* gene lineage evolutionary progression within the Oncidiinae family.

3.4.2 CRISPR-Cas mutations in KfePEPC1 impacted the biochemical activity and protein abundance of PEPC

The knockdown of *KfePEPC1* transcript abundance in line 1 of the *kfepepc1* mutant led to a significant reduction (> 70 %) of the extractable *in vitro* activity of the PEPC enzyme. In contrast, the knockdown of transcript abundance of the *KfePEPC2* gene in both mutant lines of *kfepepc2* did not affect *in vitro* activity of the PEPC enzyme. This observation can be compared to what Boxall et al. (2020) observed when the *KfePEPC1* gene was silenced in *Kalanchoë laxiflora*. Observations in the present chapter for *kfepepc1* Line 1 and both of the double mutants (i.e. *kfepepc1*/2 Line 1 and *kfepepc1/2* Line 2) indicate that the *KfePEPC1* gene encodes the bulk of PEPC protein in *K. fedtschenkoi* and supports the hypothesis that *KfePEPC1* encodes the CAM-specific isoform of phosphoenolpyruvate carboxylase (Taybi et al. 2017; Boxall et al. 2020; Chia-Yun et al. 2018; Taybi and Cushman 2002). The data indicated that the *KfePEPC2* gene is not actively involved in regulating CAM activity in *K. fedtschenkoi*, confirming that some *KfePEPC* gene isoforms have non-photosynthetic roles in CAM plants (Silvera et al. 2014; O'Leary et al. 2011).

Incomplete knockdown of the *KfePEPC1* gene was noted in *kfepepc1* line 2, and in this mutant line, *in vitro* activity of the PEPC enzyme was not significantly different to that of the wild type. This finding can be attributed to the mutant retaining the gene's function and, by extension, the enzyme. This observation is similar to Xing et al. (2014) that mismatches caused poor performance of T1B-TC gRNAs vectors in CRISPR/Cas9 mediated mutations in *Arabidopsis*.

Knocking down the abundance of *KfePEPC1* gene transcripts led to a loss of the PEPC protein in *kfepepc1* Line 1, *kfepepc1* Line 2, *kfepepc1/2* Line 1 and *kfepepc1/2* Line 2 mutants. In contrast, when the *KfePEPC2* gene was knocked down, there was no observable change in the abundance of the PEPC enzyme protein, which was clearly visible in the blots. This observation supports the hypothesis above that the *KfePEPC1* gene encodes the bulk of PEPC protein which can be attributed to the vital role of the *KfePEPC1* gene isoform in CAM and agrees with the findings of Boxall et al. (2020) that despite upregulation of the *PPC2* gene in the RNAi *rPPC1-B* mutant, no PPC protein was detected. Loss of PEPC protein was also observed in the *kfepepc1* Line 2 mutant, but the mutant retained comparable *in vitro* PEPC activity to that of the wild type as described above. Liu et al. (2019b) reported

that CRISPR produces mutations at the DNA and RNA levels and does not guarantee the non-synthesis of functional proteins.

Further work is required to understand why western blot failed to indicate the presence of PEPC proteins in *kfepepc1* Line 2 despite a substantial level of PEPC activity measured. However, the present study also found no significant change in day/night extractable PEPC activity in any mutants and wild type assayed. In the absence of malate's inhibitory effect, the activity of the PEPC enzyme over 24 hours remained the same and phosphorylation/dephosphorylation affected the sensitivity to malate. These findings agree with the results of Nimmo et al. (1984), who showed that extractable *in vitro* PEPC activity did not change over a day/night cycle in *K. fedtschenkoi.* However, the observation differed from the results of Theng et al. (2007) as they showed that PEPC activity in *Kalanchoë pinnata, Kalanchoë daigremontiana* and *Ananas comosus* significantly changed over a day/night period. This is due to the presence of two PEPC protein sub-units in these plants, which were not dictated in *K. fedtschenkoi*.

Results obtained from measuring the percentage inhibition in PEPC activity due to malate sensitivity showed a higher inhibition from malate in daytime PEPC activity as opposed to nighttime PEPC activity in wildtype and all *KfePEPC* single mutants (*kfepepc1* and *kfepepc2*) lines. For the double mutants, the percentage inhibition in *kfepepc1/2* Line 1 was the same in daytime/nighttime, while in *kfepepc1/2* Line 2, the percentage inhibition was higher at nighttime. The observation made in the percentage inhibition of wildtype, *kfepepc1* Line 1, *kfepepc1* Line 2, *kfepepc2* Line 1, and *kfepepc2* Line 2 can all be attributed to the PEPC enzyme being highly sensitive to malate inhibition during the day due to the protein undergoing dephosphorylation at the end of the dark period to avoid CAM futile cycling (Borland et al. 2014; Borland and Taybi 2004; Boxall et al. 2017). To be less sensitive to malate inhibition and become efficient for nocturnal CAM activity, PEPC undergoes post-translational regulation by the phosphoenolpyruvate carboxylase kinase (PPCK) phosphorylates the serine residue near the N-terminus of the protein. In the double mutants (*kfepepc1/2* Line 1 and *kfepepc1/2* Line 2), the different observations made from measuring the percentage inhibition are likely an effect of the loss of function activity from CRISPR-Cas9 suppressing the expression of the *KfePEPC* genes. The disruption could have perturbed the activity of the *KfePEPCK* gene as a knock-on effect of the mutation. This observation

agrees with Ray and Mukherjee (2021) that CRISPR knockout can disrupt the expression and transcript abundance of non-target genes.

3.4.3 KfePPCK gene expression is perturbed by knocking down KfePEPC1 and KfePEPC2 genes.

The regulatory role of phosphoenolpyruvate carboxylase kinase (PPCK) on the PEPC enzyme has been extensively studied in CAM plants and *K. fedtschenkoi.* PEPC is regulated post-translationally via reversible protein phosphorylation, which is controlled by the abundance of *KfePPCK* (Boxall et al. 2017; Borland et al. 2009; Theng et al. 2007; Nimmo 2000; Chia-Yun et al. 2018). Studies show that nocturnal phosphorylation of PEPC makes the enzyme less sensitive to feedback inhibition by malate, thereby avoiding futile cycling (Taybi et al. 2004). However, little information is available on the effect of knocking down *KfePEPC* genes on the transcript abundance of the *PPCK* gene.

In this present study, the impact of knocking down *KfePEPC1* and *KfePEPC2* genes on the gene expression of *KfePPCK* was investigated. Boxall et al. (2020) reported that silencing the *PPC1* gene led to the downregulation of some key clock genes implicated in the diel expression of CAM, and the *PPCK1* gene was also downregulated during the dark phase. In contrast, Boxall et al (2020) found a slight upregulation of *PPCK1* in the early light phase when the *PPC1* gene was completely knocked down in *K. laxiflora*. Hence, there is the possibility that knocking down *KfePEPC* genes will affect the functioning of the *KfePPCK* gene. Comparing the diel gene expression of *KfePPCK* in wildtype, *kfepepc1* and *kfepepc2* independent lines of *K. fedtschenkoi* indicated similar day/night transcript abundance patterns. Thus, the highest abundance of the *KfePPCK* gene occurred at night as observed in the wild type and the *KfePEPC1* and *KfePEPC2* mutants. These findings indicate that *KfePPCK* catalysed phosphorylation of *KfePEPC* at night to ensure the enzyme drives nocturnal carboxylation (Boxall et al. 2017). However, results also showed a significant down-regulation in the actual level of transcripts of *KfePPCK* at night in both *kfepepc1* and *kfepepc2* mutants compared to the wildtype, suggesting that *KfePPCK* transcription is indeed perturbed by knocking down *KfePEPC* genes. Thus, knocking down *KfePEPC* would appear to perturb the regulatory function of the PPCK enzyme in CAM photosynthesis. This observation agrees with Boxall et al. (2020) that silencing *PPC1* in *K. laxiflora* led to a

downregulation of the *PPCK1* gene in the mutant. However, as discussed above, this disruption to *KfePPCK* transcription at night did not affect the extractable *in vitro* activity of PEPC in the *kfepepc2* mutants or line 2 of the *kfepepc1* mutant. Whilst Boxall et al, (2017) proposed that nocturnal PEPC phosphorylation is essential for maximal dark CO_2 uptake in CAM plants, the findings in this chapter suggest that complete knockdown of *KfePPCK* transcription at night is required to perturb PEPC activity.

3.4.4 Knocking down the KFEPEPC genes did not impact abundances of RuBisCO or RuBisCO activase proteins

Recently, efforts have been made to understand how the expression of genes chiefly linked to the CAM process affects the protein level of the enzymes they encode and that of other proteins and enzymes linked to the process. Little information is currently available on how knocking down PEPC will impact RuBisCO-mediated C_3 carboxylation processes; hence, the effect of knocking down the *KfePEPC1* and *KfePEPC2* genes in the present study on the abundances of RuBisCO and RuBisCO activase proteins was evaluated.

Results from western blot analysis of RuBisCO and RuBisCO activase proteins in the wildtype and PEPC single and double mutants of *K. fedtschenkoi* showed that knocking down either of the *KfePEPC* genes did not affect the production of enzyme proteins of RuBisCO and RuBisCO activase. Therefore, we hypothesise that knocking down the *KfePEPC* genes will not impair the C_3 carboxylation activities catalysed by RuBisCO or RuBisCO activase. The results suggest that the CO_2 concentration mechanism catalysed by PEPC is uncoupled from the CO_2 uptake catalysed by RuBisCO in CAM plants. This observation agrees with the observation made by Maxwell et al. (1999) and Griffiths et al. (2002), who suggested the diel abundance of RuBisCO protein in CAM plants and the high carboxylation activity in CAM plants suggests that RuBisCO activity does not limit CAM activity. To be active during phase 3 of CAM, RuBisCO undergoes carbamylation, which is assisted by RuBisCO activase, making for an efficient CO_2 assimilation activity (Maxwell et al. 1999; Gonçalves et al. 2020). Determining how perturbing PEPC transcript abundance and activity affects the protein level of RuBisCO activase can indicate how efficient the carbamylation process was in these plants. However, results from western blot analysis of RuBisCO activase protein showed that the amount of RuBisCO activase protein in all the mutants remained unchanged from that in the wild type. These observations suggest that RuBisCO activity and carbamylation/activation status in CAM plants are not reliant on PEPC activity. This

observation also agrees with the report from Gonçalves et al. (2020) that despite nutrient and water deficits in CAM-performing bromeliads, RuBisCO activity remained unaffected.

*3.4.5 Knocking down the KfePEPC2 isoform perturbed the peak transcript abundance of rbc*L *genes.*

In C_3 plants, one of the significant drawbacks of RuBisCO is the ability of the enzyme to bind with O_2, thereby reducing the efficiency of photosynthesis. In CAM plants, it would appear that altering the catalytic context of RuBisCO by increasing CO_2 availability should curtail the chances of photorespiration and improve daytime photosynthetic efficiency (Hermida-Carrera et al. 2020). Despite efforts being made to understand how RuBisCO activity is regulated in CAM plants fully, there is a need to thoroughly investigate if there are molecular implications in losing PEPC/ CAM activity on RuBisCO regulation. Attempts have been made to investigate the regulation of the RuBisCO gene expression in C4 plants. Berry et al. (2016) reported that regulating RuBisCO genes in C_4 plants might include transcriptional, post-transcriptional and post-translational processes.

This chapter investigated the impact of knocking down *KfePEPC* genes on the transcript abundance of the RuBisCO large chain *rbc*L gene. Knocking down the *KfePEPC1* gene did not significantly influence *rbcL* transcript abundance, with both *kfepepc1* mutant lines showing peak expression in the middle of the light period, which was comparable to that in the wild type. However, in the case of *kfepepc2* mutants, *rbcL* transcription was impacted, with a key difference being the time of maximum transcript abundance, which occurred at the beginning of the light period in the *kfepepc2* mutants rather than at mid-day as seen in wild type. These observations indicate that different *KfePEPC* isogenes show contrasting modes of interaction with *rbcL* transcription in *K. fedtschenkoi*. The subsequent chapters in this thesis will examine the physiological implications of these disruptions in gene expression in terms of diel gas exchange, carbohydrate turnover and plant growth

3.5 Conclusions

Complete knockdown of the *KfePEPC1* gene led to a total loss of PEPC enzyme activity and PEPC protein in the *kfepepc1* line 1 and the double mutants. In contrast, the partial knockdown of *KfePEPC1* and the complete knockdown of *KfePEPC2* genes did not significantly affect

PEPC enzyme activity or protein abundance, suggesting that *the KfePEPC1* isogene is hugely significant in the nocturnal carboxylation processes mediated by the PEPC enzyme.

Knocking down *KfePEPC1* and *KfePEPC2* genes did not lead to a loss of RuBisCO or RuBisCO activase proteins. However, knocking down the *KfePEPC2* isogene perturbed the expression of the RuBisCO *rbc*L gene leading to the maximum transcript abundance of the gene reached early in both lines of the *kfepepc2* mutants. This observation suggests a possible implication of the *KfePEPC2* gene in the regulation of the *rbc*L gene in *K. fedtschenkoi*.

Chapter 4 Investigating how the knockdown of different PEPC isoforms impacts leaf gas exchange and diel metabolite turnover in *Kalanchoë fedtschenkoi*.

4.1 Introduction.

CAM plants are characterized by physiological traits that make them stand out from plants with other forms of photosynthesis. These traits include, among other things, a nocturnal stomatal opening and uptake of CO_2, which results in nocturnal accumulation of leaf titratable acidity, and enhanced water–use efficiency due to daytime stomatal closure (Hermida-Carrera et al. 2020; Borland et al. 2016a). As a syndrome, CAM has led to significant anatomical, metabolic and physiological modifications to support adequate CO_2 availability to Ribulose-1,5-bisphosphate carboxylase/oxygenase (RuBisCO) and enhance plants' water–use efficiency growing in arid and semi-arid areas of the world (Abraham et al. 2020). Nocturnal CO_2 uptake is key to the traits described above, and this process is catalysed by the enzyme phosphoenolpyruvate carboxylase (PEPC) (Cushman 2001; Nimmo 2000; Dodd et al. 2002). During the dark, PEPC is activated by the phosphorylation of a serine residue near the N- terminus of the protein, which makes the enzyme more sensitive to phosphoenolpyruvate and positive effectors, glucose-6-phosphate, and triose phosphate and less sensitive to malate inhibition (Boxall et al. 2020; Taybi et al. 2017). With the stomata open, atmospheric CO_2 enters the stomata and is converted to bicarbonate via the enzyme carbonic anhydrase. The bicarbonate reacts with 3-carbon substrate phosphoenolpyruvate (PEP) to form oxaloacetate. Oxaloacetate is reduced to malate via the enzyme malate dehydrogenase, stored in the vacuoles as malic acid overnight and acts as a store of carbon needed to drive the process of CAM (Nimmo 2000; Boxall et al. 2017; Borland and Taybi 2004; Osmond 1978). The PEP is generated from the degradation of carbohydrates, starch or soluble sugars, depending on the plant species (Carnal and Black 1989).

PEPC has photosynthetic and non-photosynthetic isoforms, which are responsible for different plant processes. The photosynthetic isoform is responsible for fixing CO_2 to PEP in CAM plants, and the non – photosynthetic isoform has been shown to catalyse other housekeeping roles that include supporting the carbon-nitrogen interaction, seed formation and germination, and guard cell metabolism during stomatal opening (O'Leary et al. 2011; Silvera et al. 2014; Chia-Yun et al. 2018). Genetically, PEPC has three gene subfamilies

which are PPC-1 (plant-type PEPC), PPC-2 (bacterial-type), and PPC-3 and all these genes are derived from chlorophyte algae as a common ancestor (Deng et al. 2016). PEPC found in CAM originates from PPC-1m1, a clade derived from whole-genome duplication (WGD) of the eudicot PPC-1 genome (Silva et al. 2014). To gain more insight into the role of the *KfePEPC1* isoform in CAM plants, Boxall et al. (2020) silenced *KfePEPC1* in *Kalanchoë laxiflora* and observed that perturbing this isoform led to a loss of nocturnal CO_2 uptake, causing the *KfePEPC1* mutants to open their stomata during the day and taking up CO_2. Despite what is known about the role of the *KfePEPC1* isoform in CAM, not much is known about the role that the *KfePEPC2* isoform plays in the entire CAM process. Yang et al. (2017) observed that *KfePEPC1* and *KfePEPC2* genes are the most abundantly expressed isogenes in *Kalanchoë fedtschenkoi*. Investigating how knocking down the two most abundant isoforms of PEPC in *K. fedtschenkoi* impacts gas exchange properties and diel malate turnover will provide insight into the roles of *KfePEPC1* and *KfePEPC2* in the operation of the CAM pathway (Zhang et al. 2021).

Nocturnal CO_2 uptake in CAM plants has been linked directly to diel turnover of starch as well as soluble sugars, which are building blocks for the CO_2 capturing substrate phosphoenolpyruvate (PEP), and the enzymatic activity of PEPC depends on the level of starch and soluble sugars (Taybi et al. 2017). Suppose both PPC isoforms are critical for the operation of CAM. In that case, it might be predicted that knocking down the genes encoding these isoforms will affect the diel content of metabolites like starch and soluble sugars and the diel turnover of malate, thereby affecting growth performance (Boxall et al. 2020).

To understand the role of different PEPC isoforms in CAM, studying the impact of knocking down *KfePEPC1* and *KfePEPC2* genes on the diel patterns of leaf gas exchange and diel metabolic turnover is vital. This chapter addressed the following hypotheses:

Hypothesis 1: Phosphoenolpyruvate carboxylase (PEPC) activity encoded by the *KfePEPC1* gene is primarily responsible for nocturnal carbon fixation in CAM plants.

Hypothesis 2: Perturbing the *KfePEPC1 gene* leads to a switch in CO_2 uptake from CAM mode to C_3 mode.

Hypothesis 3: Diel patterns of acidity accumulation will be significantly reduced in line with *KfePEPC1* gene loss of function but will be unaffected in plants with *KfePEPC2* gene loss of function.

Hypothesis 4: Knocking down the *KfePEPC1* gene will perturb the diel pattern of starch synthesis and degradation but there will be no change in starch turnover with *KfePEPC2* knockdown.

Hypothesis 5: Knocking down the *KfePEPC1* and *KfePEPC2* genes will affect stomatal regulation in *Kalanchoë fedtschenkoi.*

4.2 Materials and methods.

4.2.1 Plant material

Kalanchoë fedtschenkoi, a CAM model plant, was used for experiments carried out in this study. Both wildtype and mutant lines were propagated vegetatively using methods described in section 2.2 (Chapter 2).

4.2.2 Gas exchange analysis

Photosynthetic activity of the wild type and four (4) mutants were evaluated by measuring net CO_2 uptake (µmol m^{-2} s^{-1}), stomatal conductance (mmol H_2O $m^{-2}s^{-1}$) and transpiration rate (mmol m^{-2} s^{-1}) using leaf gas exchange analysis. The methods used are described in section 2.3 (Chapter 2).

4.2.3 Titratable acidity, soluble sugar, and starch analysis methods.

To understand how the plants' titratable acidity, soluble sugars and starch content are affected by the knockdown of PEPC, leaf pairs 7 and 8, numbered from the tip of the plant, were sampled over a 24-hr period. These samples were collected at six (6) time points every four (4) hours, wrapped in foil, snap-frozen in liquid nitrogen and stored in a -80 ^{o}C freezer. The titratable acidity method was described in section 2.4, while the soluble sugar and starch analysis methods were described in section 2.5 (Chapter 2).

4.2.4 Statistical analysis.

Data collected were analysed to determine whether there were significant differences in the data collected from wild–type and PEPC mutant lines. The analytical tools and software used are described in section 2.14 (Chapter 2).

4.3 Results.

4.3.1 Gas exchanges.

Gas exchange analysis results gave an insight into the impact of knocking out the two most abundantly expressed PEPC (*KfePEPC1 and KfePEPC2*) genes on the CAM activity of *Kalanchoë fedtschenkoi*. Knocking out *KfePEPC1* led to a loss of CAM and a switch to the C_3 mode of photosynthesis in the *kfepepc1* Line 1 while *kfepepc1* Line 2 continued to do CAM (Figure 4.1A&B). On the other hand, knocking down *KfePEPC2* did not affect CAM photosynthesis in any of the *KfePEPC2* independent lines. They all retained nocturnal carboxylation ability like that in the wild type (Figure 4.1A&B).

The reduced nocturnal stomatal opening was observed in the *kfepepc1* Line 1. In contrast, the *kfepepc1* Line 2 had a nocturnal stomatal opening similar to that observed in the wild type, with the difference being that the stomata in the mutant opened more in the late photoperiod with *kfepepc1* Line 2 having a maximum stomatal conductance value of 0.027 µMol H_2O m^{-2} s^{-1}, *kfepepc2* Line 1 with 0.021 µMol H_2O m^{-2} s^{-1} compared to the wild type which had a maximum stomatal conductance of 0.011 µMol H_2O m^{-2} s^{-1} at the end of the photoperiod (Figure 4.1D). The nocturnal stomata opening in the two *KfePEPC2* mutant lines were similar to the wild type. Still, light period late afternoon stomatal opening was higher in the mutants compared to the wild type as *kfepepc2* Line 1 had a stomatal conductance value of 0.021 µMol H_2O m^{-2} s^{-1}, *kfepepc2* Line 2 with 0.030 µMol H_2O m^{-2} s^{-1} compared to wild type stomatal conductance of wild type 0.011 µMol H_2O m^{-2} s^{-1} (Figure 4.1D).

Results from the light and dark period integrated rate of transpiration show that *kfePEPC1* Line 1 mutant lost more water during the light period with a transpiration rate of 2.41 ± 0.46 mmol H_2O compared to PPC 1 Line 2 at 1.17 ± 0.50 mmol H_2O, PPC 2 Line 1 at 1.02 ± 0.41 mmol H_2O, PPC 2 Line 2 at 1.32 ± 0.67 mmol H_2O and the wild type at 0.70 ± 0.40 mmol H_2O, respectively. At night *kfepepc1* Line 1 rate of transpiration was lower but not

significantly different compared to the wild type despite the reduced stomatal conductance at night. *kfepepc1* Line 2 and the two *kfepepc2* mutant lines had transpiration rates over light and dark periods, which were not significantly different from the wild type. (Table 4.1).

Results from the light period and night-time integrated CO_2 uptake show that *kfepepc1* Line 1 mutant took up more CO_2 during the light period than other mutants and the wild type. *kfepepc2* Line 1, on the other hand, had the highest nocturnal CO_2 uptake, while *kfepepc1 Line 1* had the lowest nocturnal CO_2 uptake when compared to wild type and other mutants (Table 4.2).

Instantaneous water–use efficiency data show that the *kfpepc1* Line 1 had significantly reduced water–use efficiency level at p 0.05 compared to the wild type over a day/night period because of completely knocking down *the KfePEPC1* gene (Table 4.3). However, a level of water–use efficiency like that of the wild type was observed in *kfepepc1* Line 2, *kfepepc2* Line 1 and *kfepepc2* Line 2 mutants, respectively, over the same period (Table 4.3).

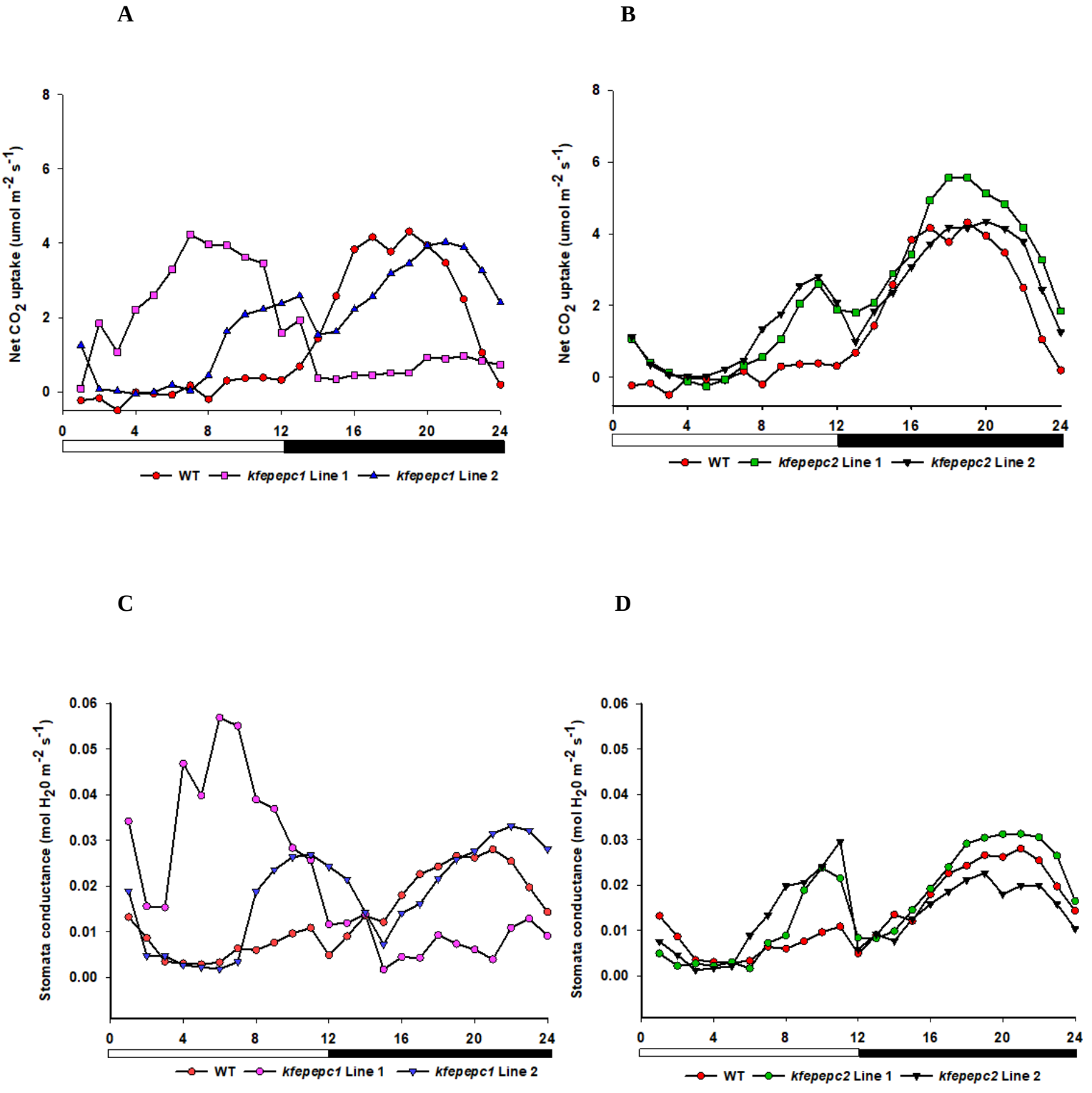
A
B
C
D
Net CO_2 uptake (umol m^{-2} s^{-1})
Stomata conductance (mol H_20 m^{-2} s^{-1})
0
2
4
6
8
0.00
0.01
0.02
0.03
0.04
0.05
0.06
0
4
8
12
16
20
24
WT
kfepepc1 Line 1
kfepepc1 Line 2
kfepepc2 Line 1
kfepepc2 Line 2

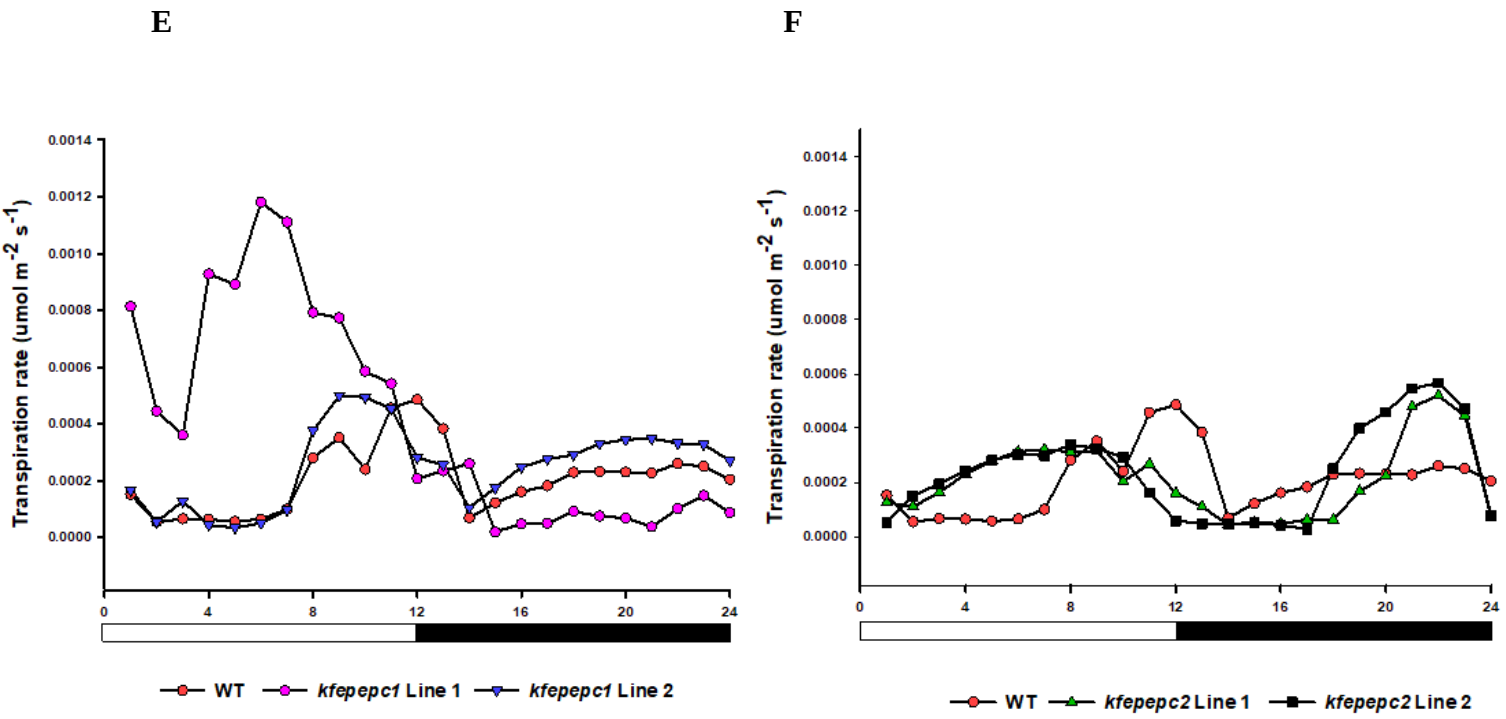

Figure 4.1. Comparing Net CO_2 uptake (a,b), Stomatal conductance (c,d) and Transpiration rate (e,f) of *kfepepc1* Line 1 (pink), *kfepepc1* Line 2 (blue), *kfepepc2* Line 1 (green), and *kfepepc2* Line 2 (black) mutant lines against wild – type (red) in a 24 hr period. Leaf pair eight (8) was used, and each measurement was done in 3 biological replicates. White and black bars represent the light period (12-h) and dark period (12-h), respectively.

Table 4.1. Light and dark period integrated rate of transpiration (TRi) for wild type, *kfepepc1* Line 1, *kfepepc1* Line 2, *kfepepc2* Line 1, and *kfepepc2* Line 2 mutant lines. TRi was computed from the area under the curve of the net transpiration rate graph. Leaf pair eight (8) was used, and each measurement was done in 3 biological replicates. * Shows mean difference significant at p 0.05, while ^{NS} shows no mean significant difference when compared to the wild type.

	Integrated transpiration rate (mmol H_2O)	
	DAY	**NIGHT**
Wildtype	0.70 ± 0.40	0.59 ± 0.07
***kfepepc1* Line 1**	2.41 ± 0.46*	0.21 ± 0.05^{NS}
***kfepepc1* Line 2**	1.17 ± 0.50^{NS}	0.76 ± 0.07^{NS}
***kfepepc2* Line 1**	1.02 ± 0.41^{NS}	0.78 ± 0.15^{NS}
***kfepepc2* Line 2**	1.32 ± 0.67^{NS}	0.58 ± 0.23^{NS}

Table 4.2. Light and dark period integrated CO_2 uptake (Gsi) for wild type, *kfepepc1* Line 1, *kfepepc1* Line 2, *kfepepc2* Line 1, and *kfepepc2* Line 2 mutant lines. GSi was computed from the area under the curve of the net CO_2 uptake graph. Leaf pair eight (8) were used, and each measurement was done in 3 biological replicates. * Shows mean difference significant at p 0.05 while ^{NS} shows no mean significant difference when compared to the wild type.

Integrated CO_2 uptake (mmol CO_2)		
	DAY	**NIGHT**
Wildtype	0.38 ± 0.30	11.17 ± 4.78
***kfepepc1* Line 1**	11.83 ± 1.31*	1.30 ± 0.56*
***kfepepc1* Line 2**	3.13 ± 1.52 ^{NS}	7.20 ± 1.45 ^{NS}
***kfepepc2* Line 1**	2.81 ± 1.80 ^{NS}	15.96 ± 1.32 ^{NS}
***kfepepc2* Line 2**	4.63 ± 1.56 ^{NS}	10.07± 2.34 ^{NS}

Table 4.3. Instantaneous water use efficiency (WUEi) for wild type, *kfepepc1* Line 1, *kfepepc1* Line 2, *kfepepc2* Line 1, and *kfepepc2* Line 2 mutant lines over 24 hours. WUEi was computed from the ratio of integrated CO_2 uptake to integrated transpiration rate. Leaf pair eight (8) were used, and each measurement was done in 3 biological replicates. * Shows mean difference significant at p 0.05 while ^{NS} shows no mean significant difference when compared to the wild type.

Instantaneous water use efficiency (mmol CO_2: mol H_2O)			
	DAY	**NIGHT**	**24HRS**
Wildtype	0.50 ± 0.21	20.02 ± 4.78	10.12 ± 4.06
***kfepepc1* Line 1**	4.91 ± 0.99*	7.91 ± 3.61*	4.39 ± 0.96 ^{NS}
***kfepepc1* Line 2**	2.24 ± 0.92^{NS}	9.90 ± 2.49^{NS}	7.62 ± 2.54 ^{NS}
***kfepepc2* Line 1**	2.66 ± 0.86^{NS}	20.03 ± 3.46^{NS}	11.91 ± 4.02 ^{NS}
***kfepepc2* Line 2**	4.22 ± 0.81*	20.38 ± 4.09^{NS}	10.35 ± 2.31 ^{NS}

4.3.2 Titratable acidity analysis.

Titratable acids are vital indicators of how well the CAM plants perform (Taybi et al. 2017). Comparing 24- hour titratable acidity analysis in all the mutants and wild type showed some interesting results. These results showed a significant amount of titratable acids in *kfepepc2* Line 2 at the beginning of the light period (Figure 4.2 B). There was no significant change in titratable acids content of *kfepepc1* Line 2, *kfepepc2* Line 1 and *kfepepc2* Line 2 mutants compared to the wild type from the middle of the light to the end of the dark period (Figure 4.2 A&B). However, nocturnal titratable acid accumulation was significantly reduced in the *kfepepc1* line 1 mutant of a day/night cycle (Figure 4.2A). As the dark period approached, a gradual increase in acidity was observed again in wild type and all mutants except *kfepepc1* Line 1. This increased level of titratable acids was at its highest between 10 to 12 hours into

the dark period. In the light period, it was observed that at time point one (4 hours into the light period), the amount of titratable acids measured in *kfepepc2* Line 2 was significantly ($p \leq 0.05$) higher than the wild type (Figure 4.2B) and as the light period progressed, the amount of titratable acid accumulated in the wild type and *kfepepc1* Line 2, *kfepepc2* Line 1 and *kfepepc2* Line 2 mutants reduced which is an indication that the acids have been broken down to liberate CO_2 to RuBisCO. These results suggest that knocking down the *KfePEPC1* gene affects the ability to accumulate titratable acids in *kfepepc1* Line 1 mutant at night, which is consistent with the perturbation of nocturnal net CO_2 uptake in this mutant line.

The diel titratable acid content of the double mutants (*kfepepc1/2* Line 1 and *kfepepc1/2* Line 2) *was* measured at dawn and dusk time points. Both independent double mutant lines had significantly reduced ($p \leq 0.05$) titratable acid at dawn timepoint compared to the wild type. However, at the dusk time point, the *kfepepc1/2* Line 2 had significantly reduced ($p \leq 0.05$) titratable acids compared to the wild type (Figure 4.2C).

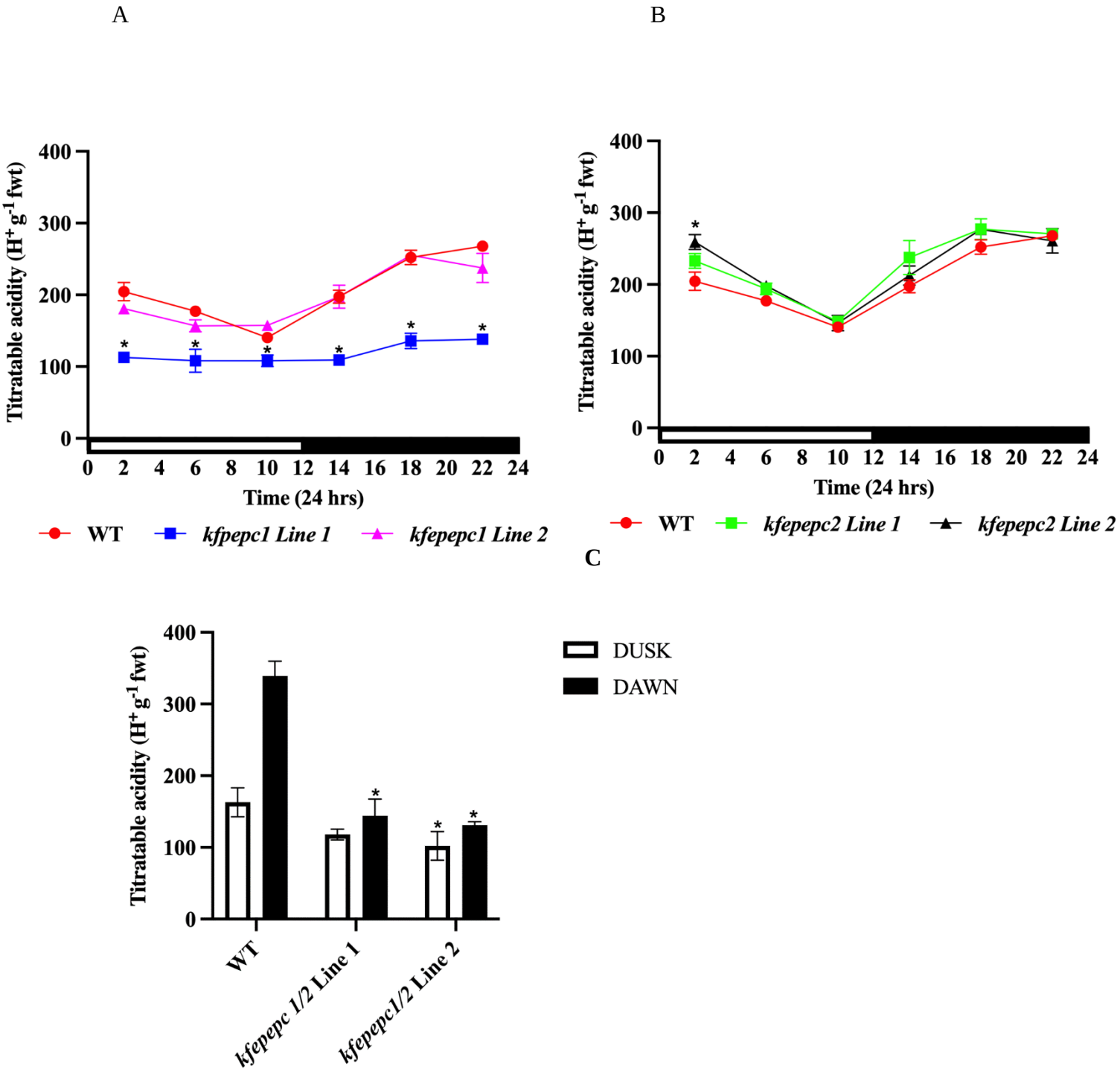

Figure 4.2. Comparing titratable acidity levels of (a) *kfepepc1* Line 1 (blue), *kfepepc1* Line 2 (purple), (b) *kfepepc2* Line 1 (green), *kfepepc2* Line 2 (black) mutant lines against wild type (red) over a 24-hr period and (c) titratable acidity of *kfepepc1/2* mutants at dawn and dusk timepoints. Leaf pair eight (8) was used, and each measurement was done in 3 biological replicates. White and black bars represent the light period (12-h) and dark period (12-h), respectively. * Mean difference significant at p 0.05 when compared to the wild type.

4.3.3 Soluble sugars and starch turnover

Measurements over 24 hours of soluble sugar levels in the wild type and *KfePEPC* mutants of *Kalanchoë fedtschenkoi* were made at six (6) time points of 4-hour intervals. Results showed that *kfepepc1* Line 2 had significantly higher soluble sugar levels than the wild type and *kfepepc1* Line 1 throughout the day and night (Figure 4.3A). In *kfepepc1* Line 1, there was a sharp increase in the level of soluble sugars at eight (8) hours into the light period and an evident decrease in soluble sugar levels by the end of the light period (Figure 4.3A). The diel soluble sugar pattern observed in *kfepepc2* Line 1 showed a steady decline in soluble sugar content as the light period progressed, being at its lowest amount at the start of the dark period before increasing again over the dark period (Figure 4.3B). In *kfepepc2* Line 2 and wild type, this soluble sugar depletion and accumulation were less apparent over the day/night cycle (Figure 4.3B).

Results from the starch analysis showed similar patterns of nocturnal starch accumulation and light period degradation in WT, *kfepepc1* Line 2, *kfepepc2* Line 1 and *kfepepc2* Line 2 mutants, respectively. (Figure 4.3D&E). Higher starch levels were observed in the *kfepepc1* Line 1 mutant at the night's end and the light period's start compared to WT and *kfepepc1* Line 2 (Figure 4.3C). In *kfepepc2* Line 1, starch content at the start of the day was significantly ($p \leq 0.05$) reduced compared to WT, and *kfepepc2* Line 2 and starch content in *kfepepc2* Line 1 increased significantly over the first half of the day (Figure 4.3E). It is clear from these results that the knockdown of the different PEPC isoforms impacted diel starch turnover in different ways.

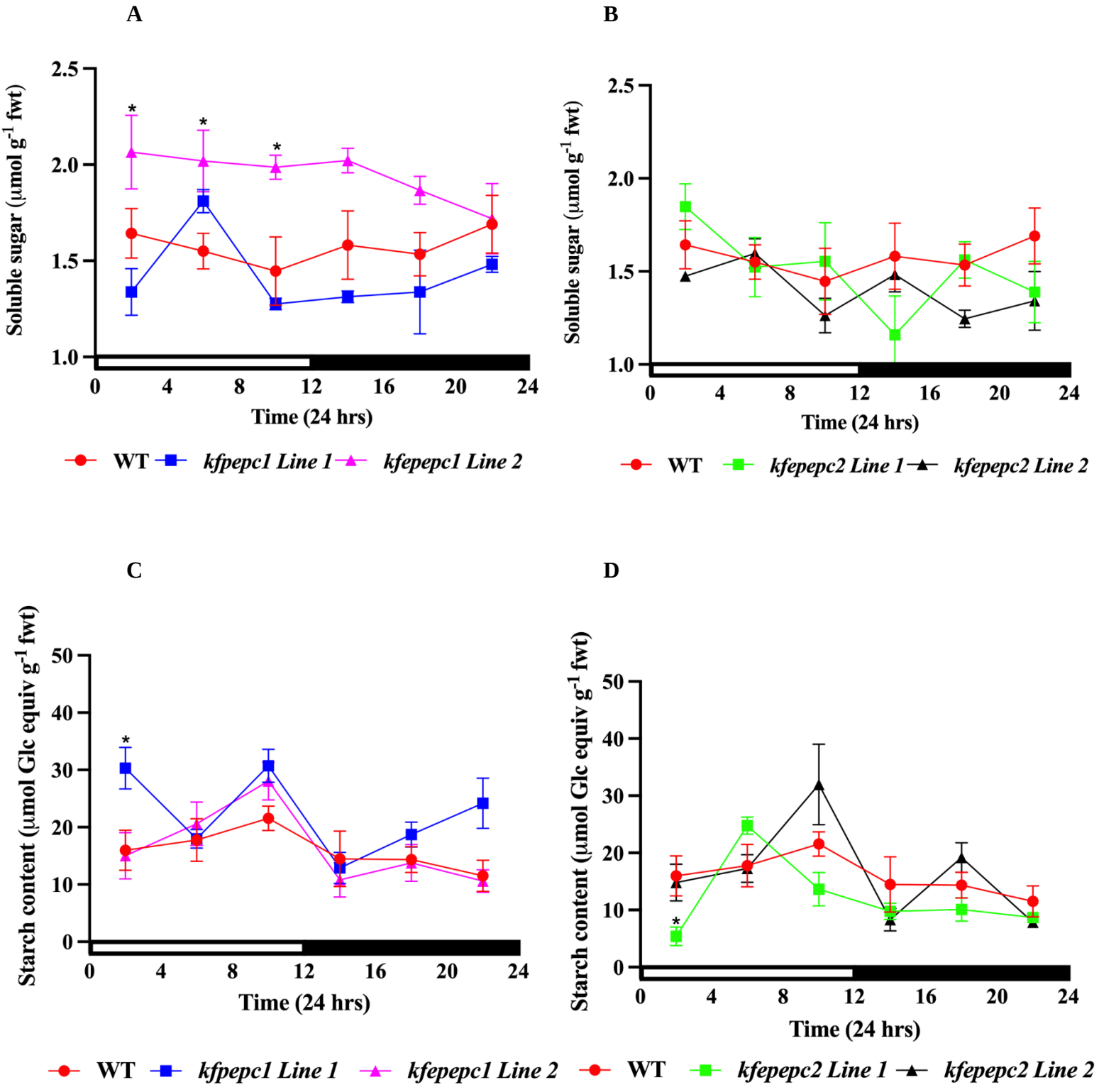

Figure 4.3. Comparing soluble sugar (a,b) and starch levels (c,d) of *kfepepc1* Line 1 (blue), *kfepepc1* L2 (purple), *kfepepc2* Line 1 (green), and *kfepepc2* Line 2 (black) mutant lines against wild type (red) *Kalanchoë fedtschenkoi* over a 24 hr period. Leaf pair eight (8) were used, and each measurement was done in 3 biological replicates. White and black bars represent the light period (12-h) and dark period (12-h), respectively. * Mean difference significant at p 0.05 when compared to the wild type.

4.4 Discussion

4.4.1 Knocking down KfePEPC1 switched the mutants from CAM to C_3 mode while KfePEPC2 knockdown affects stomatal conductance.

The involvement of the PEPC enzyme in the CAM pathway is well-known and widely reported (Chia-Yun et al. 2018; Borland et al. 2016a; Heyduk et al. 2021). A multigene family encodes PEPC with five genes (5) reported for *Kalanchoë fedtschenkoi* (Shu et al. 2020; Yang et al. 2017). Therefore, one of the aims of this thesis was to identify the PEPC isoform with a photosynthetic role in CAM. Gas exchange results showed that knocking out *KfePEPC1* led to a loss of nocturnal CO_2 uptake ability in the *kfepepc1* Line 1 mutant forcing the plant to switch to C_3 mode (Figure 4.1A). These results support the hypothesis that *KfePEPC1* encodes the CAM-specific isoform of phosphoenolpyruvate carboxylase and is in line with suggestions from several other researchers (Taybi and Cushman 2002; Chia-Yun et al. 2018; Boxall et al. 2020). *kfepepc1* Line 1 completely lost the ability to do CAM and, by implication, severely reduced the water use efficiency, increased the rate of water loss through transpiration, reduced the amount of CO_2 taken up at night and reversed the stomatal movement pattern. *kfepepc1* Line 2 did not show a reduction in nocturnal net CO_2 uptake, and this observation can be linked to the incomplete knockdown of the *KfePEPC1* gene in the mutants (Chapter 3). This incomplete knockdown also suggests a mismatch of the gRNA vector during the loss of function activity of the CRISPR-Cas9 process and is in line with findings by Xing et al. (2014) that mismatches caused the poor performance of T1B-TC gRNAs vectors in CRISPR/Cas9 mutation of *Arabidopsis*.

In contrast to the *kfepepc1* Line 1 mutant, both *KfePEPC2* mutants (*kfepepc2* Line 1 and *kfepepc2* Line 2) could take up CO_2 nocturnally, thereby maintaining 24 h carbon balance and optimal levels of water–use efficiency that was comparable to those in wild type. This observation supports the report that, of the most abundant PEPC isoforms found in *K. fedtschenkoi*, only the *KfePEPC1* isoform is involv26.ed in CAM (Boxall et al. 2020; Yang et al. 2017). Since CAM activity was not affected in the two *KfePEPC2* mutant lines (*kfepepc2* Line 1 and *kfepepc2* Line 2), water use efficiency in these lines was not altered compared to the wild type. However, stomatal behaviour in the two *KfePEPC2* mutants (*kfepepc2* Line 1 and *kfepepc2* Line 2) was different from what was observed in the wild type, as these mutants opened their stomata more during phase four (4) of CAM, which occurs towards the end of the light period and led to substantial net CO_2 uptake. This observation might indicate an

alteration in the circadian clock controlling stomatal behaviour in the *KfePEPC2* lines. The involvement of PEPC in the diel regulation of the circadian clock in CAM species has been reported by Males and Griffiths (2017) and Boxall et al. (2020). Boxall et al. (2020) reported that three (3) important core circadian clock genes, *Circadian Clock Associated1* (*CCA1-2), Lightnight-Inducible-Clock-Regulated3-like (LNK3), Early-Phytochrome-Responsive1 (EPR1)* and three (3) stomatal genes *Cryptochrome2 (CRY2), High leaf Temperature1* (*HT1), and Transcriptional regulator MYB61 gene* was downregulated while *Phototropin 2 (PHOT2)* gene was upregulated during the light period and down-regulated during the dark period as a result of silencing *PPC1* gene. Together, the data indicate that stomatal regulation in CAM can be affected by disrupting the activities of key enzymes like PEPC. *KfePEPC2* has been suggested to be a non -photosynthetic isoform with several physiological functions which could include control of stomatal movement which is achieved by influencing the internal CO_2 concentration in the mesophyll cells of the leaves and directly regulating organic acid metabolism in the guard cell to regulate stomatal conductance (Silvera et al. 2014; Cousins et al. 2007; Engineer et al. 2016; Bandyopadhyay et al. 2007).

Water–use efficiency, an essential attribute of the CAM mode of photosynthesis, was severely affected in the *kfepepc1* Line 1 mutant and manifested as an increased transpiration rate. This observation can be attributed to the mutation perturbing the activity of key genes linked to stomatal movement and the circadian clock system, leading to the mutant switching to the C_3 mode of photosynthesis and losing so much water via transpiration because of the daytime opening of stomata. Furthermore, Boxall et al. (2020) observed that silencing *PPC1* led to the upregulation of the *Phototropin1 (PHOT1)* gene, which encodes a protein kinase that acts as a blue light receptor. This meant that *PHOT1* transcripts peaked around 8-hrs into to light period relative to the wild type. Also, the *Cryptochrome2 (CRY2)* gene, which encodes a photoreceptor for blue light and entrainment of endogenous circadian rhythm and stomatal conductance, was upregulated because of *PPC1* silencing and reached maximum at dusk in contrast to the wild type, which peaked in the dark (Boxall et al., 2020). These reverse peaks in the transcript abundance of key genes implicated in stomatal conductance could explain the change in the pattern of stomatal behaviour in the *kfepepc1* Line 1 mutant. In *kfepepc1* Line 2, water – use efficiency level was like that of the wild type, probably because of the incomplete knockdown of *KfePEPC1* genes allowing the mutant to retain a considerable amount of CAM activity. This is because the mutant is not perturbing the activities of genes like *PHOT1* and *CRY2* linked to blue light reception and endogenous

circadian rhythm. In *KfePEPC2* mutants, water–use efficiency was maintained, and this can be attributed to the fact that knocking down the *KfePEPC2* gene did not lead to the plants opening their stomata until the later part of the light period when the temperature is cooler, thus helping to reduce water loss via transpiration.

4.4.2 Diel titratable acid turnover is affected by knocking down KfePEPC1.

A strong relationship between nocturnal CO_2 uptake and malic acid accumulation has been firmly established as a distinguishing feature of CAM photosynthesis (Nimmo et al. 1984; Taybi et al. 2004; Dodd et al. 2002; Boxall et al. 2020). CAM plants store the CO_2 captured at night in the form of malic acid and release the CO_2 during phase three (3) through the decarboxylation process so that RuBisCO can fix CO_2 into the Calvin cycle whilst stomata remain closed. These acids, when formed, are stored overnight in the vacuoles located in the mesophyll cells of the leaves (Borland et al. 2016a). The results described above showed significantly reduced nocturnal acid accumulation, and indeed titratable acid levels were lower than the wild type throughout the entire day/night cycle level in *kfepepc1* Line 1, where the *KfePEPC1* gene was fully knocked down. Furthermore, measuring titratable acid levels at dawn and dusk phases in the double mutant plants (*kfepepc1/2* Line 1 and *kfepepc1/2* Line 2) revealed reduced accumulation of nocturnal titratable acids, highlighting the implication of *KfePEPC1* isogene in CAM. In *kfepepc1* Line 2, nocturnal CO_2 uptake and titratable acid accumulation were not perturbed, and this seems to be a result of partial knockdown of the *KfePEPC1* gene. This observation is similar to that reported by Boxall et al. (2020) when the expression of the *KfePEPC1* gene was suppressed using RNAi. This observation of reduced titratable acidity is a piece of strong evidence that *KfePEPC1* is the isoform that performs the photosynthetic function. However, to have a noticeable change in CAM activity and titratable acidity contents, a complete knockdown of *KfePEPC1* is required. Knocking down the *KfePEPC2* gene did not affect nocturnal acid accumulation. Acid accumulation patterns in the two (2) *kfepepc2* lines were similar to those in the wild type, an indication that knocking down this isoform did not affect the process of CAM and confirmed reports from O'Leary et al. (2011) and Arias-Baldrich et al. (2017) of the presence of PEPC isoforms with a non-photosynthetic function.

4.4.3 Carbon homeostasis is affected by perturbing the activity of PEPC.

The importance of starch and soluble sugars in the CAM process is well known. Starch, in particular, serves as a source for producing the substrate phosphoenolpyruvate (PEP) in

Kalanchoë species, which captures the CO_2 from air at night in the form of HCO_3^- before use in the CAM process (Borland et al. 2016a). A key observation made from this study is that knocking down the *KfePEPC1* gene completely in the Line 1 mutant of *K. fedtschenkoi* affected the availability of carbohydrate reserves; hence, starch content increased overnight. This observation was the opposite of what was observed in the wild type, *kfepepc1* Line 2, *kfepepc2* Line 1 and *kfepepc2* Line 2, where the amount of starch decreased at night. In CAM photosynthesis, it has been observed that starch accumulated during the light and dark periods is broken down to produce the substrate (PEP) needed to capture atmospheric CO_2 (Weise et al. 2011; Boxall et al. 2020; Taybi et al. 2017). Thus, starch accumulated in the *KfePEPC1* deficient Line 1 at night because starch is no longer used to make substrate like PEP, which is needed to capture atmospheric CO_2 by PEPC during the process of CAM (Chen et al. 2002; Taybi et al. 2017; Boxall et al. 2020). Altered timing of diel starch in turnover in *kfepepc1* Line 1 mutant may also be an indication of circadian clock alteration, which would further confirm the hypothesis that CAM genes are regulated by an endogenous circadian clock system (Borland and Taybi 2004; Lüttge et al. 2000; Dodd et al. 2002). Since it is well known that the *KfePEPC1* isoform is involved in the CAM, knocking down the gene will lead to noticeable changes in key metabolic indicators of the CAM process. This finding is in agreement with the observation by Boxall et al. (2020), who found that dawn-phased transcription of genes implicated in the starch breakdown, such as β-amylase 1*(BAM1),* β-amylase 3 *(BAM3),* and β-amylase 9 *(BAM9),* as well as the sugar transporter gene Glucose-6-phosphate transporter 2 (*GPT2*), were downregulated as a result of silencing the *KfePEPC1* gene.

Furthermore, day/night soluble sugar data show that in partially knockdown *kfepepc1* Line 2 mutant, there is a high accumulation of soluble sugars during the light period and depletion of this soluble sugar by the end of the dark period. These soluble sugars may be used to synthesize substrates like D-2-Phosphoglycerate (2GP) which is converted to phosphoenolpyruvate (PEP), a substrate for nocturnal β-carboxylation. In contrast, the complete knockdown of *KfePEPC2* had no such effect on the metabolic carbon homeostasis of *K. fedtschenkoi*. Knocking down the *KfePEPC2* gene did not affect the pattern of carbohydrate use in CAM. This observation can be attributed to the non-photosynthetic role of the *KfePEPC2* isoform.

4.5 Conclusions

Results have confirmed that completely knocking down the *KfePEPC1* gene has severe implications for CAM photosynthesis, causing the plants to switch to a C_3 mode of photosynthesis, altering the diel carbohydrate and starch turnover patterns reducing the level of titratable acids accumulated overnight.

Partially knocking down the *KfePEPC1* gene does not significantly affect key CAM attributes already mentioned and completely knocking down the *KfePEPC2* gene did not affect the process of CAM in *K. fedtschenkoi*.

Results showed that stomatal behaviours of both *KfePEPC1* and *KfePEPC2* mutants were altered due to the knockdown leading to the mutant plants significantly opening their stomata more than wild type during phase four (4) of CAM in *kfepepc1* Line 2, *kfepepc2* Line 1 and *kfepepc2* Line 2 mutants, respectively. This observation confirmed that both *KfePEPC1* and *KfePEPC2* genes have functions implicated in stomatal regulation.

Chapter 5 Effect of PEPC knockdown on the growth performance, stomatal anatomy, and drought response of *Kalanchoë fedtschenkoi*

5.1 Introduction.

CAM, as a mode of photosynthesis, enables plants to perform several functions essential to their continued existence. These functions include concentrating much-needed carbon for improved photosynthesis, enhancing water–use efficiency and improving the ability to tolerate drought (Taybi et al. 2017; Borland et al. 2009; Borland et al. 2016b). There is still some debate about whether the water-conserving and drought-tolerating benefits of CAM come at a cost. Studies have indicated that CAM requires more substrate and energy inputs than C_3 photosynthesis to function effectively, suggesting that CAM is expensive and could potentially compromise growth (Schweiger et al. 2021). However, recent modelling efforts have indicated that the ability of CAM plants to liberate a massive amount of CO_2 behind closed stomata can suppress photorespiration in some CAM phases, and the adoption of an energy-conserving phosphorolytic pathway to break down starch predicts that CAM maintains high productivity in some CAM plants compared to C_3 photosynthesis (Shameer et al. 2018). The generation of *kfepepc1* mutants deficient in CAM (Chapter 3, Chapter 4) presents a novel opportunity for examining how the operation of CAM impacts plant growth and drought tolerance.

Aside from CAM, other strategies exist for conserving water and surviving drought in plants that grow in arid, semiarid, and marginal lands. One of these adaptations is succulence, with succulent leaves and stems providing water-filled tissue, which acts as a buffer against water loss via transpiration (Males and Griffiths 2017; Ogburn and Edwards 2012). Succulence can exist as an all-cell or a storage form in plants (Griffiths and Males 2017). In the all-cell forms of succulence, plants utilise their leaves as single-use water stores to cushion the effect of water loss via transpiration. In contrast, in the storage succulence form, the plants store water in specialised hydrenchyma over a long period to buffer against transpiration and drought. When water is available, they refill the hydrenchyma (Males 2017; Griffiths and Males 2017). Succulent plant species use various types of photosynthesis to cater to their carbon assimilation needs. However, CAM photosynthesis has been identified as integral to succulence (and vice versa) with the vacuole available for water and malate storage, suggesting that CAM is optimised in the presence of adequate succulence (Griffiths and

Males 2017; Males 2017; Barrera Zambrano et al. 2014). The CAM-deficient *kfepepc1* mutants described in this thesis present an opportunity for examining the interdependence of succulence and CAM. Measuring succulence in plants is usually a difficult and time consuming process but measuring the saturated water content which relates to capacitance in leaves provides a crucial insight to the tissue succulence of the leaves (Ogburn and Edwards 2012).

Tolerance to drought stress is an essential advantage that plants gain from using the CAM form of photosynthesis (Borland et al. 1998; Maiquetía et al. 2008; Yang et al. 2015b; Abraham et al. 2016). This is due to CAM equipping these plants with storage capacities that help them adjust to drought stress and an improved water use efficiency compared to those with C_3 and C_4 photosynthesis. Thus, CAM increases survivability in marginal lands where the threat of drought stress is a real possibility (Nada et al. 2015; Yan et al. 2015; Yang et al. 2015a; Lüttge 2004). Adverse effects of drought stress in plants include reduced growth and increased production of reactive oxygen species (ROS), which causes oxidative stress that affects, among other things, photosynthetic pigments like chlorophyll and carotenoids (Ślesak et al. 2008; Miszalski et al. 2003). Measuring pigment composition can serve as a way of examining how plants respond to drought stress (Habibi 2018). A further aim of this chapter is also to examine how CAM deficiency, as seen in the *kfepepc1* mutants, impacts pigment composition under drought.

Another adaptation found in plants that inhabit water-limited habitats concerns stomatal patterning. Stomata play an essential role in regulating the amount of CO_2 plants access from the air. The amount of water lost to the environment and stomatal patterning is crucial for understanding strategies for optimising water use efficiency and mitigating drought stress (Bertolino et al. 2019). Factors that affect stomatal density, stomatal size (pore length), stomatal pore index and stomatal function, in general, include CO_2 concentration, light intensity, and water availability (Bertolino et al. 2019; Doheny-Adams et al. 2012; Dodd et al. 2002). In CAM plants, the unique day/night pattern of stomatal closing/opening is central to the water-conserving properties of the pathway, suggesting that stomatal patterning is less critical in influencing water use (Males and Griffiths 2017; Borland et al. 2018). The CAM-deficient *kfepepc1* mutants enable the testing of hypotheses regarding the interdependence of CAM and stomatal patterning and are a further aim of the present chapter.

This chapter examines the importance of CAM to growth, drought tolerance, and the interdependence of CAM with succulence and stomatal patterning in *Kalanchoë fedtschenkoi*.

Chapter 4 showed that CRISP-Cas9 knockdown of *KfePEPC1* compromised CAM activity, whilst knockdown of *KfePEPC2* altered stomatal behaviour without compromising nocturnal CAM activity. By comparing the growth, succulence, stomatal patterning, and drought tolerance traits of these different CRISPR-Cas9 mutants (including *kfepepc1/2* double mutants) to those of wild type, the following hypotheses were tested:

Hypothesis 1: Growth is compromised when CAM is knocked down in CAM plants.

Hypothesis 2: Knocking down CAM leads to reduced stomatal density.

Hypothesis 3: The ability of *K. fedtschenkoi* to tolerate drought is severely reduced when CAM is knocked down.

Hypothesis 4: Knocking down CAM reduces the requirement for leaf succulence in *K. fedtschenkoi*.

5.2 Material and methods

5.2.1 Plant material

Kalanchoë fedtschenkoi, a CAM model plant, was used for experiments carried out in this study. Our colleagues at Oakridge National Laboratories, United States of America, used clusters of randomly interspaced short palindromic repeats and CRISPR associated protein 9 (CRISPR-Cas9) loss of function technique to generate PEPC-deficient plants and two independent lines for each mutant. These lines lost *KfePEPC1* and *KfePEPC2* in the single mutant lines and *KfePEPC1* and *KfePEPC2* together in the double mutant lines, respectively.

The wildtype and mutant lines were propagated vegetatively, and the process is described in section 2.1 (Chapter 2).

5.2.2 Growth measurements

All the growth measurements carried out on the plants and their methods are described in section 2.2 (Chapter 2).

5.2.3 Drought treatment

Details of how the plants were exposed to drought stress conditions are described in section 2.10 (Chapter 2).

5.2.4 Succulence measurement

The methods used to measure the saturated water content of the plants are described in section 2.11 (Chapter 2).

5.2.5 Chlorophyll and carotenoid content assay

Chlorophyll and carotenoid content of the well-watered and drought-stressed *Kalanchoë fedtschenkoi* were measured using a method described in section 2.12 (Chapter 2).

5.2.6 Stomatal density, pore length and stomatal pore area index (SPI) measurements.

Stomatal density and pore length were measured using section 2.13 (Chapter 2). The stomatal pore area index (SPI) was calculated using the formula described in section 2.13 (Chapter 2).

5.3 Results.

5.3.1 Plant height

The growth performance of *Kalanchoë fedtschenkoi* wildtype and *KfePEPC* mutant plants was accessed by measuring the increase in plant height per week, the rate of leaves proliferation per week, and the total leaf area of the plants.

Examining the rate of increase in plant height per week showed that in *kfepepc1* mutants, there was no significant difference ($p \leq 0.05$) compared to the wildtype in week one and week four and week six (A). However, in week five, the rate of increase in plant height for *kfepepc1* Line 2 was significant ($p \leq 0.05$) compared to the wildtype (Figure 5.1A). For the *kfepepc2* mutants, results show no significant difference ($p \leq 0.05$) in the increase in plant height per week for week one and week four. However, at weeks five and six, the *kfepepc2* Line 1 mutant showed a significant reduction ($p \leq 0.05$) in the rate of increase in height (Figure 5.1B). For the double mutants (*kfepepc1/2* Line 1 and *kfepepc1/2* Line 2), there was a

significant decrease ($p \leq 0.05$) in the rate of increase in plant height per week from week two to week six (Figure 5.1C) compared to that of wild type.

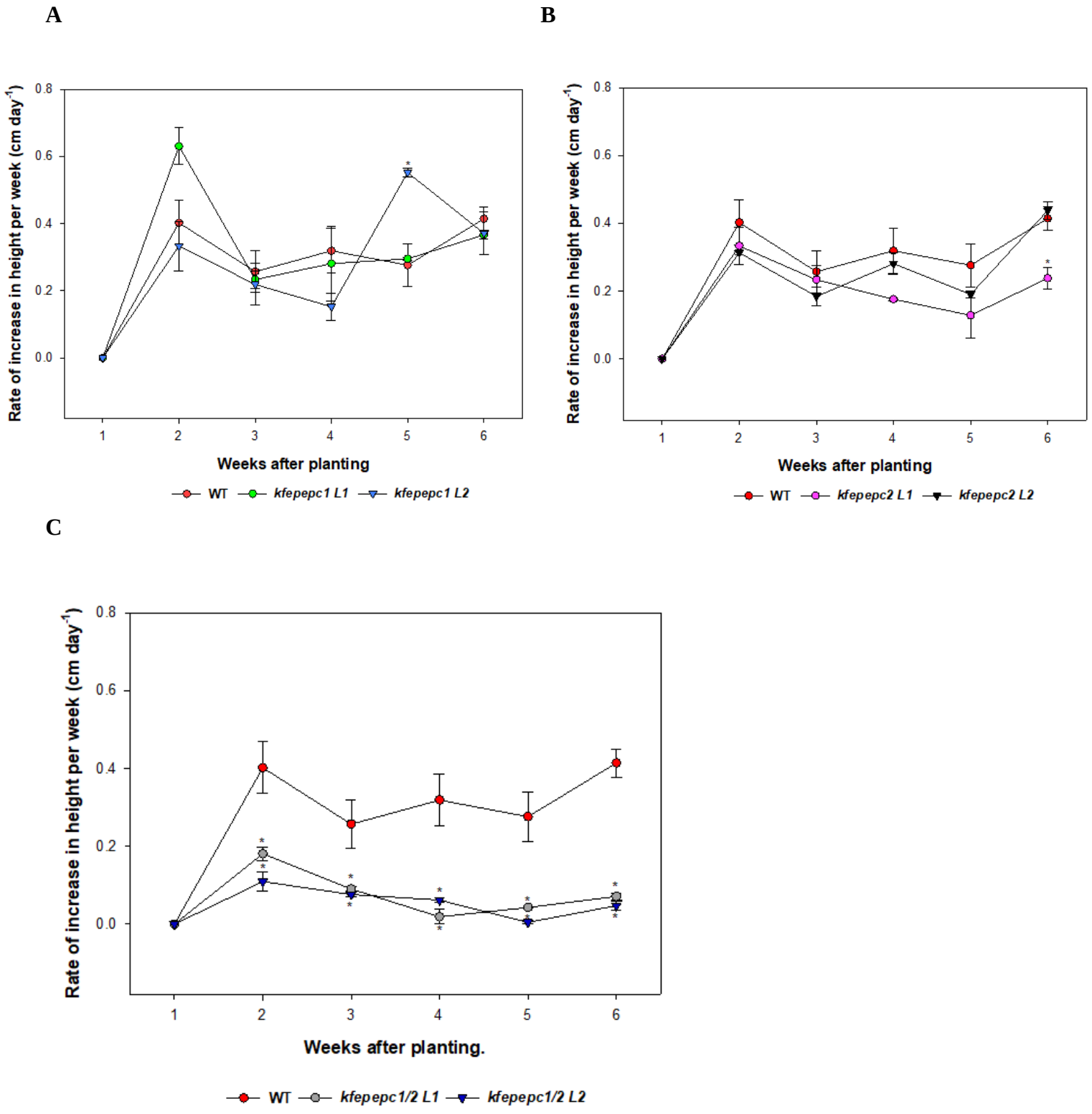

Figure 5.1. The plant height results presented as both the rate of increase in height per week for wildtype (red), *kfepepc1* Line 1 (blue), *kfepepc1* Line 2 (purple), *kfepepc2* Line 1 (green) and *kfepepc2* Line 2 (black), *kfepepc1/2* Line 1 (grey) and *kfepepc1/2* Line 2 (black) over six (6) weeks.

The error bars represent the standard error of three (3) biological replicates. * Mean difference is significant ($p \leq 0.05$) compared to the wildtype.

5.3.2 Number of leaves and leaf area

As part of investigating the growth performance of the plants, the rate of leaf proliferation per week and the total leaf area of the plants were measured in this study. The results from the rate of leaf proliferation per week showed no significant increase ($p \leq 0.05$) in the rate of leaf proliferation of the *kfepepc1* mutants (*kfepepc1* Line 1 and *kfepepc1* Line 2) and the *kfepepc2* mutants (*kfepepc2* Line 1 and *kfepepc2* Line 2) compared to the wildtype (Figure 5.2A&B). In the double mutants, there was a significant reduction ($p \leq 0.05$) in the rate of leaf proliferation in week three, week four, and week five. However, in week two, *kfepepc1/2* Line 1 showed a significant increase in the rate of leaf proliferation ($p \leq 0.05$). Furthermore, in week six, *kfepepc1/2* Line 2 showed a significant increase ($p \leq 0.05$) in the rate of leaf proliferation (Figure 5.2C).

Results from measuring the mean total leaf area of all the *K. fedtschenkoi* genotypes used in this study showed there was no statistically significant difference between the total leaf area of the *kfepepc1* (*kfepepc1* Line 1 and *kfepepc1* Line 2) mutants and *kfepepc2* (*kfepepc2* Line 1 and *kfepepc2* Line 2) mutants ($p \leq 0.05$) when compared to the wildtype while the double mutants (*kfepepc1/2* Line 1 and *kfepepc1/2* Line 2) showed significantly reduced total leaf area ($p \leq 0.05$) when compared to the wildtype (Figure 5.2D).

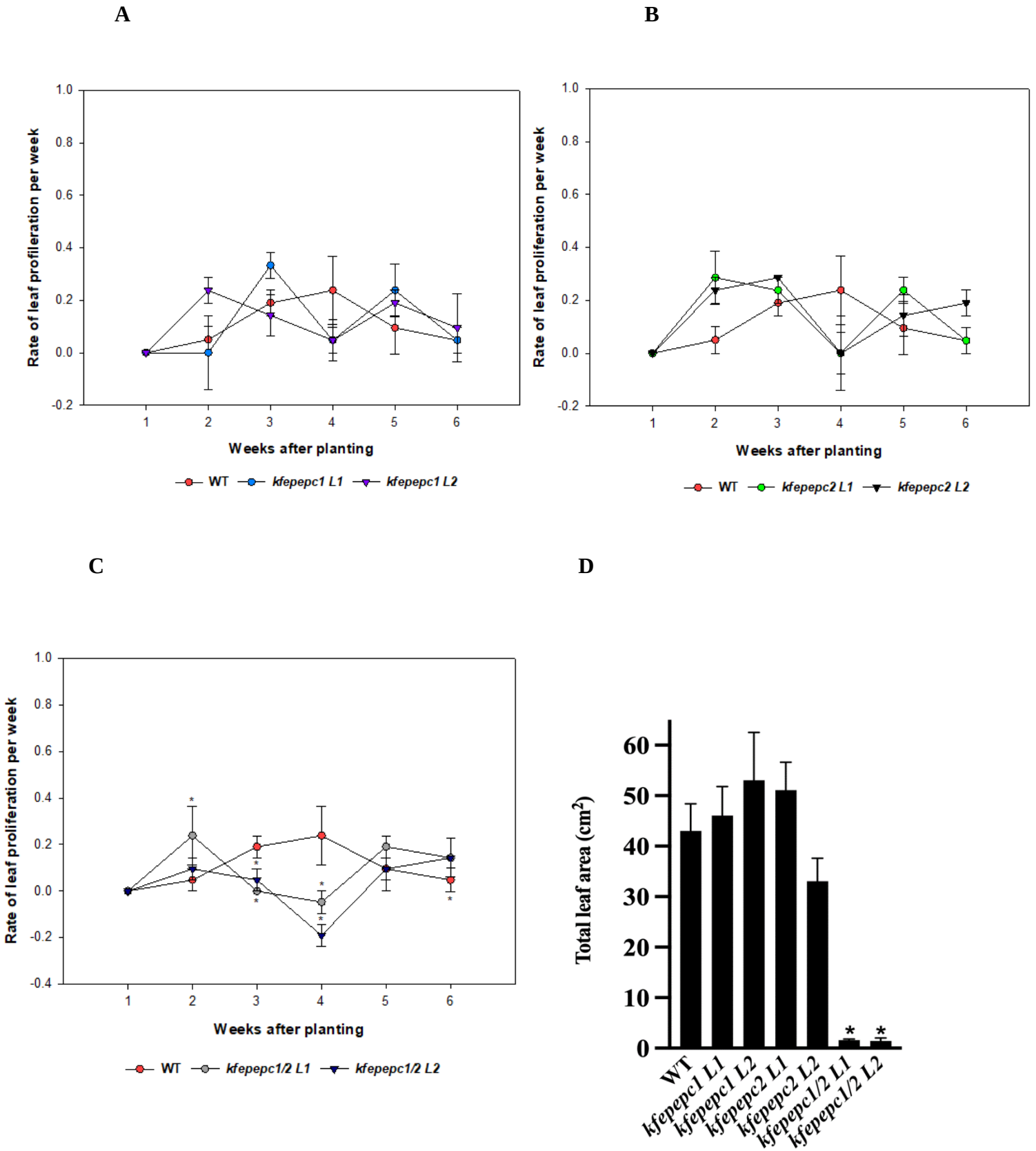

Figure 5.2. The mean number of leaves results presented as the rate of leaf proliferation per week (a-c) for wildtype (red), *kfepepc1* Line 1 (blue), *kfepepc1* Line 2 (purple), *kfepepc2* Line 1 (green) and *kfepepc2* Line 2 (black), *kfepepc1/2* Line 1 (grey) and *kfepepc1/2* Line 2 (black) over six (6) weeks and the total leaf area (d) for all the *K. fedtschenkoi* phenotype used for the study. The error bars

represent the standard error of three (3) biological replicates. * shows a significant difference at $p \leq 0.05$.

5.3.3 Fresh and dry weight analysis

The mean shoot fresh weight results showed no significant difference between *kfepepc1* and *kfepepc2* mutants ($p \leq 0.05$) compared to the wild type. In contrast, the double mutants (*kfepepc1/2* Line 1 and *kfepepc1/2* Line 2) showed a statistically significant reduction in fresh shoot weight ($p \leq 0.05$) compared to the wild type shoot fresh weight (Table 5.1)

The mean shoot dry weight results showed that *kfepepc1* Line 1 mutant had a significantly higher mean dry weight ($p \leq 0.05$) when compared to the wild type mean dry weight (Table 5.1). Conversely, there was no significant difference ($p \leq 0.05$) between the mean shoot dry weight of *kfepepc1* Line 2, and *kfepepc2* Line 1 compared to the mean shoot dry weight of the wild type (Table 5.1). However, the *kfepepc1* Line 1 and double mutants (*kfepepc1/2* Line 1 and *kfepepc1/2* Line 2) had significantly reduced mean shoot dry weight compared to that of the wild type (Table 5.1).

The root fresh weights of *kfepepc1* Line 1, *kfepepc2* Line 2, *kfepepc1/2* Line 1 and *kfepepc1/2* Line 2 showed significantly reduced weights ($p \leq 0.05$) when compared to the wildtype (Table 5.1).

kfepepc1 and *kfepepc2* mutants showed significantly increased ($p \leq 0.05$) root dry weight when compared to the wild type (Table 5.1).

The shoot-to-root fresh weight ratio results are shown in (Table 5.1). These results indicated no mutant had a statistically significant ($p \leq 0.05$) difference in the shoot-to-root fresh weight ratio compared to the wild type.

The mean shoot-to-root dry weight ratio recorded showed that only the *kfepepc1* Line 1 mutant had a significantly higher ($p \leq 0.05$) shoot-to-root dry weight than the wild type.

Table 5.1. The shoot/root fresh and dry weights and shoot/root fresh and dry weight ratios of the wildtype, *kfepepc1* Line 1, *kfepepc1* Line 2, *kfepepc2* Line 1, *kfepepc2* Line 1, *kfepepc1/2* Line 1, and *kfepepc1/2* Line 2 mutants of *Kalanchoë fedtschenkoi*. Data are presented as the mean and standard error of three (3) biological replicates. ^{NS} represents no significant difference ($p \leq 0.05$) while * represents a significant difference at $p \leq 0.05$ when compared to the wild type.

Sample	Shoot fresh weight	Shoot dry weight	Root fresh weight	Root dry weight	Shoot-to-root fresh weight ratio	Shoot-to-root dry weight ratio
Wildtype	37.40 ± 4.77	3.16 ± 0.54	2.20 ± 0.46	0.43 ± 0.08	19.74 ± 6.56	8.06 ± 2.54
***kfepepc1* Line 1**	33.94 ± 4.77^{NS}	5.19 ± 0.75*	1.06 ± 0.12*	0.25 ± 0.02*	31.99 ± 0.89^{NS}	20.93 ± 3.26*
***kfepepc1* Line 2**	34.76 ± 6.96^{NS}	3.87 ± 1.05^{NS}	1.58 ± 0.32^{NS}	0.26 ± 0.05*	23.57 ± 6.20^{NS}	16.32 ± 5.57^{NS}
***kfepepc2* Line 1**	41.65 ± 1.91^{NS}	2.60 ± 0.43^{NS}	1.42 ± 0.20^{NS}	0.33 ± 0.07*	30.08 ± 2.93^{NS}	9.26 ± 3.04^{NS}
***kfepepc2* Line 2**	25.76 ± 2.87^{NS}	2.15 ± 0.22^{NS}	0.85 ± 0.08*	0.19 ± 0.04*	30.48 ± 3.63^{NS}	11.78 ± 1.82^{NS}
***kfepepc1/2* Line 1**	7.85 ± 0.52*	0.43 ± 0.06*	0.53 ± 0.11*	0.07 ± 0.02*	16.67 ± 4.95^{NS}	6.79 ± 2.11^{NS}
***kfepepc1/2* Line 2**	9.40 ± 4.27*	0.39 ± 0.20*	0.71 ± 0.30*	0.10 ± 0.03*	12.76 ± 0.71^{NS}	3.47 ± 0.87^{NS}

5.3.4 Stomatal anatomy measurements.

The parameters measured include stomatal density, stomatal pore (guard cell) length, and stomatal pore area index (SPI).

The mean adaxial stomatal density results showed that knocking down *kfepepc1* and *kfepepc2* mutants led to a significantly reduced adaxial stomatal density ($p \leq 0.05$) compared to the wild type. However, knocking down *KfePEPC1* had no significant effect on the abaxial stomatal density of *kfepepc1* Line 1 and *kfepepc1* Line 2 mutants ($p \leq 0.05$) (Figure 5.3A). Knocking down *KfePEPC2* significantly reduced the abaxial stomatal density of *kfepepc2* Line 1 ($p \leq 0.05$) but did not significantly affect the stomatal density of *kfepepc2* Line 2 mutant when compared to the wildtype. (Figure 5.3A).

The mean adaxial pore length results showed that the mean adaxial pore lengths of *kfepepc1* Line 1, *kfepepc2* Line 1, and *kfepepc2* Line 2 were significantly higher ($p \leq 0.05$) when compared to that of the wildtype. At the same time, the adaxial stomatal pore length of *kfepepc1* Line 2 was not significantly different ($p \leq 0.05$) when compared to the wild type (Figure 5.3B).

There was no significant difference ($p \leq 0.05$) in the abaxial stomatal pore length of the mutants compared to the wild type (Figure 5.3B). In contrast, the abaxial stomatal pore length of *kfepepc2* Line 2 was significantly higher ($p \leq 0.05$) when compared to the wild type (Figure 5.3B).

There was no significant difference ($p \leq 0.05$) in the stomatal pore area index (SPI) of either the adaxial or abaxial epidermis of the *kfepepc1* and *kfepepc2* mutants when compared to the wildtype (Table 5.2).

A

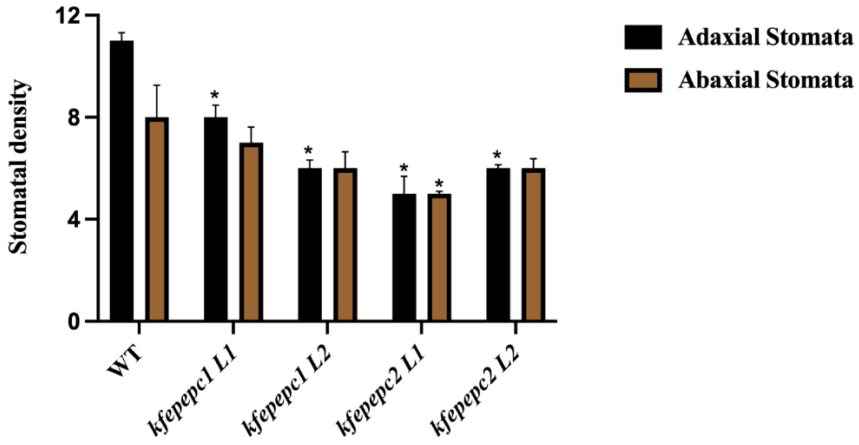

B

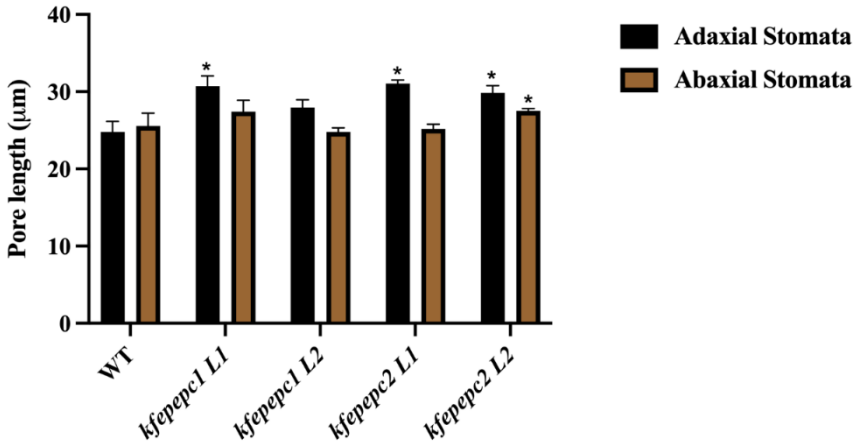

Figure 5.3. Adaxial (black), abaxial (brown), stomatal density (a) and pore length (b) of the wild type and all mutants. The shoot-to-root fresh weight is shown in (black) bars, while the shoot-to-root dry weight is shown (in grey) bars. The error bars represent the standard error of three (3) biological replicates. *Mean difference significant at p 0.05 when compared to the wild type.

Table 5.2. The stomatal pore area index (SPI) of the adaxial and abaxial stomata of wildtype, *kfepepc1* Line 1, *kfepepc1* Line 2, *kfepepc2* Line 1 and *kfepepc2* Line 2 mutants of *Kalanchoë fedtschenkoi*. The formula proposed by Bucher et al. (2016) SPI = (Guard cell length)^2 *Stomatal density was used to calculate SPI. Data were presented as the mean of three (3) biological replicates. ^{NS} represents no significant difference at p 0.05 compared to the wildtype SPI.

Genotype	**Adaxial Stomatal pore area index (SPI) (x10^2)**	**Abaxial Stomatal pore area index (SPI) (x10^2)**
Wildtype	64.94 ± 6.09	45.10 ± 10.89
***kfepepc1* Line 1**	73.78 ± 10.90^{NS}	55.46 ± 8.47^{NS}
***kfepepc1* Line 2**	45.19 ± 4.70^{NS}	38.31 ± 2.87^{NS}
***kfepepc2* Line 1**	52.17 ± 8.31^{NS}	31.53 ± 1.75^{NS}
***kfepepc2* Line 2**	54.74 ± 2.78^{NS}	48.92 ± 3.67^{NS}

5.3.5 Succulence measurement and drought response

The effect of knocking down *KfePEPC* genes on the succulence of the *kfepepc1* and *kfepepc2* mutants of *K. fedtschenkoi* plants and their physiological response to two weeks of drought stress were measured. These results are presented as saturated water content (Figure 5.4A), chlorophyll content (Figure 5.4B-5.4D), and carotenoid content (Figure 5.4E).

The saturated water content results showed that there was no significant difference ($p \leq 0.05$) between the well-watered and drought-stressed plants of each genotype (wildtype and *kfepepc1* and *kfepepc2* mutant lines) (Figure 5.4A). however, the saturated water content results also showed that well-watered plants of *kfepepc1* Line 1 mutant had significantly higher ($p \leq 0.05$) saturated water content than the wild type (Figure 5.4A). Comparing the saturated water content amongst drought-stressed plants showed that *kfepepc1* Line 1 and *kfepepc1* Line 2 mutants were significantly higher ($p \leq 0.05$) than the wild type (Figure 5.4A).

The chlorophyll a content measurement results showed that in well-watered conditions, *kfepepc1* Line 1 and *kfepepc1* Line 2 mutants had significantly higher ($p \leq 0.05$) chlorophyll

a content than the wildtype (Figure 5.4B). In drought-stressed conditions, however, *kfepepc1* Line 1 and *kfepepc2* Line 1 had significantly higher ($p \leq 0.05$) chlorophyll a content than the wild type (Figure 5.4B). Furthermore, comparing the chlorophyll a content between well-watered and drought-stressed plants between each genotype showed that drought-stressed *kfepepc1* Line 1, *kfepepc2* Line 1, and *kfepepc2* Line 2 mutants had significantly higher ($p \leq 0.05$) chlorophyll a content compared to their well-watered pair (Figure 5.4B).

The chlorophyll b content measurement results showed that in well-watered conditions, *kfepepc1* Line 1 had significantly higher ($p \leq 0.05$) chlorophyll b content than the wild type (Figure 5.4C). In drought-stressed conditions, however, *kfepepc1* Line 1 and *kfepepc2* Line 1 had significantly higher ($p \leq 0.05$) chlorophyll b content than the wild type (Figure 5.4C). Furthermore, comparing the chlorophyll b content between well-watered and drought-stressed plants between each genotype showed that drought-stressed *kfepepc1* Line 1mutant had significantly higher ($p \leq 0.05$) chlorophyll b content compared to their well-watered pair (Figure 5.4C).

The total chlorophyll content measurement results showed that in well-watered conditions, *kfepepc1* Line 1 and *kfepepc1* Line 2 had significantly high ($p \leq 0.05$) total chlorophyll content compared to the wildtype (Figure 5.4D). In drought-stressed conditions, *kfepepc1* Line 1 and *kfepepc2* Line 1 had significantly higher ($p \leq 0.05$) total chlorophyll content compared to the \wild type (Figure 5.4D). Furthermore, comparing the total chlorophyll content between well-watered and drought-stressed plants between each genotype showed that drought-stressed *kfepepc1* Line 1, *kfepepc2* Line 1 and *kfepepc2* Line 2 mutants had significantly higher ($p \leq 0.05$) total chlorophyll contents compared to their well-watered pairs (Figure 5.4D)

The carotenoid content measurement results showed that in well-watered conditions, *kfepepc1* Line 1 had significantly higher ($p \leq 0.05$) carotenoid content compared to the wild type (Figure 5.4E). In drought-stressed conditions, again, *kfepepc1* Line 1 had significantly higher ($p \leq 0.05$) carotenoid content compared to the wild type (Figure 5.4E). Furthermore, comparing the carotenoid content between well-watered and drought-stressed plants between each genotype showed that drought-stressed wildtype, *kfepepc1* Line 1, *kfepepc2* Line 1, and *kfepepc2* Line 2 mutants had significantly higher ($p \leq 0.05$) carotenoid contents compared to their well-watered pairs (Figure 5.4E)

A

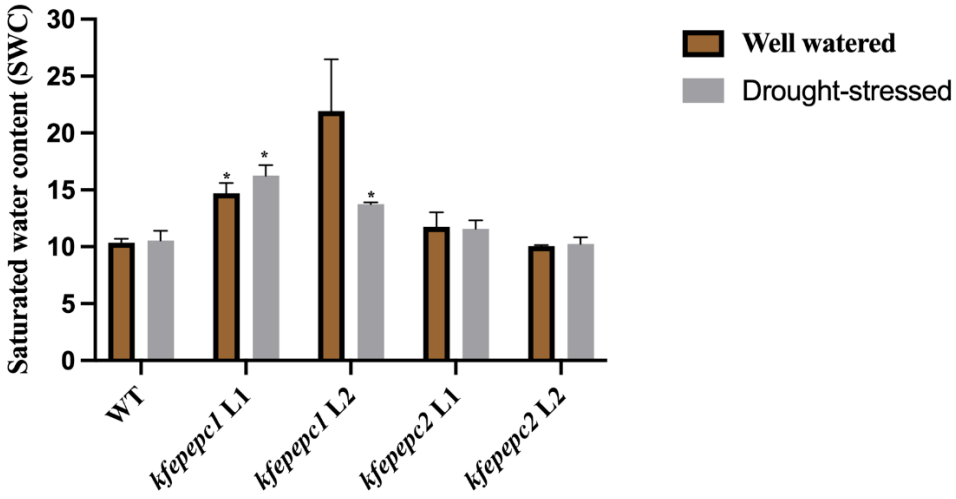
Saturated water content (SWC)
30
25
20
15
10
5
0
WT
kfepepc1 L1
kfepepc1 L2
kfepepc2 L1
kfepepc2 L2
Well watered
Drought-stressed

B

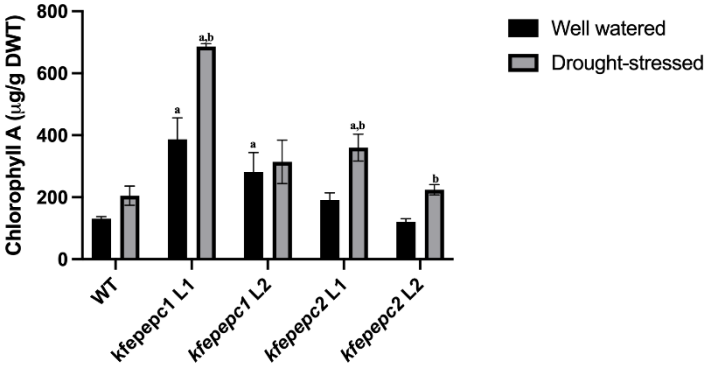
Chlorophyll A (µg/g DWT)
800
600
400
200
0
a
a,b
a
a,b
b
WT
kfepepc1 L1
kfepepc1 L2
kfepepc2 L1
kfepepc2 L2
Well watered
Drought-stressed

C

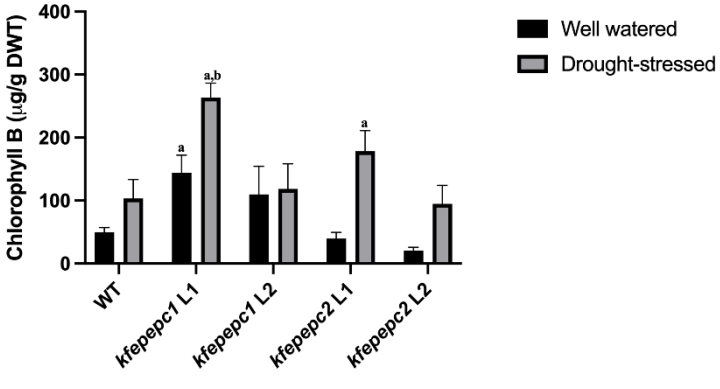
Chlorophyll B (µg/g DWT)
400
300
200
100
0
a
a,b
a
WT
kfepepc1 L1
kfepepc1 L2
kfepepc2 L1
kfepepc2 L2
Well watered
Drought-stressed

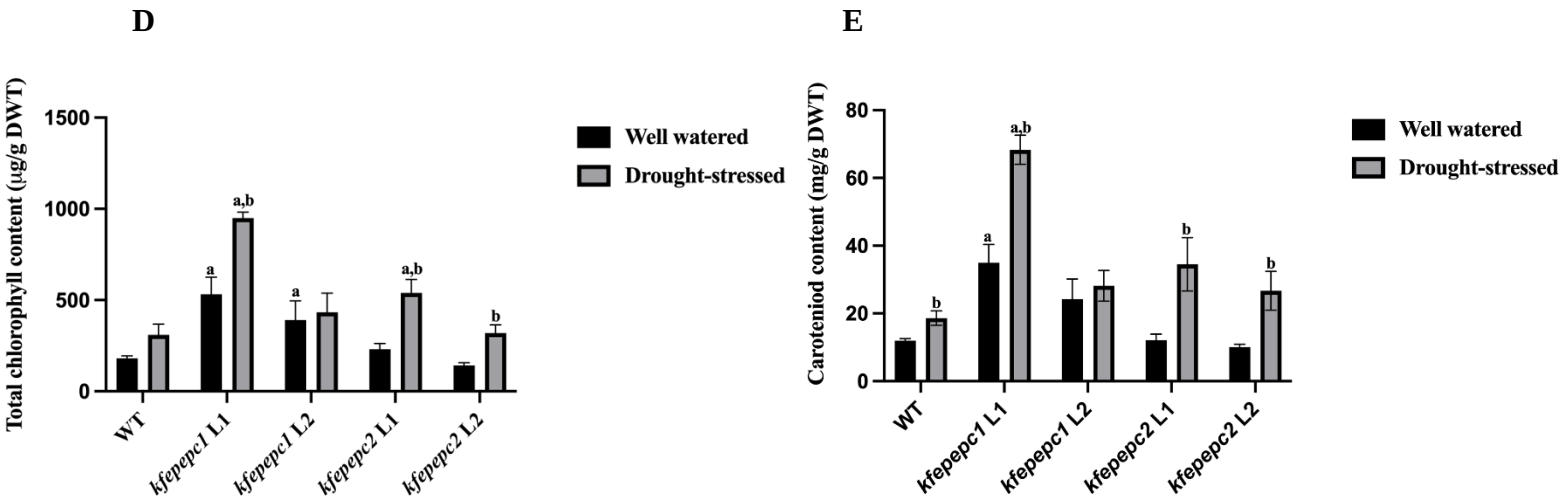

Figure 5.4. Saturated water content (a) for well-watered (brown) and drought-stressed (grey), chlorophyll A content (b), chlorophyll B content (c), total chlorophyll content (d), carotenoid content (e) for well-watered (black) and drought-stressed (grey) *K. fedtschenkoi* wildtype, *kfepepc1,* and *kfepepc2* mutant plants. Data presented as the mean of three (3) biological replicates. **a** show a significant difference ($p \leq 0.05$) in pigment content compared to the wildtype, while **b** show a significant difference ($p \leq 0.05$) when pigment contents of well-watered and drought-stressed pairs of each genotype were compared.

5.4 Discussion

5.4.1 Knocking down KfePEPC2 gene suppressed the growth of K. fedtschenkoi mutants while knocking down KfePEPC1 did not affect growth.

For CAM plants, one key benefit of enhanced water use efficiency (WUE) is the ability to maintain optimal growth conditions and yield with a minimal supply of water in marginal lands (Boxall et al. 2017; Borland et al. 2009; Borland et al. 2014; Liu et al. 2019a). To fully understand the role of phosphoenolpyruvate carboxylase (PEPC) in the CAM process of *K. fedtschenkoi*, there is a need to investigate the effect of knocking down key *KfePEPC* genes on the growth performance of the mutants. This investigation is essential because there is an argument that CAM is an expensive energetic process; however, studies have shown that the productivity level of CAM is on the same level as that of C3 plants (Shameer et al. 2018).

In this study, the effect of knocking down *KfePEPC1* and *KfePEPC2* genes on growth parameters like plant height, rate of leaf proliferation, leaf area, fresh and dry weight of the shoots and roots were measured. Both lines of the *kfepepc1* single mutants maintained steady and comparable stem elongation and leaf proliferation to that of the wild type over the six weeks of investigation compared to the wild type, despite the finding that the *kfepepc1* line 1 mutant was CAM-deficient (Chapter 4). If CAM imposed a metabolic cost, it might have been predicted that the CAM-deficient mutants would enhance growth relative to wild type.

However, this was not the case, indicating that CAM does not compromise growth in *K. fedtschenkoi*. In contrast, results showed that knocking down *KfePEPC2* reduced the stem elongation of *kfepepc2* mutants. This observation can be attributed to *KfePEPC2* gene involvement in key non-photosynthetic roles like nitrogen metabolism (Shi et al. 2015; O'Leary et al. 2011). Other roles for the PEPC enzyme that are not directly connected to photosynthesis in plants have been studied in *Arabidopsis thaliana* and knocking down the *PPC2* gene in this species has been linked to growth arrest in the plant (Feria et al. 2016; Abraham et al. 2016; Shi et al. 2015).

Knocking down *KfePEPC1* and *KfePEPC2* genes in the single mutants did not significantly affect the rate of leaf proliferation or the total leaf area of the plants, and shoot/root fresh and dry weights showed no negative impact of knocking down the *KfePEPC1* and *KfePEPC2* genes individually. However, in the double mutants (*KfePEPC1/2*), knocking down the two most abundant PEPC genes led to significant reductions in stem elongation, leaf proliferation, total leaf area, and shoot/root fresh dry weights. This growth arrest in the double mutants could be attributed to reduced nitrogen metabolism (PEPC2) and reduced photosynthetic/CAM activity (PEPC1; see Chapter 4). That the double PEPC knockdown was much more detrimental to growth than individual PEPC knockdown indicates some level of redundancy in terms of how *KfePEPC1* and *KfePEPC2* impact growth. There is interest in how PEPC influences nitrogen metabolism and associated enzymes in CAM plants. Some evidence is that nitrate reductase activity is optimised in an active CAM state (Gajewska et al. 2018). Furthermore, the availability and concentration of nitrogen have also been implicated in CAM performance in the CAM plant *Kalanchoë lateritia* (Pereira and Cushman 2019). Knocking down the two *KfePEPC* genes together, as in the double mutants, is thus severely damaging to plant growth.

5.4.2 Knocking down *KfePEPC1* and *KfePEPC2* genes reduced stomatal density and increased pore length.

Stomata of obligate CAM plants are uniquely designed to improve water-use efficiency, a key trait of CAM photosynthesis (Males and Griffiths 2017). There have also been studies on C3-CAM intermediate stomata which suggest structure changes such as reduced stomata density (Heyduk et al. 2016). Unlike C_3 and C_4 plants, stomata in these plants do not depend on light signal transduction through photoreceptors to regulate opening or closing (Lee 2010). Because the stomata are usually closed during most parts of the photoperiod and open at night when the air is a lot cooler, the rate of transpiration is reduced drastically (Hartwell et al. 2016).

In this study, knocking down *KfePEPC1* and *KfePEPC2* genes created an opportunity to understand how relevant these genes are to CAM by studying the response of stomatal patterning of the mutants. The results revealed that knocking down *KfePEPC1* and *KfePEPC2* genes might have led to a reduction in the stomatal density of the mutants. This observation seems to be linked to these mutants adjusting to the disruptions to CAM (PEPC1, see Chapter 4) and stomatal behaviour (PEPC2, see Chapter 4) and might be a mechanism for reducing the metabolic cost of maintaining stomatal numbers in plants experiencing disrupted carbon and/or nitrogen assimilation processes. Reduced stomatal density in CAM plants compared to C_3 plants has been reported by Barrera Zambrano et al. (2014) to cut down the metabolic cost and reduce conductance to water vapour. Knocking down the *KfePEPC1* gene has a profound effect on CAM performance. Reduced stomatal density could reduce water loss when CAM is compromised.

The effect of knocking down *KfePEPC1* and *KfePEPC2* genes on the pore length of the stomata shows that most of the mutants had larger pore sizes due to the mutation. Pore length is an indication of the guard cell length/size Furthermore, the results showed a negative correlation between stomatal densities and stomatal size/aperture. A negative correlation between stomatal density and size seems to hold for many C_3 species and may even be more complicated. Plants with lower stomatal densities show a greater mean stomatal size, and smaller stomata are found in leaves with higher density stomatal densities (Doheny-Adams et al. 2012; Lawson and Blatt 2014). This relationship is attributed to spatial limits in placing stomata on the leaf surface that constrains stomata's maximum size and density (Beaulieu et al. 2008; Franks and Beerling 2009). In a comparative study of stomatal patterning across nine Clusia species that possess varying CAM capacities, it was found that stomata were

present in lower densities in the thicker-leaved CAM-performing species (Barrera Zambrano et al. 2014). However, the stomatal pore areas tended to be larger in CAM Clusias compared to C_3 Clusias, which supports the spatial limitation view described above for C_3 species (Barrera Zambrano et al. 2014).

Both the size and density of stomata have an impact on the gas exchange, so Sack et al. (2003) and later Holland and Richardson (2009) proposed the stomatal pore area index (SPI) as a potential conductance index (PCI), both taking size (as squared guard cell length^2) as well as density into consideration. Another explanation for the observation is that differences in environmental conditions such as elevational gradients affect SPI. Studies show that plants growing in high altitudes have reduced SPI due to exposure to high irradiance, causing decreased stomatal opening (Bucher et al. 2016; Nogués et al. 1999). However, since the study was done in a controlled environment, the elevational gradient was not altered, eliminating any effect on SPI.

5.4.3 Knocking down KfePEPC1 impacted succulence and significantly affected drought tolerance.

One of the key advantages of the CAM mode of photosynthesis is coping with abiotic stress conditions like drought (Pintó-Marijuan et al. 2017; Griffiths et al. 2002; Yang et al. 2015b; Heyduk et al. 2021; Abraham et al. 2016). In addition, there is strong evidence to show that plants adopted the CAM mode of photosynthesis as a carbon-concentrating mechanism to cope in marginal lands whilst maintaining the optimal growth and biomass production (Borland et al. 2009; Silva et al. 2014; Yang et al. 2015b). In this present study, the leaf-saturated water content (SWC) was measured in well-watered and drought-stress conditions to assess the impact of the mutation on the plant's level of succulence. The SWC results revealed that *kfepepc1* mutants had higher saturated water content in drought conditions than wildtype, despite the reduced CAM in at least line 1 of the mutant. This observation suggests that plants can acquire succulence as a trait irrespective of their mode of photosynthesis, as in *kfepepc1* Line 1, which lost the ability to do CAM (Ogburn and Edwards 2010). Ogburn and Edwards (2012) report that plants with strong CAM activity have high water contents but not necessarily a high SWC and that CAM is efficient with some degree of succulence (Barrera Zambrano et al. 2014). The results in the present chapter suggest that when CAM is compromised, as, in the *kfepepc1* mutants, the development of a higher saturated water content under drought could be a compensatory mechanism to help maintain water status in the absence of CAM. Thus, the hypothesis that knocking out CAM will significantly impact succulence in CAM plants was proven.

Measuring the impact of drought stress on the pigment content of the plants is one way of assessing how plants can handle the stress. Drought may have elicited significant increases in chlorophyll and carotenoid contents of the *kfepepc1* Line 1 and *kfepepc2* Line 1 mutant plants which were significantly higher than those of the wild type. Elevation of pigment content was particularly marked in the droughted CAM deficient mutant *kfepepc1* Line 1, suggesting that these plants struggled to cope with the stress. Enhanced carotenoid levels could help protect the *kfepepc1* mutants from oxidative damage, with carotenoids serving as a non-enzymatic antioxidant (Egert and Tevini 2002; Habibi 2018; Rustioni and Bianchi 2021; Ahmad et al. 2010) since the CAM-associated drought tolerance mechanism (i.e., enhanced water-use efficiency) was compromised in these mutants. The results agree with the hypothesis that knocking out CAM reduces the plant's ability to tolerate drought and points to the need for

CAM-compromised plants to exploit other metabolic options to deal with drought's potentially destructive oxidative stress.

5.5 Conclusion.

Knocking down the *KfePEPC1* gene had little or no effect on the growth performance while knocking down *KfePEPC2* led to a significant reduction in growth and knocking down both *KfePEPC1/2* genes resulted in severe growth arrest in the *kfepepc1/2* double mutants. These observations indicate that whilst CAM-compromised mutants such as the *kfepepc1* plants did not show altered growth compared to the wild type, both PEPC genes are essential for growth.

Reductions in stomatal density and increased stomatal pore length were observed when *KfePEPC2* genes were knocked down while knocking down the *KfePEPC1* gene reduced stomatal density. This points to a link between CAM and stomatal patterning but also a link between non-photosynthetic PEPC function (i.e., PEPC2) and stomatal patterning.

Knocking down the *KfePEPC1* gene enhanced the saturated water content of the *kfepepc1* line 1 mutant which was also compromised in CAM. Such results indicate that succulence as a trait is not dependent on the plants' ability to perform CAM photosynthesis since plants which use other forms of photosynthesis (C_3 and C_4 photosynthesis) can still be succulent. Results also showed that when CAM is compromised, other mechanisms for drought tolerance are required, as indicated by the *kfepepc1* Line 1 mutant which show greatly enhanced production of pigments like chlorophyll and carotenoids when subjected to drought.

Chapter 6 General Discussion

The use of *Kalanchoë fedtschenkoi* as a model CAM plant has provided unprecedented opportunities for functional genomics research into this photosynthetic specialisation. Key reasons for using *K. fedtschenkoi* as a model are the relatively small size of its genome at approximately 260Mb, which has been sequenced and is available (Yang et al. 2017), and the ease with which this species can be genetically transformed (Hartwell et al, 2016). Yang et al. (2017) reported that of all the genes identified in *K. fedtschenkoi*, which encode PEPC, the key nocturnal carboxylase in CAM, two isoforms, namely *KfePEPC1* and *KfePEPC2*, showed the highest diel transcript abundance. This observation prompted the targeted knockdown of these genes in *K. fedtschenkoi* via CRISPR-Cas9, and the mutants generated were used in this study.

The results collected have provided an exciting insight into the roles of different isoforms of *KfePEPC* genes in the CAM pathway. This chapter will highlight the key findings in this study, suggest areas of further research based on the findings, and show how findings from this research would benefit my home country of Nigeria, which has funded this PhD research.

6.1 Key findings from the study

6.1.1 KfePEPC1 is the CAM-specific isoform in K. fedtschenkoi.

The knockdown of the *KfePEPC1* gene using the CRISPR-Cas9 loss of function technique resulted in an almost complete loss of diel transcript abundance of the *KfePEPC1* gene in line 1 and partial loss of diel transcript abundance in line 2, and this observation was discussed in detail in Chapter 3 of this thesis.

The knockdown led to a significant reduction in the *in vitro* biochemical activity of PEPC and loss of PEPC protein in the *kfepepc1* Line 1 mutant. In contrast, in the *kfepepe1* Line 2 mutant, the knockdown did not affect the *in vitro* activity of the PEPC enzyme, but the protein abundance of the PEPC enzyme was reduced compared to that in the wild type. Previous large-scale proteomics analysis of *K. fedtschenkoi* (Abraham et al, 2020) indicated that *KfePEPC1* encodes the bulk of PEPC protein, as was also found to be the case for the PPC1 gene in *K. laxiflora* (Boxall et al, 2020). Thus, the substantial reduction in PEPC protein abundance in both *kfepepc1* mutant lines reflects that the *KfePEPC1* gene encodes the

bulk of the PEPC enzyme protein. Again, the western blot assay is known to be qualitative, and there is a possibility that little protein left in the *kfepepc1* Line 2 mutant after the knockdown was still active but could not be dictated by the assay; hence why the enzyme activity was measured. The differences in PEPC enzyme activity can be possibly explained by the fact that CRISPR-Cas9 completely knocked down the *KfePEPC1* gene in line 1 but partially knocked down the *KfePEPC1* gene in line 2. However, the knockdown of *KfePEPC1* led to a significant downregulation of the transcript abundance of the *KfePPCK* gene compared to the wild type, which encodes the PEPC phosphorylating enzyme PPCK during the dark period. The downregulation of the *KfePPCK* gene can be attributed to the mutation impacting the amount of PEPC enzyme available for phosphorylation with *kfepepc1* Line 2 likely having enough PEPC enzyme to be active during the dark period. The PEPC enzymes in both *kfepepc1* lines showed a considerable level of malate sensitivity, as measuring their percentage inhibition revealed in the *kfepepc1* Line 2 where CAM photosynthesis still occurs, the malate inhibition is actively preventing futile cycling of the CAM pathway, agreeing with findings of Boxall et al. (2017).

The observations made in the manner that PEPC lost its catalytic ability and protein abundance confirmed that *KfePEPC1* is the CAM-specific isoform in the CAM model plant *K. fedtschenkoi* and is central to the effectiveness of the CAM pathway. Furthermore, the observation that *kfepepc1* Line 2 retained a reasonable amount of diel transcript abundance and PEPC activity despite losing a significant amount of the PEPC protein has opened an area for further studies to provide more insight into how PEPC is regulated in this model CAM plant.

Knocking down *the KfePEPC1* gene led to a down-regulation in the transcript abundance of the *rbc*L gene during the day, which encodes RuBisCO and catalyses C_3 carboxylation during the light period of both lines of the *kfepepc1* mutant. However, knocking down *KfePEPC1* did not affect the abundance of the RuBisCO or RuBisCO activase proteins, an indication that despite the slight downregulation of the *rbc*L gene, the potential activity of C_3 carboxylation in *kfepepc1* mutants was comparable to that in wild type.

A key discovery from the successful knockdown of *KfePEPC1* in *kfepepc1* Line 1 was the switch from nocturnal β-carboxylation to daytime C_3 carboxylation (Chapter 4). This meant

that the *kfepepc*1 line 1 plant completely lost the ability to take up CO_2 at night as the stomata remained closed throughout the night but opened at the end of the dark period (Chapter 4). The implication of this shift in the pattern of carboxylation was a significant increase in the daytime uptake of CO_2 in *kfepepc1* line 1 compared to the wild type. Interestingly, the enhanced direct C_3 carboxylation activity in the *kfepepc1* line 1 plants was not accompanied by an enhanced abundance of RuBisCO or RuBisCO activase proteins (Chapter 3), suggesting that C_3 carboxylating capacity in *K. fedtschenkoi* is not limiting for daytime gas exchange. This observation agrees with Ceusters et al. (2021a), who reported a gradual increase in RuBisCO and RuBisCO activase activity as malate decarboxylation progresses in phase 3 of CAM. The gas exchange analyses also indicated an increase in the rate of daytime transpiration in *kfepepc1* and a significant reduction in the water-use efficiency, a critical feature that CAM confers on plants that have adopted it as their preferred mode of photosynthesis (Yang et al. 2015a).

Furthermore, the switch from β-carboxylation to C_3 carboxylation also led to the stomatal opening during the daytime in the *kfepepc1* line 1, as in C_3 plants. There was a significant reduction in the amount of organic acids accumulated overnight in k*fepepc1* line 1, indicating again that CAM has been disrupted in this line. This was accompanied by a significant accumulation of starch during the dark period. The inability to use starch during the night also supported the previously described findings that CAM was absent, thus affecting the system's carbon balance. These observations were similar to what Boxall et al. (2020) observed when they silenced the *PPC1* gene using RNAi in *K. laxiflora.*

Despite the perturbations to CAM activity observed in the *kfepepc1* line 1 mutant, knocking down the *KFePEPC1* gene did not affect growth performance; however, Boxall et al. (2020) observed that suppressing *PPC1* in *K. laxiflora* led to a 21% reduction in shoot dry weight in well-watered conditions. In all growth parameters measured during the current research described, the *kfepepc1* mutants maintained a level of growth comparable to the wild type. This difference in growth performance can be attributed to differences in growth conditions and how the plant species responded to the mutation. The mutation in *KfePEPC1* affected stomatal patterning with reduced stomatal density in both *kfepepc1* lines but increased stomatal pore length compared to the wild type. However, this negative relationship between stomatal density and pore length did not affect the stomatal pore index indicating that the anatomical potential for gas exchange in the *kfepepc1* mutants remained optimal

irrespective of the type of photosynthesis (C_3 or CAM) that the plant adopted due to the mutation.

In the absence of CAM photosynthesis, *kfepepc1* line 1 subjected to drought stress had a high saturated water content. This was because the leaf's ratio of water to biomass was higher. But the absence of CAM compromised succulence since studies have shown that CAM and succulence co-depend on each other, with the magnitude of CAM higher for more succulent leaves (Males 2017; Griffiths et al. 2008; Barrera Zambrano et al. 2014). Succulence, however, is a major adaptive syndrome which occurs in various anatomical forms making it difficult to measure. So, the high saturated water content in the droughted *kfepepc1* Line 1 leaf did not co-relate to succulence broadly. Therefore, this thesis measured succulence as saturated water content. Still, a future detailed anatomical study on these mutants' cell size and intracellular spaces would be informative regarding succulence in these mutants in the absence of CAM.

Furthermore, the higher pigment content observed in *kfepepc1* Line 1 under drought conditions could disrupt the plants' mechanism to cope with drought stress. Chloroplastic pigment contents are commonly used to measure the level of abiotic stress a plant is undergoing (Pintó-Marijuan and Munné-Bosch 2014). Therefore, these observations indicate that knocking down CAM compromises the drought tolerance ability of *K. fedtschenkoi*, leading to the plant engaging other potential mechanisms, to deal with the adverse effects of drought stress.

*6.1.2 KfePEPC2 is implicated in growth, stomatal regulations, and the possible regulation of rbc*L *genes.*

CRISPR-Cas9 successfully knocked down the *KfePEPC2* gene in lines 1 and 2, as diel gene expression data revealed (Chapter 3). However, this knockdown neither affected the activity of the PEPC enzyme nor reduced the enzyme's protein abundance when measured using Western blotting. Since the *KfePEPC1* gene encodes the bulk of the PEPC protein (Abraham et al, 2020) and was not targeted in this knockdown, the PEPC enzyme's protein abundance in the *kfepepc2* lines remained comparable to that of the wild type. Significant down-regulation of *rbc*L gene transcript abundance in the middle of the light period and of the *KfePPCK* gene over most of the dark period indicates a possible perturbing of the circadian rhythm of these genes due to *KfePEPC2* knockdown (Chapter 3). This observation should be further studied to understand if/how knocking down *KfePEPC2* affects core clock genes like *Circadian*

Clock Associated1 (*CCA1-2), Lightnight-Inducible-Clock-Regulated3-like (LNK3), Early-Phytochrome-Responsive1 (EPR1)* since Boxall et al. (2020) reported that these core clock genes were upregulated during the light period and down-regulated during the dark period when *PPC1* gene was silenced in *K. laxiflora.*

The knockdown of the *KfePEPC2* gene did not affect CAM activity, as observed from nocturnal CO_2 uptake and nocturnal stomatal conductance of the *kfepepc2* mutants, which was like that of the wild type (Chapter 4). Since CAM activity was primarily retained in these mutants, the water-use efficiency levels were comparable to wild type ones. Moreover, the diel starch, soluble sugar turnover, and nocturnal acidification of the *kfepepc2* mutants were comparable to the wild type. However, it was observed that *kfepepc2* mutants opened their stomata widely just before dusk, which was in marked contrast to the wildtype, in which stomata opened only slightly its stomata at this same period. These data reveal a difference in the regulation of stomatal behaviour in the *kfepepc2* mutants (Chapter 4). Knocking down the *KfePEPC2* gene may have altered the circadian clock and perturbed the abundance of genes like *Cryptochrome2 (CRY2), High leaf Temperature1* (*HT1), and Transcriptional regulator MYB61,* which control stomatal behaviour. Previous studies on perturbations arising from knocking down or silencing of genes in a mutant have shown the tendency to alter the functioning of genes closely linked to the mutated gene (Boxall et al. 2017). Hence analysing the gene expression of these clock genes in the mutant may give more insight. Together, the observations described above indicated that the *KfePEPC2* gene was a housekeeping isoform, which might be involved in other physiological roles in the plant and so knocking it down would have little or no effect on the actual operation of CAM in *K. fedtschenkoi* (Sánchez et al. 2006; Chia-Yun et al. 2018).

Since it was clear that knocking down the *KfePEPC2* isoform did not affect CAM activity but seems to be involved in some form of circadian control and/or other physiological processes, there was the need to explore other roles that the *KfePEPC2* gene could underpin. The growth performance study of the *kfepepc2* mutants revealed that this PEPC isoform underpinned the enzyme's crucial role in maintaining proper growth (Chapter 5). This observation may be linked to important physiological roles such as nitrogen metabolism, to which knocking down the gene may have undermined its contribution to the plant's growth, and there is evidence to show that PEPC activity is optimised when nitrogen supply is adequate (Shi et al. 2015; Pereira and Cushman 2019). The *PEPC* gene in Arabidopsis is a

major target of the transcription factor of the plant-specific Dof1 (DNA binding with one finger) implicated in organic acid metabolism. *Dof1* expression led to improved nitrogen assimilation in plants like *A. thaliana* and *Zea mays* (Yanagisawa et al. 2004; O'Leary et al. 2011). Further analyses of genes and enzymes implicated in nitrogen metabolism in the *kfepepc2* lines could be informative.

Stomatal development was significantly disrupted by knocking down the *KfePEPC2* gene with reduced stomatal density and increased stomatal pore length compared to the wild type (Chapter 5). This observation could suggest a way of adjusting to the apparent alteration in daytime stomatal behaviour whilst retaining the benefits of features such as high water-use efficiency (Borland et al. 2018). However, the *KfePEPC2* mutation did not impact the stomatal pore index or overall anatomical potential for leaf gas exchange. With CAM activity retained and fully functioning, knocking down the *KfePEPC2* gene on succulence and drought tolerance ability was investigated to provide insight into the importance of this PEPC isoform on these processes. However, there was no observed impact of the *KfePEPC2* mutation on either succulence level or drought tolerance ability. Furthermore, the measured parameters showed no significant difference between well-watered and drought-stressed conditions compared to those observed in the wild type (Chapter 5). This observation confirms that CAM boosts the ability to tolerate drought, and a certain succulence level is required for CAM efficiency (Males 2017).

6.1.3 KfePEPC1 and KfePEPC2 gene expressions underpinned vital functions of the PEPC enzymes.

Knocking down both *KfePEPC1/2* genes led to a severely affected catalytic ability of the PEPC enzyme, leading to a hugely reduced enzyme activity compared to the wildtype and a complete loss of the PEPC enzyme protein in the *kfepepc1/2* mutants (Chapter 3). The loss of enzyme activity was an effect of knocking down the CAM-specific isoform, the *KfePEPC1* gene, and because the *KfePEPC1* gene encodes the bulk of the PEPC enzyme protein, that explains why the protein of the enzyme was lost.

Data measuring the effect of knocking down the *KfePEPC* genes 1 and 2 on nocturnal acid accumulation revealed a significant reduction in titratable acids (Chapter 4). A key feature of CAM photosynthesis is the ability to store atmospheric CO_2 as malic acid in the vacuole. When measured, there is usually a high amount of organic acid in the leaves of CAM plants

at dawn. So, a significant drop in the concentration of organic acid in the leaves of *kfepepc1/2* mutants at dawn indicates nocturnal carboxylation did not occur.

With growth parameters such as stem elongation, rate of leaf proliferation, leaf area, shoot fresh/dry weight, and root fresh/dry weight significantly reduced compared to the wildtype, it was evident that knocking down both *KfePEPC1/2* genes severely affects the growth of *K. fedtschenkoi* (Chapter 5). On visually inspecting the *kfepepc1/2* mutants, the apparent difference between other mutants and the wild type is clear. O'Leary et al. (2011) observed that knocking out *AtPEPC1/2* led to significant growth arrest in *Arabidopsis thaliana.* For Arabidopsis, it was suggested that in the absence of PEPC, the anaplerotic flux from PEP to malate and hence 2-oxoglutarate is reduced, suppressing the Gln synthetase and GOGAT cycle, ultimately leading to suppressed ammonium assimilation (Shi et al., 2015). This anaplerotic process of PEPC is vital for plants because it replenishes the tricarboxylic acids with intermediates used during a variety of biosynthetic processes (Masumoto et al. 2010; Willick et al. 2019). These observations in this thesis confirm that the *KfePEPC iso*genes 1 and 2 are crucial in *K. fedtschenkoi* for underpinning photosynthetic and non-photosynthetic functions in CAM plants, making them top candidate genes needed for CAM to C_3 bioengineering. While it is evident that PEPC is involved in carbon-nitrogen interactions in CAM plants like *K. fedtschenkoi,* further studies are required to determine the exact role of this protein in the complex responses of higher plants to carbon-nitrogen coupling.

6.2 Future work

This thesis achieved two significant milestones in the quest to expand scientific knowledge into the inner workings of CAM. These milestones are (1) Discovering the different roles that two isoforms of the PEPC gene play in the physiology of the model CAM plant *K. fedtschenkoi,* and (2) The potentials inherent in the novel CRISPR-Cas9 technology and how it could be harnessed as a viable tool for in-depth and precise plant molecular studies. With these in mind, findings from this study have cleared the way for further work that would benefit efforts to optimise CAM bioengineering.

6.2.1 Role of other KfePEPC isoforms in CAM activity of K. fedtschenkoi

One of the key discoveries made during the genome sequencing of *K. fedtschenkoi* by Yang et al. (2017) was the presence of the five (5) isoforms of the *KfePEPC* genes with *KfePEPC1* and *KfePEPC2* isoforms showing higher transcript abundance in the CAM leaves. Since this thesis worked with mutants of *KfePEPC1*, *KfePEPC2* and the double *KfePEPC1/2* to investigate their roles in *K. fedtschenkoi*, there is a need also to investigate the roles of the other isoforms of *KfePEPC* genes. This can be achieved by conducting in-depth transcriptomic, proteomic and metabolomic investigations of these PEPC isoforms *in K. fedtschenkoi* grown under a range of environmental conditions and in the *kfepepc1* and *kfepepc2* mutants. CRISPR-Cas could also knock down these other *KfePEPC* genes in *K. fedtschenkoi*. Transcriptomic data would give insight into the diel expression of these genes and reveal any possible temporal shift in expression compared to their C3 orthologs in *A. thaliana.* In addition, they could explain why their transcripts are not as abundant as those of *KfePEPC1* and *KfePEPC2* over a day/night cycle. A detailed proteomic analysis in *KfePEPC* mutants would help explain how these isoforms affect the PEPC protein expression and other proteins implicated in CAM and nitrogen metabolism. The metabolomic analysis would show how the different PEPC isoforms affect the abundance and diel cycling of key metabolites like starch, soluble sugars (glucose and fructose), and organic acids. CRISPR-Cas could knock down these PEPC isoforms individually, making it possible for their expression in mesophyll and perhaps in guard cells of *K. fedtschenkoi* to be studied separately. This would give insights into how involved these isoforms are in the CAM pathway and possibly in stomatal regulation. Also, their possible implication in drought tolerance in *K. fedtschenkoi* would make an interesting study. Finally, there is a huge possibility that knocking these genes in pairs, for instance, *KfePEPC3/4, KfePEPC3/5, and KfePEPC4/5* might disrupt a critical biochemical or physiological process in the plant necessary to its CAM activity, such was the case in this work (Chapter 3,4).

6.2.2 Possible co-dependency of PEPC and RuBisCO enzyme activity in CAM photosynthesis.

This thesis proved that knocking down CAM photosynthesis by perturbing the diel transcript abundance of *KfePEPC1* led to a switch to C_3 photosynthesis in *K. fedtschenkoi*. This observation was similar to what Boxall et al. (2020) reported when *PPC1* was suppressed in *K. laxiflora.* This switch in photosynthetic mode was facilitated by the fact that RuBisCO

protein abundance, together with that of RuBisCO activase, remained unperturbed by these genetic manipulations of PEPC. The questions now are how would the PEPC enzyme cope if RuBisCO activity was reduced? Conversely, what would happen if RuBisCO activation was perturbed? This can only be answered if CAM plants deficient in RuBisCO activity were created by possibly knocking down *rbc*L and *KfeRCA*α gene expressions. Ceusters et al. (2021a) suggest that RuBisCO activase plays important activating and regulating roles in RuBisCO activity and C3 carboxylation patterns in CAM plants. Therefore, perturbing the activity of RuBisCO activase would give insights into how CAM RuBisCO can sustain secondary carboxylation. Carboxylation is known to be a crucial component of CAM photosynthesis, playing a key role in optimising the process. Studies on CAM activity have shown that these carboxylating enzymes (PEPC and RuBisCO) tend to be active at different stages in the diel process without undermining the activity of each other (Dodd et al. 2002; Boxall et al. 2017; Winter and Smith 2022). Further work to explore the possible co-dependency of these two carboxylating enzymes in no small way could reveal exciting findings that would deepen our understanding of the evolutionary similarities and differences between C3 and CAM.

6.2.3 Evolution C_3 and CAM and necessity of photorespiration.

RuBisCO's dual affinity nature allows it to bind to CO_2 or O_2 molecules resulting in photosynthesis or photorespiration, respectively (Lüttge 2010b). It has long been believed that a key benefit of CAM over C_3 photosynthesis is suppressing oxygenase activity and promoting carboxylase activity in RuBisCO during phase 3 of CAM (Bräutigam et al. 2017; Yin et al. 2018; Pedersen et al. 2011). However, another school of thought is seriously promoting the idea that photorespiration is not completely harmful to plants, as the process can serve as a way to indicate a possible anomaly with a plant's photosynthetic process (Busch 2020). To understand the benefits or drawbacks of photorespiration to CAM, there is an urgent need to investigate this to establish in proper terms what the role of CAM in suppressing photorespiration might be or if truly photorespiration could be beneficial to plants using CAM photosynthesis. So interesting questions on CAM's role in photorespiration include (a) Why is photorespiration important to plants? (b) Why does it also occur in cyanobacteria? (c) If CAM is curtailed, does the activity of photorespiratory enzymes increase? (d) Are there changes in the diel transcript abundance of genes implicated in photorespiration when the main carboxylating enzymes PEPC and RuBisCO are active? The best approach to tackling these questions is to assay protein abundance and activity of some

known photorespiratory enzymes in both wild type and CAM-deficient mutants of *K. fedtschenkoi* to observe any change in their activity over a diel cycle and to conduct a detailed transcriptome analysis of the genes that encode these enzymes comparing their expression with the C3 orthologues. Genes of interest could include the glutamate synthase *GLU1* gene, which encodes a ferredoxin-dependent Glutamate synthase (Fd-GOGAT) enzyme. This enzyme is responsible for assimilating photorespiration-produced ammonium into glutamine and glutamate (Lancien et al. 2002). Ammonium is an essential compound which in vascular plants can be produced via nitrate assimilation, breakdown of nitrogenous compounds and, interestingly, photorespiration (Hirel and Lea 2001). With molecular tools currently available, it may be easier to investigate CAM's impact on diel gene expression of the *KfeGLU1* gene. Suppose CAM promotes carboxylase activity of RuBisCO whilst inhibiting photorespiration in that case, a possible downregulation of the *KfeGLU1* gene should be expected, discouraging glutamine production activity of the Fd-GOGAT enzyme via photorespiratory-ammonium assimilation.

Since the goal of bioengineering CAM to C3 is to optimise the photosynthetic capability of C3 crops and enhance their ability to adapt to marginal lands, eliminating another bottleneck to the efficiency of photosynthesis (e.g., photorespiration) would go a long way to solidify the inevitability of this process further.

6.3 Benefits of this thesis research to my home country Nigeria.

Nigeria is among the fastest-growing economies globally, with a very youthful population whose growth rate currently stands at 2.86% annually and is expected to double by 2045 (Olanrewaju et al. 2020). An integral part of sustaining this high population growth rate has a viable agricultural system to ensure a sustainable food supply. However, according to the food and agricultural organisation (FAO), the United Nations body that leads the international effort to defeat hunger, Nigeria's annual agricultural output contributes just 22.35% of the country's total gross domestic product (GDP) (FAO 2022). This results from several problems plaguing the system, making it impossible for sufficient agricultural output to be attained and posing a severe threat to food security. Some of these problems include poor land tenure systems, low levels of irrigation farming, climate change and land degradation. Others are low technology, high production cost, poor distribution of inputs, limited financing, high post-harvest losses, and poor access to markets (FAO 2022).

Climate change is a global problem whose effect is felt in many ways. For example, one of the severe effects of climate is shifting weather patterns which means that areas with hitherto sufficient rainfall now get little or no rainfall, thereby increasing the chances of desertification and high risk of crop failure (Koetse and Rietveld 2009). This is a real problem facing Nigeria's agricultural sector, and despite every effort made by the government, it seems there is no end in sight.

The current study was made to broaden the knowledge of CAM photosynthesis, a system that offers a potential biological solution to climate change. To achieve this aim, cutting-edge molecular tools were used to manipulate a plant genetically, *Kalanchoë fedtschenkoi* (lavender scallops), to learn the function of genes that confers it with the ability to perform crassulacean acid metabolism (CAM) photosynthesis. This plant is known to grow well in the tropics of Madagascar, an area known to be plagued by low rainfall. CAM photosynthesis equips the plant to cope with low rainfall as well as other plants that adopt the pathway with a trait known as water-use efficiency. This trait allows the plants to grow optimally with half the amount of water required by a typical C3 plant and enables them to tolerate the frequent drought stress in these environments. Since most crops like rice, wheat, cowpea, and other staple crops primarily grown in Nigeria to provide food and feed livestock use C3 photosynthesis, they lack possible physiological adaptations to cope with low precipitation, hence running the risk of crop loss, reducing food security. The features and the traits inherent in using CAM indeed provides a viable solution to tackling the broad problem of climate change as it affects crop production. With the growing understanding of genomes and molecular genetics of the pathway, scientists are optimistic that CAM photosynthesis can be bioengineered into C3 crops to equip them with these benefits to enhance their survivability and increase their productivity whilst using water efficiently.

I am confident that Nigeria's agricultural production will benefit from this ground-breaking stride made in plant biotechnology. As the CAM bioengineering systems are optimised, several CAM bioengineered staple crops will be available to grow in the future contributing to other efforts currently made to solve the country's agricultural problems and provide enough food for the growing population.

References

Abdel-Raouf HS (2012) Anatomical traits of some species of Kalanchoe (Crassulaceae) and their taxonomic value. Annals of Agricultural Sciences 57:73-79

Abraham PE, Hurtado Castano N, Cowan-Turner D, Barnes J, Poudel S, Hettich R, Flütsch S, Santelia D, Borland AM (2020) Peeling back the layers of crassulacean acid metabolism: functional differentiation between Kalanchoë fedtschenkoi epidermis and mesophyll proteomes. The Plant Journal 103:869-888

Abraham PE, Yin H, Borland AM, Weighill D, Lim SD, De Paoli HC, Engle N, Jones PC, Agh R, Weston DJ et al. (2016) Transcript, protein and metabolite temporal dynamics in the CAM plant Agave.

Ahmad P, Jaleel CA, Salem MA, Nabi G, Sharma S (2010) Roles of enzymatic and nonenzymatic antioxidants in plants during abiotic stress. Critical reviews in biotechnology 30:161-175

Arias-Baldrich C, de la Osa C, Bosch N, Ruiz-Ballesta I, Monreal JA, García-Mauriño S (2017) Enzymatic activity, gene expression and posttranslational modifications of photosynthetic and non-photosynthetic phosphoenolpyruvate carboxylase in ammonium-stressed sorghum plants. Journal of Plant Physiology 214:39-47

Bandyopadhyay A, Datta K, Zhang J, Yang W, Raychaudhuri S, Miyao M, Datta SK (2007) Enhanced photosynthesis rate in genetically engineered indica rice expressing pepc gene cloned from maize. Plant Science 172:1204-1209

Barrera Zambrano VA, Lawson T, Olmos E, Fernández-García N, Borland AM (2014) Leaf anatomical traits which accommodate the facultative engagement of crassulacean acid metabolism in tropical trees of the genus Clusia. Journal of Experimental Botany 65:3513-3523

Beaulieu JM, Leitch IJ, Patel S, Pendharkar A, Knight CA (2008) Genome size is a strong predictor of cell size and stomatal density in angiosperms. New Phytologist 179:975-986

Bertolino LT, Caine RS, Gray JE (2019) Impact of stomatal density and morphology on water-use efficiency in a changing world. Frontiers in Plant Science 10:225

Blankenship RE (1992) Origin and early evolution of photosynthesis. Photosynthesis research 33:91-111

Borland A, Taybi T (2004) Synchronization of metabolic processes in plants with Crassulacean acid metabolism. Journal Of Experimental Botany 55:1255-1265

Borland AM, Griffiths H (1997) A comparative study on the regulation of C3 and C4 carboxylation processes in the constitutive crassulacean acid metabolism (CAM) plant Kalanchoë daigremontiana and the C3-CAM intermediate Clusia minor. Planta 201:368-378

Borland AM, Griffiths H, Hartwell J, Smith JAC (2009) Exploiting the potential of plants with crassulacean acid metabolism for bioenergy production on marginal lands. Journal of Experimental Botany 60:2879-2896

Borland AM, Guo H-B, Yang X, Cushman JC (2016a) Orchestration of carbohydrate processing for crassulacean acid metabolism. Current Opinion in Plant Biology 31:118-124

Borland AM, Guo H-B, Yang X, Cushman JC (2016b) Orchestration of carbohydrate processing for crassulacean acid metabolism. Current Opinion in Plant Biology 31:118-124

Borland AM, Hartwell J, Weston DJ, Schlauch KA, Tschaplinski TJ, Tuskan GA, Yang X, Cushman JC (2014) Engineering crassulacean acid metabolism to improve water-use efficiency. Trends in Plant Science 19:327-338
Borland AM, Leverett A, Hurtado-Castano N, Hu R, Yang X (2018) Functional anatomical traits of the photosynthetic organs of plants with crassulacean acid metabolism. In: The leaf: a platform for performing photosynthesis. Springer, pp 281-305
Borland AM, Técsi LI, Leegood RC, Walker RP (1998) Inducibility of crassulacean acid metabolism (CAM) in Clusia species; physiological/biochemical characterisation and intercellular localization of carboxylation and decarboxylation processes in three species which exhibit different degrees of CAM. Planta 205:342-351
Borland AM, Yang X (2013) Informing the improvement and biodesign of crassulacean acid metabolism via system dynamics modelling. New Phytologist 200:946-949
Bowes G, Ogren W, Hageman R (1971) Phosphoglycolate production catalyzed by ribulose diphosphate carboxylase. Biochemical and biophysical research communications 45:716-722
Boxall SF, Dever LV, Kneřová J, Gould PD, Hartwell J (2017) Phosphorylation of phosphoenolpyruvate carboxylase is essential for maximal and sustained dark CO2 fixation and core circadian clock operation in the obligate crassulacean acid metabolism species Kalanchoë fedtschenkoi. The Plant Cell 29:2519-2536
Boxall SF, Kadu N, Dever LV, Kneřová J, Waller JL, Gould PJD, Hartwell J (2020) Silencing PHOSPHOENOLPYRUVATE CARBOXYLASE1 in the Obligate Crassulacean Acid Metabolism Species Kalanchoë laxiflora causes Reversion to C3-like Metabolism and Amplifies Rhythmicity in a Subset of Core Circadian Clock Genes. bioRxiv:684050
Bradford MM (1976) A rapid and sensitive method for the quantitation of microgram quantities of protein utilizing the principle of protein-dye binding. Analytical Biochemistry 72:248-254
Bräutigam A, Schlüter U, Eisenhut M, Gowik U (2017) On the evolutionary origin of CAM photosynthesis. Plant Physiology 174:473-477
Brodribb TJ, Holbrook NM, Zwieniecki MA, Palma B (2005) Leaf hydraulic capacity in ferns, conifers and angiosperms: impacts on photosynthetic maxima. New Phytologist 165:839-846
Broetto F, Lüttge U, Ratajczak R (2002) Influence of light intensity and salt-treatment on mode of photosynthesis and enzymes of the antioxidative response system of Mesembryanthemum crystallinum. Functional Plant Biology 29:13-23
Bucher SF, Auerswald K, Tautenhahn S, Geiger A, Otto J, Müller A, Römermann C (2016) Inter-and intraspecific variation in stomatal pore area index along elevational gradients and its relation to leaf functional traits. Plant Ecology 217:229-240
Busch FA (2020) Photorespiration in the context of Rubisco biochemistry, CO2 diffusion and metabolism. The Plant Journal 101:919-939
Cai J, Liu X, Vanneste K, Proost S, Tsai W-C, Liu K-W, Chen L-J, He Y, Xu Q, Bian C et al. (2015) The genome sequence of the orchid Phalaenopsis equestris. Nature Genetics 47:65-72
Caine RS, Yin X, Sloan J, Harrison EL, Mohammed U, Fulton T, Biswal AK, Dionora J, Chater CC, Coe RA (2019) Rice with reduced stomatal density conserves water and has improved drought tolerance under future climate conditions. New Phytologist 221:371-384
Carnal NW, Black CC (1989) Soluble sugars as the carbohydrate reserve for CAM in pineapple leaves: implications for the role of pyrophosphate: 6-phosphofructokinase in glycolysis. Plant Physiology 90:91-100

Carter P, Nimmo H, Fewson C, Wilkins M (1990) Bryophyllum fedtschenkoi protein phosphatase type 2A can dephosphorylate phosphoenolpyruvate carboxylase. FEBS Lett 263:233-236
Ceusters J, Borland AM, Godts C, Londers E, Croonenborghs S, Van Goethem D, De Proft MP (2011) Crassulacean acid metabolism under severe light limitation: a matter of plasticity in the shadows? Journal Of Experimental Botany 62:283-291
Ceusters J, Borland AM, Londers E, Verdoodt V, Godts C, De Proft MP (2009) Differential usage of storage carbohydrates in the CAM bromeliad Aechmea 'Maya' during acclimation to drought and recovery from dehydration. Physiologia Plantarum 135:174-184
Ceusters N, Borland AM, Ceusters J (2021a) How to resolve the enigma of diurnal malate remobilisation from the vacuole in plants with crassulacean acid metabolism? New Phytologist 229:3116-3124
Ceusters N, Ceusters J, Hurtado-Castano N, Dever LV, Boxall SF, Kneřová J, Waller JL, Rodick R, Van den Ende W, Hartwell J (2021b) Phosphorolytic degradation of leaf starch via plastidic α-glucan phosphorylase leads to optimized plant growth and water use efficiency over the diel phases of Crassulacean acid metabolism. Journal of Experimental Botany 72:4419-4434
Ceusters N, Ende WVd, Ceusters J (2016) Exploration of sweet immunity to enhance abiotic stress tolerance in plants: lessons from CAM. Progress in Botany Vol 78:145-166
Chandler J, Bartels D (2008) Drought: Avoidance and adaptation. Encyclopedia of water science Taylor and Francis group, London 224
Chen LS, Lin Q, Nose A (2002) A comparative study on diurnal changes in metabolite levels in the leaves of three crassulacean acid metabolism (CAM) species, Ananas comosus, Kalanchoë daigremontiana and K. pinnata. Journal of Experimental Botany 53:341-350
Chia-Yun P, Fure-Chyi C, Teen-Chi C, Huey-Ling L, Tzong-Shyan L, Wen-Ju Y, Yung IL (2018) Expression Profiles of Phosphoenolpyruvate Carboxylase and Phosphoenolpyruvate Carboxylase Kinase Genes in Phalaenopsis, Implications for Regulating the Performance of Crassulacean Acid Metabolism. Frontiers in Plant Science 9
Chomthong M, Griffiths H (2020) Model approaches to advance crassulacean acid metabolism system integration. The Plant Journal 101:951-963
Christin P-A, Arakaki M, Osborne CP, Bräutigam A, Sage RF, Hibberd JM, Kelly S, Covshoff S, Wong GK-S, Hancock L et al. (2014) Shared origins of a key enzyme during the evolution of C 4 and CAM metabolism. Journal of Experimental Botany 65
Christopher JT, Holtum J (1996) Patterns of Carbon Partitioning in Leaves of Crassulacean Acid Metabolism Species during Deacidification. Plant Physiology 112:393-399
Cousins AB, Baroli I, Badger MR, Ivakov A, Lea PJ, Leegood RC, von Caemmerer S (2007) The Role of Phosphoenolpyruvate Carboxylase during C₄ Photosynthetic Isotope Exchange and Stomatal Conductance. Plant Physiology 145:1006-1017
Cushman JC (2001) Crassulacean Acid Metabolism. A Plastic Photosynthetic Adaptation to Arid Environments. Plant Physiology 127:1439-1448
Cushman JC, Bohnert HJ (1999) CRASSULACEAN ACID METABOLISM: Molecular Genetics. Annual Review of Plant Physiology and Plant Molecular Biology 50:305-332
Deng H, Zhang L-S, Zhang G-Q, Zheng B-Q, Liu Z-J, Wang Y (2016) Evolutionary history of PEPC genes in green plants: Implications for the evolution of CAM in orchids. Molecular Phylogenetics and Evolution 94:559-564

DePaoli HC, Borland AM, Tuskan GA, Cushman JC, Yang X (2014) Synthetic biology as it relates to CAM photosynthesis: challenges and opportunities. Journal of Experimental Botany 65:3381-3393
Descoings B (2006) Le genre Kalanchoe structure et définition. Journal de Botanique de la Société Botanique de France 33:3-28
Dever LV, Boxall SF, Kneřová J, Hartwell J (2015) Transgenic perturbation of the decarboxylation phase of Crassulacean acid metabolism alters physiology and metabolism but has only a small effect on growth. Plant Physiology 167:44
Dodd AN, Borland AM, Haslam RP, Griffiths H, Maxwell K (2002) Crassulacean acid metabolism: plastic, fantastic. Journal of Experimental Botany 53:569-580
Doheny-Adams T, Hunt L, Franks PJ, Beerling DJ, Gray JE (2012) Genetic manipulation of stomatal density influences stomatal size, plant growth and tolerance to restricted water supply across a growth carbon dioxide gradient. Philosophical Transactions of the Royal Society B: Biological Sciences 367:547-555
Doudna JA, Charpentier E (2014) The new frontier of genome engineering with CRISPR-Cas9. Science 346:1258096
Dubois M, Gilles K, Hamilton J, Rebers P, Smith F (1956) Colorimetric Method for Determination of Sugars and Related Substances. Analytical Chemistry 28:350-356
Eaton SL, Roche SL, Llavero Hurtado M, Oldknow KJ, Farquharson C, Gillingwater TH, Wishart TM (2013) Total Protein Analysis as a Reliable Loading Control for Quantitative Fluorescent Western Blotting. PLOS ONE 8:e72457
Edwards EJ (2019) Evolutionary trajectories, accessibility and other metaphors: the case of C4 and CAM photosynthesis. New Phytologist 223:1742-1755
Egert M, Tevini M (2002) Influence of drought on some physiological parameters symptomatic for oxidative stress in leaves of chives (Allium schoenoprasum). Environmental and Experimental Botany 48:43-49
Engineer CB, Hashimoto-Sugimoto M, Negi J, Israelsson-Nordström M, Azoulay-Shemer T, Rappel W-J, Iba K, Schroeder JI (2016) CO2 Sensing and CO2 Regulation of Stomatal Conductance: Advances and Open Questions. Trends in Plant Science 21:16-30
FAO in Nigeria (2022) https://www.fao.org/nigeria/fao-in-nigeria/nigeria-at-a-glance/en/. Accessed 31/05/2022
Feitosa-Araujo E, da Fonseca-Pereira P, Pena MM, Medeiros DB, Perez de Souza L, Yoshida T, Weber AP, Araújo WL, Fernie AR, Schwarzländer M (2020) Changes in intracellular NAD status affect stomatal development in an abscisic acid-dependent manner. The Plant Journal 104:1149-1168
Feria AB, Bosch N, Sánchez A, Nieto-Ingelmo AI, de la Osa C, Echevarría C, García-Mauriño S, Monreal JA (2016) Phosphoenolpyruvate carboxylase (PEPC) and PEPC-kinase (PEPC-k) isoenzymes in Arabidopsis thaliana: role in control and abiotic stress conditions. Planta 244:901-913
Franks PJ, Beerling DJ (2009) Maximum leaf conductance driven by CO2 effects on stomatal size and density over geologic time. Proceedings of the National Academy of Sciences 106:10343-10347
Fulton DC, Stettler M, Mettler T, Vaughan CK, Li J, Francisco P, Gil M, Reinhold H, Eicke S, Messerli G (2008) β-AMYLASE4, a noncatalytic protein required for starch breakdown, acts upstream of three active β-amylases in Arabidopsis chloroplasts. The Plant Cell 20:1040-1058
Gajewska E, Surówka E, Kornas A, Kuźniak E (2018) Nitrogen metabolism-related enzymes in Mesembryanthemum crystallinum after Botrytis cinerea infection. Biologia Plantarum 62:579-587

García-Caparrós P, De Filippis L, Gul A, Hasanuzzaman M, Ozturk M, Altay V, Lao MT (2021) Oxidative stress and antioxidant metabolism under adverse environmental conditions: a review. The Botanical Review 87:421-466
Garcia-Moya E, Romero-Manzanares A, Nobel P (2011) Highlights for Agave productivity. GCB Bioenergy 3:4-14
Gehrig H, Gaußmann O, Marx H, Schwarzott D, Kluge M (2001) Molecular phylogeny of the genus Kalanchoe (Crassulaceae) inferred from nucleotide sequences of the ITS-1 and ITS-2 regions. Plant Science 160:827-835
Gibson DG, Young L, Chuang R-Y, Venter JC, Hutchison CA, Smith HO (2009) Enzymatic assembly of DNA molecules up to several hundred kilobases. Nature Methods 6:343-345
Gilman IS, Edwards EJ (2020) Crassulacean acid metabolism. Current Biology 30:R57-R62
Gonçalves AZ, Latansio S, Detmann KC, Marabesi MA, Neto AA, Aidar MP, DaMatta FM, Mercier H (2020) What does the RuBisCO activity tell us about a C3-CAM plant? Plant Physiology and Biochemistry 147:172-180
Grace OM (2019) Succulent plant diversity as natural capital. Plants, People, Planet 1:336-345
Griffiths H, Helliker B, Roberts A, Haslam RP, Girnus J, Robe WE, Borland AM, Maxwell K (2002) Regulation of Rubisco activity in crassulacean acid metabolism plants: better late than never. Functional Plant Biology 29:689-696
Griffiths H, Males J (2017) Succulent plants. Current Biology 27:R890-R896
Griffiths H, Robe WE, Girnus J, Maxwell K (2008) Leaf succulence determines the interplay between carboxylase systems and light use during Crassulacean acid metabolism in Kalanchoë species. Journal of Experimental Botany 59:1851-1861
Gross SM, Martin JA, Simpson J, Abraham-Juarez MJ, Wang Z, Visel A (2013) De novo transcriptome assembly of drought tolerant CAM plants, Agave deserti and Agave tequilana. BMC genomics 14:563
Habibi G (2018) Effects of mild and severe drought stress on the biomass, phenolic compounds production and photochemical activity of Aloe vera (L.) Burm. f. Acta Agriculturae Slovenica 111:463-476
Hanjra MA, Qureshi ME (2010) Global water crisis and future food security in an era of climate change. Food policy 35:365-377
Hartwell J, Dever LV, Boxall SF (2016) Emerging model systems for functional genomics analysis of Crassulacean acid metabolism. Current Opinion in Plant Biology 31:100-108
Hatch MD, Tsuzuki M, Edwards GE (1982) Determination of NAD Malic Enzyme in Leaves of C₄ Plants. EFFECTS OF MALATE DEHYDROGENASE AND OTHER FACTORS 69:483-491
Hermida-Carrera C, Fares MA, Font-Carrascosa M, Kapralov MV, Koch MA, Mir A, Molins A, Ribas-Carbó M, Rocha J, Galmés J (2020) Exploring molecular evolution of Rubisco in C3 and CAM Orchidaceae and Bromeliaceae. BMC Evolutionary Biology 20:11
Heyduk K, Burrell N, Lalani F, Leebens-Mack J (2016) Gas exchange and leaf anatomy of a C 3 –CAM hybrid, Yucca gloriosa (Asparagaceae). Journal Of Experimental Botany 67:1369-1379
Heyduk K, Ray JN, Ayyampalayam S, Moledina N, Borland A, Harding SA, Tsai C-J, Leebens-Mack J (2021) Shared expression of crassulacean acid metabolism (CAM) genes pre-dates the origin of CAM in the genus Yucca. Journal of Experimental Botany 70:6597-6609

Hirel B, Lea P (2001) Ammonia assimilation. In ‘Plant nitrogen’.(Eds PJ Lea, JF Morot-Gaudry) pp. 79–99. Springer-Verlag: Berlin,
Jiang F, Doudna JA (2017) CRISPR–Cas9 structures and mechanisms. Annual review of biophysics 46:505-529
Kim Hong HT, Nose A, Agarie S, Yoshida T (2008) Malate metabolism in mitochondria and its role in photosynthesis during CAM phase III. Journal Of Experimental Botany 59:1819-1827
Koetse MJ, Rietveld P (2009) The impact of climate change and weather on transport: An overview of empirical findings. Transportation Research Part D: Transport and Environment 14:205-221
Lancien M, Martin M, Hsieh M-H, Leustek T, Goodman H, Coruzzi GM (2002) Arabidopsis glt1-T mutant defines a role for NADH-GOGAT in the non-photorespiratory ammonium assimilatory pathway. The Plant Journal 29:347-358
Lawson T, Blatt MR (2014) Stomatal size, speed, and responsiveness impact on photosynthesis and water use efficiency. Plant Physiology 164:1556-1570
Lee J (2010) Stomatal Opening Mechanism of CAM Plants. Journal of Plant Biology 53:19-23
Lefoulon C, Boxall SF, Hartwell J, Blatt MR (2020) Crassulacean acid metabolism guard cell anion channel activity follows transcript abundance and is suppressed by apoplastic malate. New Phytologist 227:1847-1857
Li C, Tan D-X, Liang D, Chang C, Jia D, Ma F (2014) Melatonin mediates the regulation of ABA metabolism, free-radical scavenging, and stomatal behaviour in two Malus species under drought stress. Journal of Experimental Botany 66:669-680
Liang X, He P, Liu H, Zhu S, Uyehara IK, Hou H, Wu G, Zhang H, You Z, Xiao Y (2019) Precipitation has dominant influences on the variation of plant hydraulics of the native Castanopsis fargesii (Fagaceae) in subtropical China. Agricultural and Forest Meteorology 271:83-91
Liu D, Chen M, Mendoza B, Cheng H, Hu R, Li L, Trinh CT, Tuskan GA, Yang X (2019a) CRISPR/Cas9-mediated targeted mutagenesis for functional genomics research of crassulacean acid metabolism plants. Journal of Experimental Botany 70:6621-6629
Liu D, Hu R, Palla KJ, Tuskan GA, Yang X (2016) Advances and perspectives on the use of CRISPR/Cas9 systems in plant genomics research. Current Opinion in Plant Biology 30:70-77
Liu D, Hu R, Zhang J, Guo H-B, Cheng H, Li L, Borland AM, Qin H, Chen J-G, Muchero W et al. (2021) Overexpression of an Agave Phosphoenolpyruvate Carboxylase Improves Plant Growth and Stress Tolerance. Cells 10:582
Liu Z, Johnson ST, Zhang Z, Corey DR (2019b) Expression of TNRC6 (GW182) Proteins Is Not Necessary for Gene Silencing by Fully Complementary RNA Duplexes. Nucleic Acid Therapeutics 29:323-334
Livak K, Schmittgen T (2001) Analysis of relative gene expression data using real-time quantitative PCR and the 2(T)(-Delta Delta C) method. Methods 25:402-408
Luján M, Oleas NH, Winter K (2021) Evolutionary history of CAM photosynthesis in Neotropical Clusia: insights from genomics, anatomy, physiology and climate. Botanical Journal of the Linnean Society 199:538-556
Lüttge U (2004) Ecophysiology of Crassulacean Acid Metabolism (CAM). Annals of Botany 93:629-652
Lüttge U (2008) Stem CAM in arborescent succulents. Trees 22:139-148
Lüttge U (2010a) Ability of crassulacean acid metabolism plants to overcome interacting stresses in tropical environments. AoB plants 2010

Lüttge U (2010b) Photorespiration in phase III of crassulacean acid metabolism: evolutionary and ecophysiological implications. In: Progress in Botany 72. Springer, pp 371-384
Lüttge U, Fischer-Schliebs E, Ratajczak R (2000) The Role of Vacuolar Malate-Transport Capacity in Crassulacean Acid Metabolism and Nitrate Nutrition. Higher Malate-Transport Capacity in Ice Plant after Crassulacean Acid Metabolism-Induction and in Tobacco under Nitrate Nutrition. Plant Physiology 124:1335-1347
Maher MF, Nasti RA, Vollbrecht M, Starker CG, Clark MD, Voytas DF (2020) Plant gene editing through de novo induction of meristems. Nature Biotechnology 38:84-89
Maiquetía M, Cáceres A, Herrera A (2008) Mycorrhization and phosphorus nutrition affect water relations and CAM induction by drought in seedlings of Clusia minor. Annals of Botany 103:525-532
Males J (2017) Secrets of succulence. Journal of Experimental Botany 68:2121-2134
Males J, Griffiths H (2017) Stomatal Biology of CAM Plants. Plant Physiology 174:550
Martignago D, Rico-Medina A, Blasco-Escámez D, Fontanet-Manzaneque JB, Caño-Delgado AI (2020) Drought resistance by engineering plant tissue-specific responses. Frontiers in Plant Science 10:1676
Martin K, Raun W, Solie J (2012) BY-PLANT PREDICTION OF CORN GRAIN YIELD USING OPTICAL SENSOR READINGS AND MEASURED PLANT HEIGHT. Journal of Plant Nutrition 35:1429-1439
Martín M, Rius SP, Podestá FE (2011) Two phosphoenolpyruvate carboxykinases coexist in the Crassulacean Acid Metabolism plant Ananas comosus. Isolation and characterization of the smaller 65kDa form. Plant Physiology and Biochemistry 49:646-653
Masumoto C, Miyazawa S-I, Ohkawa H, Fukuda T, Taniguchi Y, Murayama S, Kusano M, Saito K, Fukayama H, Miyao M (2010) Phospho enol pyruvate carboxylase intrinsically located in the chloroplast of rice plays a crucial role in ammonium assimilation. Proceedings of the National Academy of Sciences 107:5226-5231
Maxwell K, Borland AM, Haslam RP, Helliker BR, Roberts A, Griffiths H (1999) Modulation of Rubisco Activity during the Diurnal Phases of the Crassulacean Acid Metabolism Plant Kalanchoëdaigremontiana. Plant Physiology 121:849-856
McCue KF, Gardner E, Chan R, Thilmony R, Thomson J (2019) Transgene stacking in potato using the GAANTRY system. BMC research notes 12:1-6
Ming R, VanBuren R, Wai CM, Tang H, Schatz MC, Bowers JE, Lyons E, Wang M-L, Chen J, Biggers E et al. (2015) The pineapple genome and the evolution of CAM photosynthesis. Nature Genetics 47:1435-1442
Miszalski Z, Slesak I, Haag-Kerwer A, Surowka E, Libik M, Gawronska K, Niewiadomska E (2003) CAM induction and oxidative stress in Mesembryanthemum crystallinum. Polish Journal of Natural Sciences Supplement 1
Miszalski Z, Ślesak I, Niewiadomska E, Baczek-Kwinta R, Lüttge U, Ratajczak R (1998) Subcellular localization and stress responses of superoxide dismutase isoforms from leaves in the C3-CAM intermediate halophyte Mesembryanthemum crystallinum L. Plant, cell & environment 21:169-179
Moseley RC, Tuskan GA, Yang X (2019) Comparative genomics analysis provides new insight into molecular basis of stomatal movement in Kalanchoë fedtschenkoi. Frontiers in Plant Science 10:292
Muhammad I, Shalmani A, Ali M, Yang Q-H, Ahmad H, Li FB (2021) Mechanisms Regulating the Dynamics of Photosynthesis Under Abiotic Stresses. Frontiers in Plant Science 11

Murchie E, Pinto M, Horton P (2009) Agriculture and the new challenges for photosynthesis research. New Phytologist 181:532-552
Nada RM, Khedr AHA, Serag MS, El-Nagar NA (2015) Growth, photosynthesis and stress-inducible genes of Phragmites australis (Cav.) Trin. ex Steudel from different habitats. Aquatic Botany 124:54-62
Ng J, Guo Z, Mueller-Cajar O (2020) Rubisco activase requires residues in the large subunit N terminus to remodel inhibited plant Rubisco. Journal of Biological Chemistry 295:16427-16435
Niechayev NA, Pereira PN, Cushman JC (2019) Understanding trait diversity associated with crassulacean acid metabolism (CAM). Current Opinion in Plant Biology 49:74-85
Nimmo GA, Nimmo HG, Fewson CA, Wilkins MB (1984) Diurnal changes in the properties of phosphoenolpyruvate carboxylase in Bryophyllum leaves: a possible co valent modification. FEBS Lett 178:199-203
Nimmo HG (2000) The regulation of phosphoenolpyruvate carboxylase in CAM plants. Trends in Plant Science 5:75-80
Nogués S, Allen DJ, Morison JI, Baker NR (1999) Characterization of stomatal closure caused by ultraviolet-B radiation. Plant Physiology 121:489-496
Nosek M, Kaczmarczyk A, Śliwa M, Jędrzejczyk R, Kornaś A, Supel P, Kaszycki P, Miszalski Z (2019) The response of a model C3/CAM intermediate semi-halophyte Mesembryanthemum crystallinum L. to elevated cadmium concentrations. Journal of Plant Physiology 240:153005
O'Leary B, Park J, Plaxton WC (2011) The remarkable diversity of plant PEPC (phosphoenolpyruvate carboxylase): recent insights into the physiological functions and post-translational controls of non-photosynthetic PEPCs. Biochemical Journal 436:15-34
Ogburn RM, Edwards EJ (2010) The ecological water-use strategies of succulent plants. In: Advances in botanical research, vol 55. Elsevier, pp 179-225
Ogburn RM, Edwards EJ (2012) Quantifying succulence: a rapid, physiologically meaningful metric of plant water storage. Plant, cell & environment 35:1533-1542
Olanrewaju S, Olafioye S, Oguntade E (2020) Modelling Nigeria population growth: A trend analysis approach. International Journal of Innovative Science and Research Technology 5:52-64
Oloyede F, Illoh H, Oloyede F (2007) Taxonomical studies of selected ornamental plants. IFE Journal of Science 9:167-171
Osmond C (1978) Crassulacean acid metabolism: a curiosity in context. Annual review of plant physiology 29:379-414
Parry MA, Keys AJ, Madgwick PJ, Carmo-Silva AE, Andralojc PJ (2008) Rubisco regulation: a role for inhibitors. Journal Of Experimental Botany 59:1569-1580
Pedersen O, Colmer TD, Garcia-Robledo E, Revsbech NP (2018) CO2 and O2 dynamics in leaves of aquatic plants with C3 or CAM photosynthesis–application of a novel CO2 microsensor. Annals of Botany 122:605-615
Pedersen O, Rich SM, Pulido C, Cawthray GR, Colmer TD (2011) Crassulacean acid metabolism enhances underwater photosynthesis and diminishes photorespiration in the aquatic plant Isoetes australis. New Phytologist 190:332-339
Perdomo JA, Capó-Bauçà S, Carmo-Silva E, Galmés J (2017) Rubisco and rubisco activase play an important role in the biochemical limitations of photosynthesis in rice, wheat, and maize under high temperature and water deficit. Frontiers in Plant Science 8:490
Pereira PN, Cushman JC (2019) Exploring the Relationship between Crassulacean Acid Metabolism (CAM) and Mineral Nutrition with a Special Focus on Nitrogen. International Journal of Molecular Sciences 20:4363

Pereira PN, Niechayev NA, Blair BB, Cushman JC (2021) Chapter 10 Climate Change Responses and Adaptations in Crassulacean Acid Metabolism (CAM) Plants. In: Becklin KM, Ward JK, Way DA (eds) Photosynthesis, Respiration, and Climate Change. Springer International Publishing, Cham, pp 283-329
Peters-Wendisch PG, Wendisch VF, Paul S, Eikmanns BJ, Sahm H (1997) Pyruvate carboxylase as an anaplerotic enzyme in Corynebacterium glutamicum. Microbiology 143:1095-1103
Pfaffl MW (2006) Relative quantification. In: Dorak MT (ed) Real-time PCR. Taylor & Francis, Newcastle upon Tyne, pp 63 - 83
Pintó-Marijuan M, Cotado A, Fleta-Soriano E, Munné-Bosch S (2017) Drought stress memory in the photosynthetic mechanisms of an invasive CAM species, Aptenia cordifolia. Photosynthesis research 131:241-253
Pintó-Marijuan M, Munné-Bosch S (2014) Photo-oxidative stress markers as a measure of abiotic stress-induced leaf senescence: advantages and limitations. Journal Of Experimental Botany 65:3845-3857
Porra R, Thompson W, Kriedemann P (1989) Determination of accurate extinction coefficients and simultaneous equations for assaying chlorophylls a and b extracted with four different solvents: verification of the concentration of chlorophyll standards by atomic absorption spectroscopy. Biochimica et Biophysica Acta (BBA)-Bioenergetics 975:384-394
Raines CA (2011) Increasing photosynthetic carbon assimilation in C3 plants to improve crop yield: current and future strategies. Plant Physiology 155:36-42
Ray SK, Mukherjee S (2021) Genome Editing with CRISPR-Cas9: A Budding Biological Contrivance for Colorectal Carcinoma Research and its Perspective in Molecular Medicine. Current Molecular Medicine
Redman M, King A, Watson C, King D (2016) What is CRISPR/Cas9? Archives of disease in childhood - Education & practice edition 101:213-215
Roberts A, Borland AM, Griffiths H (1997) Discrimination processes and shifts in carboxylation during the phases of crassulacean acid metabolism. Plant Physiology 113:1283-1292
Rustioni L, Bianchi D (2021) Drought increases chlorophyll content in stems of Vitis interspecific hybrids. Theoretical and Experimental Plant Physiology 33:69-78
Sack L, Cowan P, Jaikumar N, Holbrook N (2003) The 'hydrology'of leaves: co-ordination of structure and function in temperate woody species. Plant, cell & environment 26:1343-1356
Sage RF, Sage TL, Kocacinar F (2012) Photorespiration and the Evolution of C4 Photosynthesis. Annual Review of Plant Biology 63:19-47
Sánchez R, Flores A, Cejudo F (2006) Arabidopsis phospho enol pyruvate carboxylase genes encode immunologically unrelated polypeptides and are differentially expressed in response to drought and salt stress. Planta 223:901-909
Santos MG, Davey PA, Hofmann TA, Borland A, Hartwell J, Lawson T (2022) Stomatal and Mesophyll Responses Tissue to in Light, Vicia faba CO2, and Kalanchoë fedtschenkoi. Stomatal Biology and Beyond
Schweiger AH, Nürk NM, Beckett H, Liede-Schumann S, Midgley GF, Higgins SI (2021) The eco-evolutionary significance of rainfall constancy for facultative CAM photosynthesis. New Phytologist 230:1653-1664
Shameer S, Baghalian K, Cheung C, Ratcliffe RG, Sweetlove LJ (2018) Computational analysis of the productivity potential of CAM. Nature Plants 4:165-171

Shi J, Yi K, Liu Y, Xie L, Zhou Z, Chen Y, Hu Z, Zheng T, Liu R, Chen Y (2015) Phosphoenolpyruvate carboxylase in Arabidopsis leaves plays a crucial role in carbon and nitrogen metabolism. Plant Physiology 167:671-681
Shivhare D, Mueller-Cajar O (2017) Characterization of thermostable CAM Rubisco activase reveals a Rubisco interacting surface loop. Plant Physiology:pp. 00554.02017
Shu J-P, Yan Y-H, Wang R-J (2020) Convergent Molecular Evolution of PEPC Gene Family in C4 and CAM Plants.
Shu J-P, Yan Y-H, Wang R-J (2022) Convergent molecular evolution of phosphoenolpyruvate carboxylase gene family in C4 and crassulacean acid metabolism plants. PeerJ 10:e12828
Silva H, Sagardia S, Ortiz M, Franck N, Opazo M, Quiroz M, Baginsky C, Tapia C (2014) Relationships between leaf anatomy, morphology, and water use efficiency in Aloe vera (L) Burm f. as a function of water availability. Revista Chilena de Historia Natural 87:1-10
Silvera K, Winter K, Rodriguez BL, Albion RL, Cushman JC (2014) Multiple isoforms of phosphoenolpyruvate carboxylase in the Orchidaceae (subtribe Oncidiinae): implications for the evolution of crassulacean acid metabolism. Journal of Experimental Botany 65:3623-3636
Singh J, Thakur JK (2018) Photosynthesis and abiotic stress in plants. In: Biotic and abiotic stress tolerance in plants. Springer, pp 27-46
Ślesak I, Libik M, Miszalski Z (2008) The foliar concentration of hydrogen peroxide during salt-induced C3-CAM transition in Mesembryanthemum crystallinum L. Plant Science 174:221-226
Smith GF, Figueiredo E, Van Wyk AE (2019) Kalanchoe (Crassulaceae) in Southern Africa: classification, biology, and cultivation. Academic Press,
Spalding M, Stumpf D, Ku M, Burris R, Edwards G (1979) Crassulacean acid metabolism and diurnal variations of internal CO2 and O2 concentrations in Sedum praealtum DC. Functional Plant Biology 6:557-567
Stitt M, Zeeman SC (2012) Starch turnover: pathways, regulation and role in growth. Current Opinion in Plant Biology 15:282-292
Taybi T, Cushman J, Borland A (2017) Leaf carbohydrates influence transcriptional and post-transcriptional regulation of nocturnal carboxylation and starch degradation in the facultative CAM plant, Mesembryanthemum crystallinum. Journal of Plant Physiology 218:144
Taybi T, Cushman JC (2002) Abscisic acid signaling and protein synthesis requirements for phosphoenolpyruvate carboxylase transcript induction in the common ice plant. Journal of Plant Physiology 159:1235-1243
Taybi T, Nimmo HG, Borland AM (2004) Expression of Phosphoenolpyruvate Carboxylase and Phosphoenolpyruvate Carboxylase Kinase Genes. Implications for Genotypic Capacity and Phenotypic Plasticity in the Expression of Crassulacean Acid Metabolism. Plant Physiology 135:587-598
Teeri J, Stowe L, Murawski D (1978) The climatology of two succulent plant families: Cactaceae and Crassulaceae. Canadian Journal of Botany 56:1750-1758
Theng V, Agarie S, Nose A (2007) Regulatory Properties of Phospho enol pyruvate Carboxylase in Crassulacean Acid Metabolism Plants: Diurnal Changes in Phosphorylation State and Regulation of Gene Expression. Plant Production Science 10:171-181
Visentin I, Pagliarani C, Deva E, Caracci A, Turečková V, Novák O, Lovisolo C, Schubert A, Cardinale F (2020) A novel strigolactone-miR156 module controls stomatal behaviour during drought recovery. Plant, cell & environment 43:1613-1624

Walczak A (2021) The use of world water resources in the irrigation of field cultivations. Journal of Ecological Engineering 22
Weise SE, van Wijk KJ, Sharkey TD (2011) The role of transitory starch in C, CAM, and C metabolism and opportunities for engineering leaf starch accumulation. Journal of Experimental Botany 62:3109-3118
Willick IR, Plaxton WC, Lolle SJ, Macfie SM (2019) Transcriptional and post-translational upregulation of phosphoenolpyruvate carboxylase in Arabidopsis thaliana (L. Heynh) under cadmium stress. Environmental and Experimental Botany 164:29-39
Winter K, Holtum JA, Smith JAC (2015a) Crassulacean acid metabolism: a continuous or discrete trait? New Phytologist 208:73-78
Winter K, Holtum JAM, Smith JAC (2015b) Crassulacean acid metabolism: a continuous or discrete trait? New Phytologist 208:73-78
Winter K, Smith JAC (2022) CAM photosynthesis: the acid test. New Phytologist 233:599-609
Wyka T, Bohn A, Duarte H, Kaiser F, Lüttge U (2004) Perturbations of malate accumulation and the endogenous rhythms of gas exchange in the Crassulacean acid metabolism plant Kalanchoë daigremontiana : testing the tonoplast-as-oscillator model. Planta 219:705-713
Xing H-L, Dong L, Wang Z-P, Zhang H-Y, Han C-Y, Liu B, Wang X-C, Chen Q-J (2014) A CRISPR/Cas9 toolkit for multiplex genome editing in plants. BMC Plant Biology 14:327
Yan J, Zhu C, Liu W, Luo F, Mi J, Ren Y, Li J, Sang T (2015) High photosynthetic rate and water use efficiency of Miscanthus lutarioriparius characterize an energy crop in the semiarid temperate region. GCB Bioenergy 7:207-218
Yanagisawa S, Akiyama A, Kisaka H, Uchimiya H, Miwa T (2004) Metabolic engineering with Dof1 transcription factor in plants: improved nitrogen assimilation and growth under low-nitrogen conditions. Proceedings of the National Academy of Sciences 101:7833-7838
Yang T, Liu X (2015) Comparing photosynthetic characteristics of Isoetes sinensis Palmer under submerged and terrestrial conditions. Scientific reports 5:17783
Yang X, C. CJ, M. BA, J. EE, D. WS, A. TG, A. ON, Howard G, C. SJA, C. DPH et al. (2015a) A roadmap for research on crassulacean acid metabolism (CAM) to enhance sustainable food and bioenergy production in a hotter, drier world. New Phytologist 207:491-504
Yang X, Cushman JC, Borland AM, Edwards EJ, Wullschleger SD, Tuskan GA, Owen NA, Griffiths H, Smith JAC, De Paoli HC et al. (2015b) A roadmap for research on crassulacean acid metabolism (CAM) to enhance sustainable food and bioenergy production in a hotter, drier world. New Phytologist 207:491-504
Yang X, Cushman JC, Borland AM, Liu Q (2020) Systems biology and synthetic biology in relation to drought tolerance or avoidance in plants. Frontiers in Plant Science 11:394
Yang X, Hu R, Yin H, Jenkins J, Shu S, Tang H, Liu D, Weighill DA, Cheol Yim W, Ha J et al. (2017) The Kalanchoë genome provides insights into convergent evolution and building blocks of crassulacean acid metabolism. Nature Communications 8:<xocs:firstpage xmlns:xocs=""/>
Yang X, Qi LS, Jaramillo A, Cheng Z-MM (2019) Biodesign research to advance the principles and applications of biosystems design. vol 2019. Science Partner Journal,
Yin H, Guo H-B, Weston DJ, Borland AM, Ranjan P, Abraham PE, Jawdy SS, Wachira J, Tuskan GA, Tschaplinski TJ (2018) Diel rewiring and positive selection of ancient plant proteins enabled evolution of CAM photosynthesis in Agave. BMC genomics 19:1-16

Yuan G, Hassan MM, Liu D, Lim SD, Yim WC, Cushman JC, Markel K, Shih PM, Lu H, Weston DJ (2020) Biosystems design to accelerate C3-to-CAM progression. BioDesign Research 2020

Zhang DLJ, MC, AL, H-BG, MX, G, Yuan RH, NLE, TJT, SJ et al. (2021) Metabolic control of transcriptome reprogramming associated with crassulacean acid metabolism. In press

Zhang DLJ, MC, AL, H-BG, MX, G, Yuan RH, NLE, TJT, SJ et al. (unpublished) Metabolic control of transcriptome reprogramming associated with crassulacean acid metabolism. In press

Zhang Y, Su J, Duan S, Ao Y, Dai J, Liu J, Wang P, Li Y, Liu B, Feng D (2011) A highly efficient rice green tissue protoplast system for transient gene expression and studying light/chloroplast-related processes. Plant methods 7:1-14

Appendix A. Effect of knocking down *KfePEPC1* and *KfePEPC2* gene on the plant height (stem elongation) and chlorophyll content of *KfePEPC* mutants of *K. fedtschenkoi.*

Knocking down *KfePEPC* genes had different effects on the plant height (stem elongation) when measured on weekly basis for six (6) weeks. In the *kfepepc1* Line 1 mutant, the knockdown did not cause a significant reduction in plant height over the six (6) weeks period compared to the wild type (Figure A1.A). Meanwhile, in the *kfepepc1* Line 2, there was significantly reduced plant height compared to the wild type at week 4 (Figure A1.A). In the *kfepepc2* Line 1 mutant, the knockdown led to a significant reduction in stem elongation compared to the wildtype in week 1, week 4, week 5, and week 6 (Figure A1.B). While in *kfepepc2* Line 2, the knockdown led to a significant reduction in the plant height compared to the wild type in week 1, week 3, week 4, week 5, and week 6 (Figure A1.B). The knockdown of both *KfePEPC1* and *KfePEPC2* led to a significant reduction in the plant height of *kfepepc1/2* Line 1 and *kfepepc1/2* Line 2 from week 1 to week 6 (Figure A1.C).

The effect of knocking down *KfePEPC 1* and *KfePEPC 2* genes on the ratio of chlorophyll a to chlorophyll b content was measured in well-watered and drought-stressed *K. fedtschenkoi* wildtype and *KfePEPC* mutants. In well-watered conditions, only *kfepepc2* Line 1 and *kfepepc2* Line 1 showed a significant increase in the ratio of chlorophyll a to chlorophyll b content, while in drought-stress conditions, there was no significant increase or reduction in the ratio of chlorophyll a to chlorophyll b content in the mutants compared to the wild type (Figure A2).

A

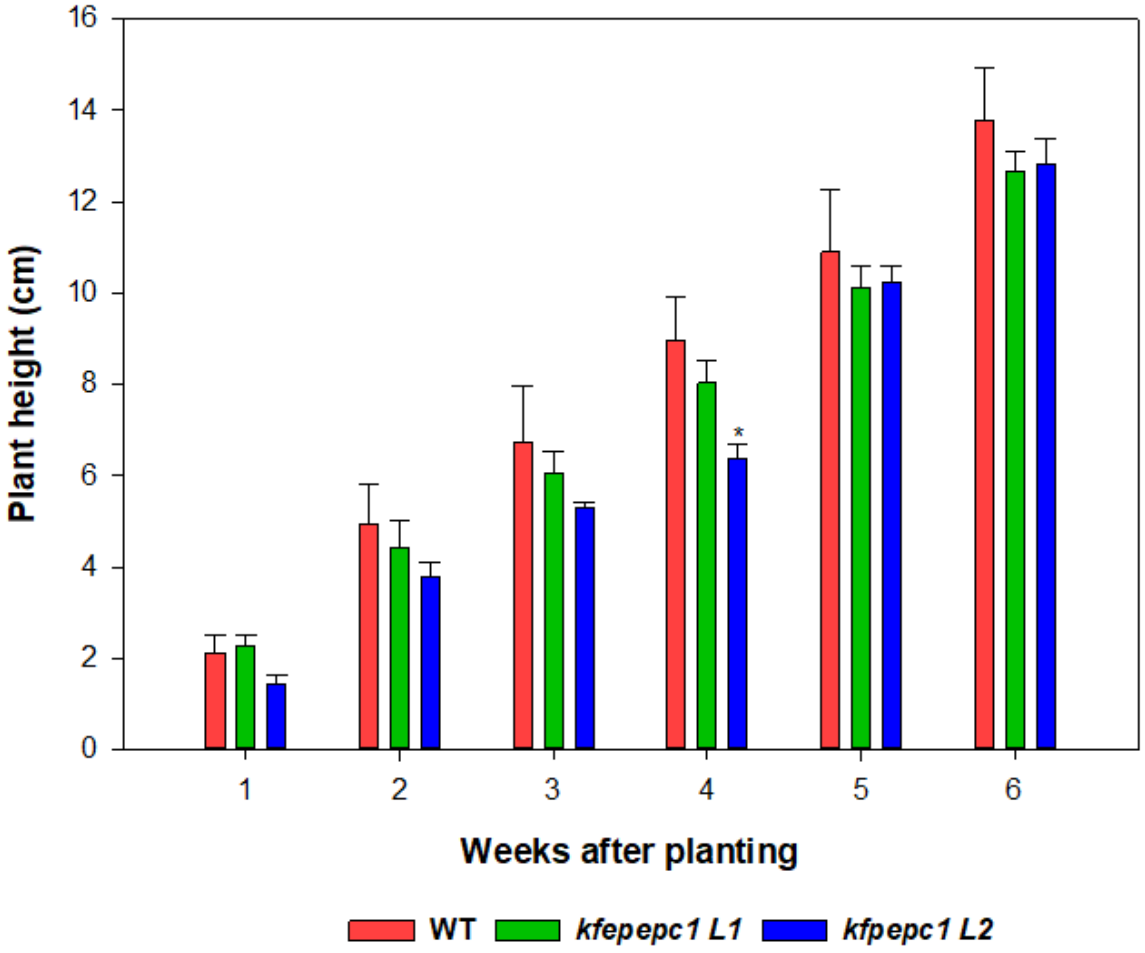
16
14
12
10
8
6
4
2
0
Plant height (cm)
*
1
2
3
4
5
6
Weeks after planting
WT
kfepepc1 L1
kfpepc1 L2

B

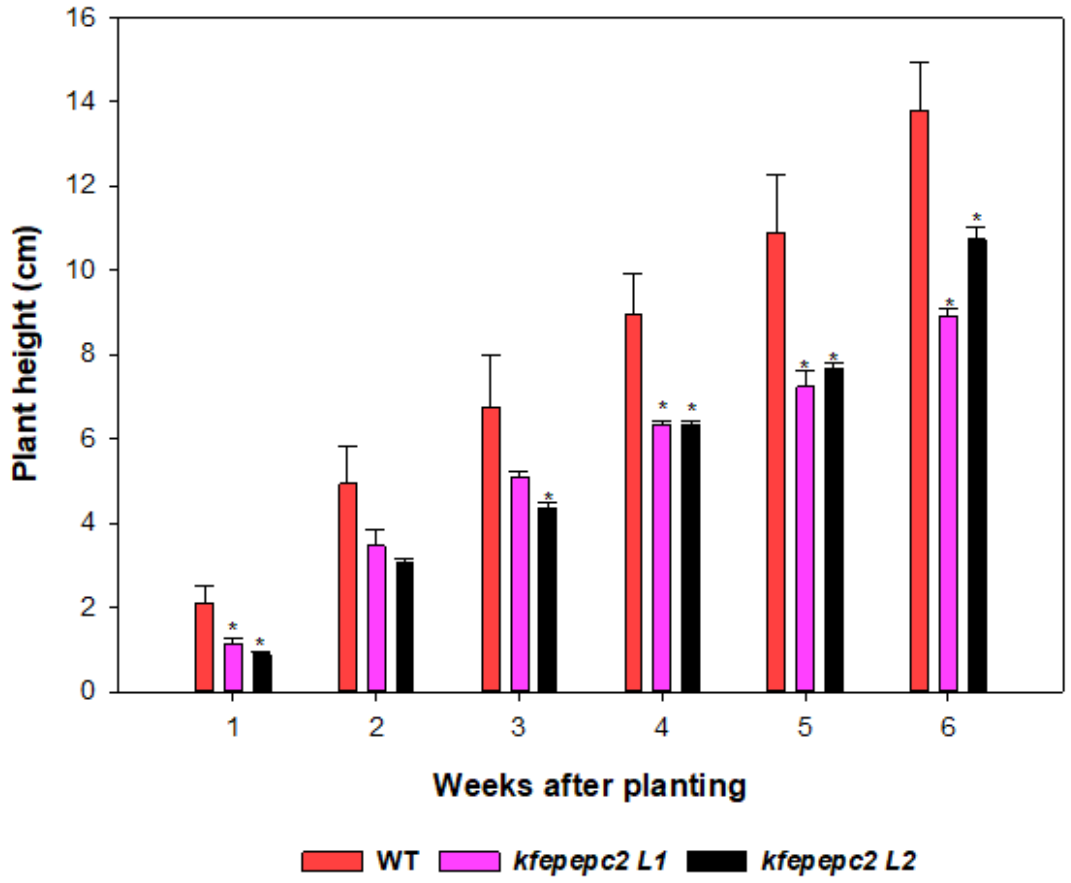
Plant height (cm)
16
14
12
10
8
6
4
2
0
1
2
3
4
5
6
Weeks after planting
WT
kfepepc2 L1
kfepepc2 L2

C

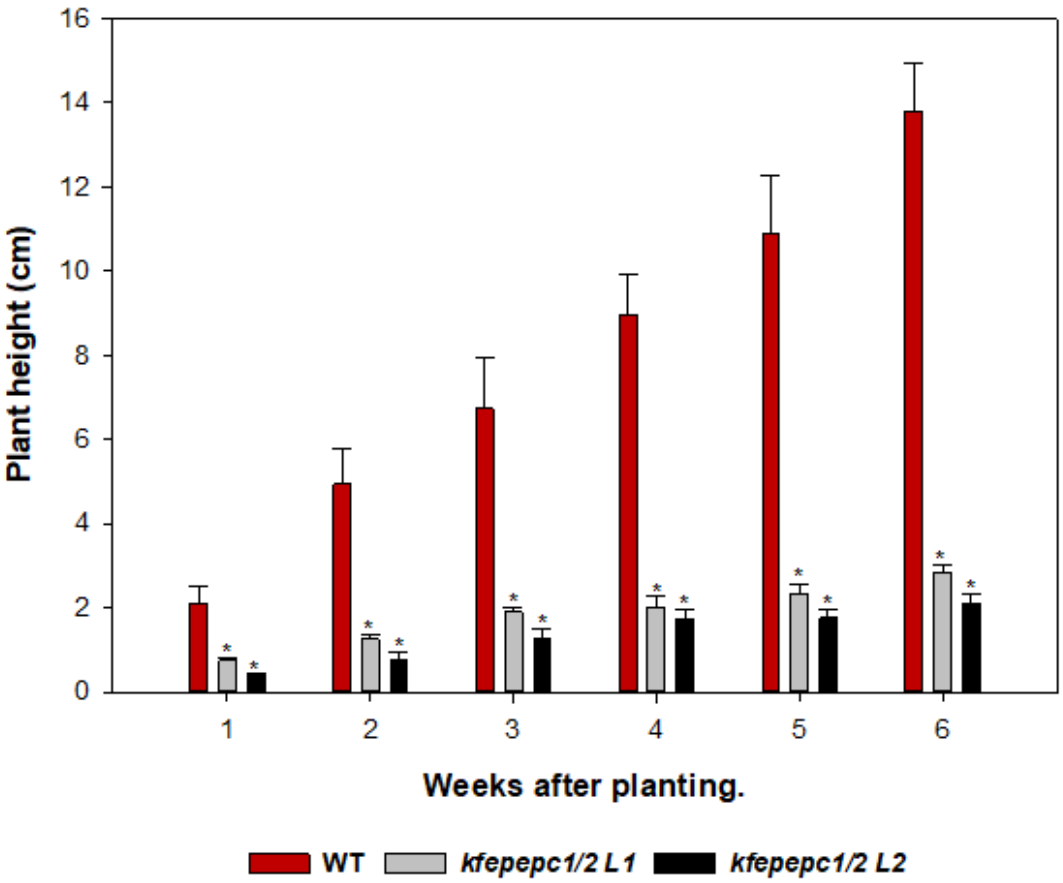

Figure A1. The mean plant height (stem elongation) of *K.fedtschenkoi* wildtype (red bars), *kfepepc1* Line 1 (green bars), *kfepepc1* Line 2 (blue bars), *kfepepc2* Line 1 (purple bars) and *kfepepc2* Line 2 (black bars), *kfepepc1/2* Line 1 (grey bars) and *kfepepc1/2* Line 2 (black bars) over six (6) weeks. Data presented as the mean of three (3) biological replicates. * Shows a significant difference at $p \leq 0.05$.

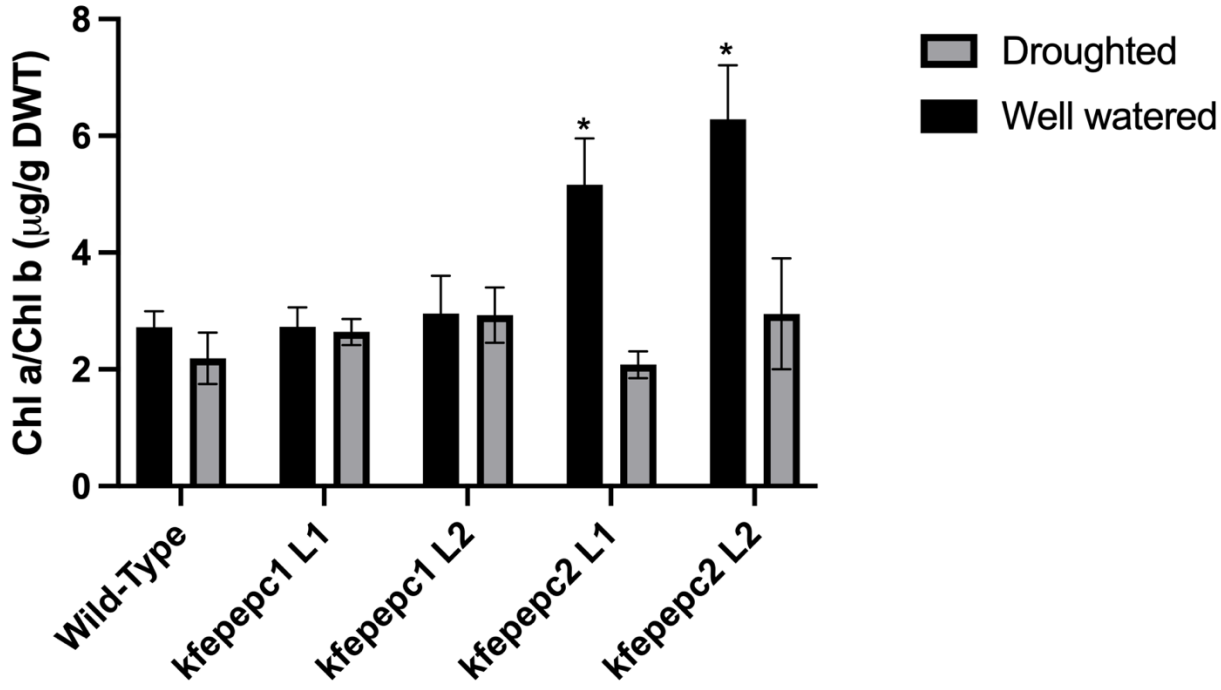

Figure A2. The mean chlorophyll a to chlorophyll b ratio for well-watered (black bars) and drought-stressed (grey bars) *K.fedtschenkoi* wildtype and *KfePEPC* mutant plants. Data presented as the mean of three (3) biological replicates. * shows a significant difference at $p \leq 0.05$.

Appendix B. Calibration curve used for measuring the qRT-PCR primer efficiency.

A.

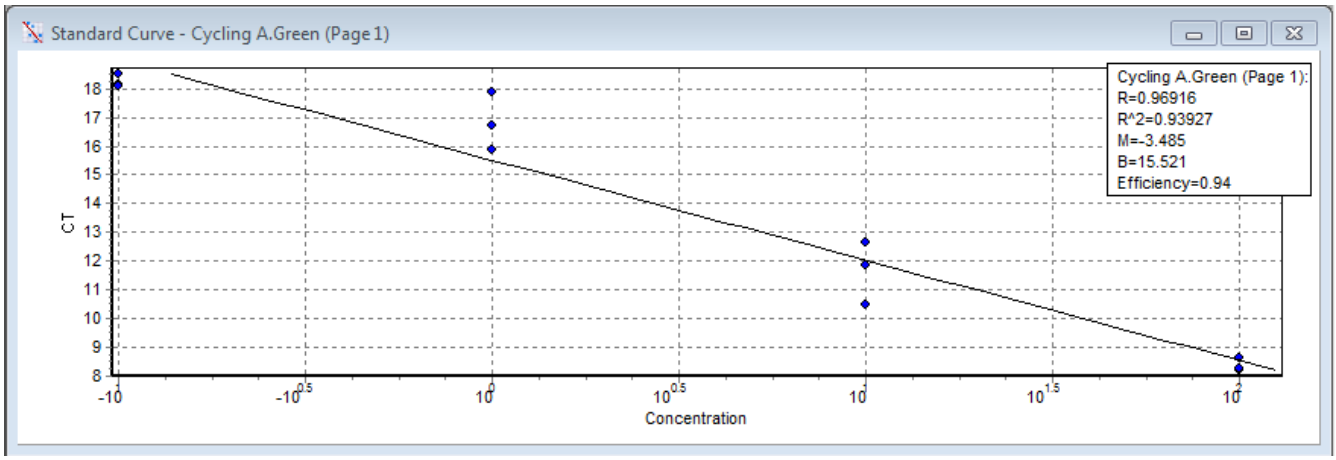

B

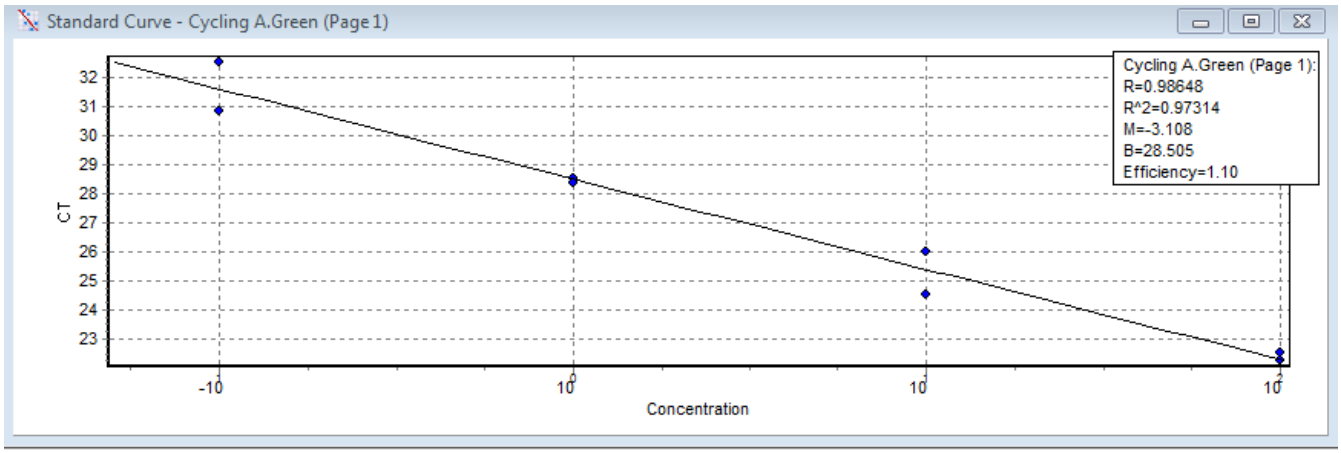

C

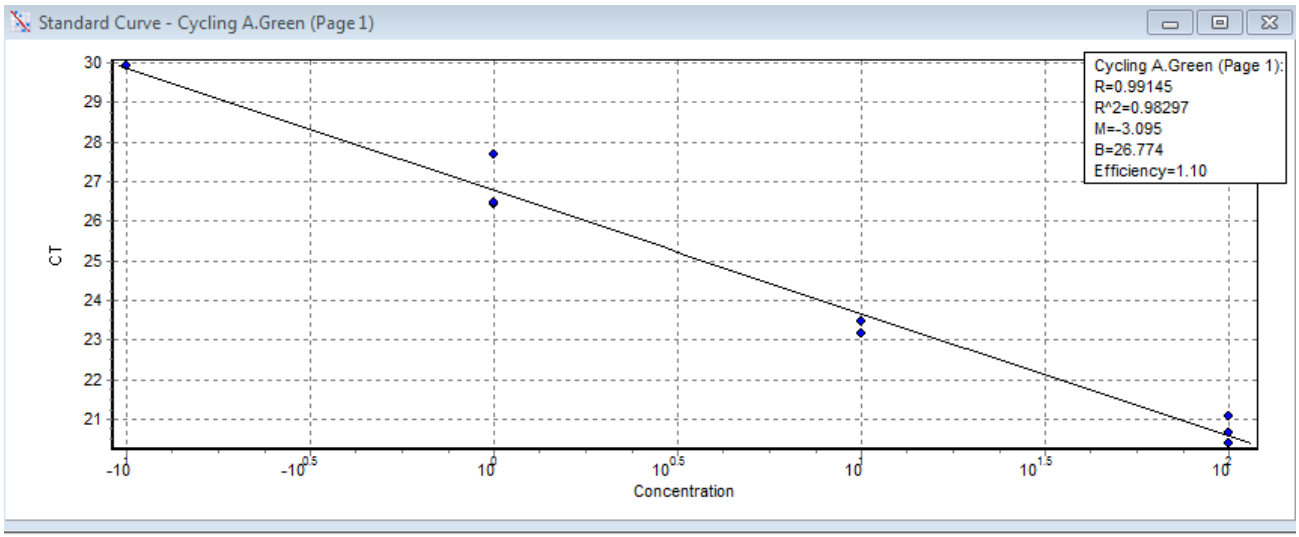

D

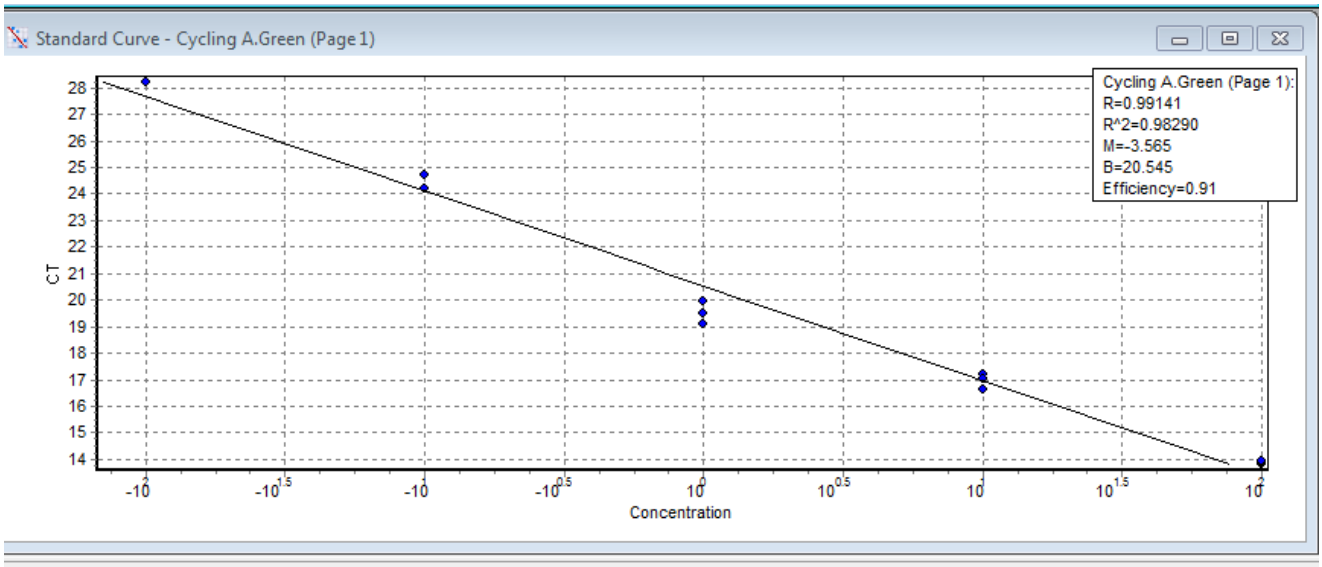

Figure A2. Calibration curve used for measuring the primer efficiency of (a) *KfePEPC1* gene, (b) *KfePEPC2* gene, (c) *KfePPCK 1* gene, and (d) *rbc*L gene.